

VOLATILE FATTY ACIDS RECOVERY IN A REACTIVE PRIMARY CLARIFIER:
A PILOT CASE STUDY

By

Michele Ponzelli, BSc, MSc

M. Eng., Università Politecnica delle Marche, 2017

B. Eng., Università Politecnica delle Marche, 2014

A thesis

presented to Ryerson University

in partial fulfillment of the

requirements for the degree of

Master of Applied Science

in the Program of

Civil Engineering

Toronto, Ontario, Canada, 2019

©Michele Ponzelli, 2019

Author's Declaration for Electronic Submission of a Thesis

I hereby declare that I am the sole author of this thesis. This is a true copy of the thesis, including any required final revisions, as accepted by my examiners.

I authorize Ryerson University to lend this thesis to other institutions or individuals for the purpose of scholarly research.

I further authorize Ryerson University to reproduce this thesis by photocopying or by other means, in total or in part, at the request of other institutions or individuals for the purpose of scholarly research.

I understand that my thesis may be made electronically available to the public.

Abstract

Volatile Fatty Acids Recovery in a Reactive Primary Clarifier:
A Pilot Case Study

Michele Ponzelli,
Master of Applied Science in Civil Engineering,
Ryerson University,
2019

Although the aim of primary clarifiers remains to remove particles, the removal of settleable solids affects downstream processes that rely on readily biodegradable oxygen demand (rbCOD) in proportion to nutrient removal demands. However, through some process modification the primary clarifier can be looked at as a physico-biochemical reactor able to accomplish: removal of settleable solids; increase rbCOD concentration in the primary effluent. Pilot-scale experiments were conducted at the 12 m³ water resource recovery facility of Université Laval to determine the effect of different factors on the fermentation process in a primary clarifier. The results showed that providing a sludge retention time larger than one day and a low recirculation flow rate from the bottom of the clarifier of about 15% of the influent flow rate are crucial factors for increased rbCOD concentration. They can lead to a VFAs yield up to 90 mgCH₃COOHequivalent/gVSS, along with a 70% solids removal efficiency.

Acknowledgements

First and foremost I would like to express all my gratitude to my supervisor professor Dr. Peter A. Vanrolleghem for his knowledgeable help and guidance during this master project. His contributions during our meetings and in particular in this project have been of paramount importance and influence in my successes. I specially thank him for making me reflect on my assumptions. I am also grateful to him for welcoming me into a tight-knit enthusiastic student group at Université Laval. I will never forget the beautiful time that I had once arrived at his dinner event.

For all the fun that I had in the pileAUte, I would like to thank all the modelEAU team. In particular, Christophe Boisvert, Sey-Hana Saing, Maryam Tohidi, Kamilia Haboub, Romain Philippe, Gamze Kirim, Asma Hafouf, Feiyi Li, and Elena Torfs. Although the snowy weather lasted almost up to May, I really had a great time in Quebec City because of you, and I am thankful.

I would like to thank my supervisor Prof. Dr. Elsayed Elbeshbishy for bringing me on board of a very valuable project in terms of room for self-improvement for my career, such as knowledge transfer, teamwork, research challenges, and so on. What I appreciate the most from him is his extreme care for his student and his ability of always treating his students as a part of a big family.

I would also like to thank my industrial supervisor Dr. Domenico Santoro who during this project, and not only this, provided me an inestimable industrial mindset to approach problems which helped me grow, since he believed in me and in my capabilities as a scientist.

Let me also express my gratitude to all the SOWC team: Tommaso, Lisha, Riccardo, John, Ted, and all the others.

Overall, I was so glad to be part of such a team and I could not have asked for better supervisors and mentors.

Furthermore, I would like to thank my family and friends for showing their support and exhibiting much support throughout my second master's program. Despite the ocean between us, they always supported me in every possible way, without which this thesis would not have happened. This last part is especially true for Giorgia who always believed in me and offered me unconditional support. Thank you.

Lastly, I want to thank the Cin Cin club for having made it possible.

Table of Contents

Author's Declaration for Electronic Submission of a Thesis	ii
Abstract	iii
Acknowledgements.....	iv
List of Tables	vii
List of Figures.....	ix
List of Appendices	xiv
Chapter 1: Introduction.....	1
Chapter 2: Background and Literature Review	2
2.1 Primary Settler Tank	4
2.2 Volatile Fatty Acids	7
2.3 Anaerobic Digestion.....	8
2.4 Reactive Primary Clarifier	10
Chapter 3: Materials and Methods.....	20
Chapter 4: Results.....	29
4.1 The Effects of SRT and Internal Recirculation Flow Rate	29
4.1.1 One day SRT and no internal recirculation flow rate.....	29
4.1.2 One day SRT and high internal recirculation flow rate.....	33
4.1.3 Three days SRT and high internal recirculation flow rate.....	39
4.1.4 Three days SRT and low internal recirculation flow rate.....	44
4.2 The Effect of Alkalinity	49
4.3 Effect of Ferric Chloride	53
4.4 Combined Effect of Alkalinity and Ferric Chloride.....	57
4.5 Effect of Temperature	60
4.6 Data Analysis and Statistical Analysis with R.....	61
4.6.1 Analysis of Plotted Data.....	62
4.6.2 ANOVA Analysis (R)	68
Chapter 5: Conclusions.....	71
Chapter 6: Recommendations and Suggestions for Further Research.....	72
Appendix.....	74

References..... 118

List of Tables

Table 1: Typical primary clarifier design information (Metcalf and Eddy, 2003).	6
Table 2: Reactive primary clarifier performance, in terms of VFA production and solids removal efficiency (Chanona et al., 2006).	12
Table 3: Main operational and performance parameters for the in-line reactive primary clarifier (Bouzas et al. 2007).	14
Table 4: Influent wastewater characteristics (Jin et al. 2016).	15
Table 5: VFA yield for different substrates and operational conditions.	17
Table 6: Online sensors and monitored parameters located at the primary effluent.	21
Table 7: Summary of the operating and environmental conditions for stages #1 to #8.	22
Table 8: Investigated parameters of the pilot experiments.	25
Table 9: Lab measurement and removal efficiency based on triplicates for total and duplicates for soluble concentrations (Stage #1).	31
Table 10: Lab measurements and removal efficiency based on triplicates and duplicates for total and soluble concentrations, respectively (Stage #2).	31
Table 11: Process performance parameters (Stage #1 and #2).	32
Table 12: Lab measurements and removal efficiency based on triplicates and duplicates for total and soluble concentrations, respectively (Stage #3).	38
Table 13: Process performance parameters (Stage #3).	38
Table 14: Summary of the main parameters for Stage #3.	38
Table 15: Lab measurements and removal efficiency based on triplicates and duplicates for total and soluble concentrations, respectively (Stage #4).	42
Table 16: Process performance parameters (Stage #4).	42
Table 17: Summary of the main parameters for Stage #4.	42
Table 18: Lab measurements and removal efficiency based on triplicates and duplicates for total and soluble concentrations, respectively (Stage #5).	47
Table 19: Process performance parameters (Stage #5).	47
Table 20: Summary of the main parameters for Stage #5.	48
Table 21: Lab measurements and removal efficiency based on triplicates and duplicates for total and soluble concentrations, respectively (Stage #6).	51
Table 22: Process performance parameters (Stage #6).	52

Table 23: Summary of the main parameters for Stage #6.	52
Table 24: Lab measurements and removal efficiency based on triplicates and duplicates for total and soluble concentrations, respectively (Stage #7).	56
Table 25: Process performance parameters (Stage #7).	56
Table 26: pH, VFA and bicarbonate alkalinity values during NaHCO ₃ and FeCl ₃ dosages (Stage #8).	57
Table 27: Lab measurements and removal efficiency based on triplicates and duplicates for total and soluble concentrations, respectively (Stage #8).	59
Table 28: Process performance parameters (Stage #8).	60
Table 29: Summary of the operating conditions and performance for stages #1 to #8.	61
Table 30: Summary of the operating conditions and performance for stages in steady state conditions.	62
Table 31: ANOVA table for VFA yield response.	69
Table 32: ANOVA table for TSS removal efficiency response.	69
Table 33: Coefficient estimates for TSS removal efficiency response.	70
Table 34: Summary of the main parameters for Stage #1.	78
Table 35: Summary of the main parameters for Stage #2.	84
Table 36: pH, VFA and alkalinity values during NaHCO ₃ dosage (Stage #6).	95
Table 37: Raw wastewater quality characteristics for dry and wet weather period.	98
Table 38: Summary of the main parameters for Stage #7.	102
Table 39: Summary of the main parameters for Stage #8.	107
Table 40: Coefficient estimates for VFA yield response.	112

List of Figures

Figure 1: 3D molecular structure of the acetic acid (CH ₃ COOH).....	8
Figure 2: Biochemical reactions involved during the primary sludge anaerobic digestion.....	9
Figure 3: Reactive primary clarifier scheme (a), side-stream fermenter (b) (Chanona et al., 2006).	11
Figure 4: Reactive primary clarifier scheme equipped with complementary side stream fermenter (Bouzas et al., 2007)	13
Figure 5: Activated primary tank scheme (Jin et al., 2016).....	15
Figure 6: Scheme of the pileAUte facility.	20
Figure 7: Process scheme of the modified primary clarifier.	22
Figure 8: Schematic mass balance representation of the primary clarifier.....	23
Figure 9: Overview of the storage tank and primary clarifier and the sampling locations.....	24
Figure 10: TSS concentration profile in primary clarifier by means of turbidity meter (Stage #1 and #2).	30
Figure 11: Internal recirculation line installed on the pileAUte primary clarifier (marked in red) (left picture source: JOHN MEUNIER INC.).....	33
Figure 12: Grabbing samples at different heights.....	34
Figure 13: TSS concentration profile comparison between turbidity meter and lab measurements (Pre-Stage #3).	35
Figure 14: TSS concentration profile in primary clarifier (Stage #3).....	35
Figure 15: pH, VFA and alkalinity profiles for Stage #3.	36
Figure 16: Bubbles on the surface - a fermentation process is occurring.....	37
Figure 17: TSS concentration profile in primary clarifier (Stage #4).....	39
Figure 18: pH, VFA and bicarbonate alkalinity profiles for Day 6 based on grabbed samples (Stage #4).	40
Figure 19: pH, VFA and bicarbonate alkalinity profiles for Day 9 based on composite samples (Stage #4).....	40
Figure 20: Comparison of pH, VFA and bicarbonate alkalinity profiles for Day 6 and 9 (Stage #4).	41
Figure 21: Rising sludge on the primary clarifier on June 11 (Stage #4).	43
Figure 22: Mass balance for Stage #4.....	44

Figure 23: TSS concentration profile in primary clarifier (Stage #5).....	45
Figure 24: Comparison of pH, VFA and bicarbonate alkalinity profiles for Day 17 and 18 (Stage #5).	46
Figure 25: Weather in Quebec City from July 21 (Day 15) to 24 (Day 18). (Source: timeanddate.com).....	46
Figure 26: Primary sludge after 30 minutes of sedimentation in an Imhoff cone.	49
Figure 27: TSS concentration profile in primary clarifier (Stage #6).....	50
Figure 28: Comparison of pH, VFA and bicarbonate alkalinity profiles for Day 7 and 8 (Stage #6).	51
Figure 29: Rising sludge on the primary clarifier on Day 4 (Stage #6).....	52
Figure 30: FeCl ₃ solution pumped into the primary clarifier's Clifford cylinder by means of a peristaltic pump.....	53
Figure 31: TSS concentration profile in primary clarifier (Stage #7).....	54
Figure 32: Comparison of pH, VFA and bicarbonate alkalinity profiles for Day 6 and 7 (Stage #7).	55
Figure 33: TSS concentration profile in primary clarifier (Stage #8).....	58
Figure 34: Comparison of pH, VFA and bicarbonate alkalinity profiles for Day 13 and 14 (Stage #8).	58
Figure 35: Temperature effect on VFAs yield, COD solubilisation, solids removal efficiency (E%TSS) and hydrolysis yield during the different stages.	60
Figure 36: Effect of the internal recirculation ratio on the VFA yield for stages #1 to #8.	62
Figure 37: TSS removal efficiency versus extra days in steady state conditions for stages #1 to #8.	63
Figure 38: VFA yield versus extra days in steady state conditions for stages #1 to #8.....	63
Figure 39: Effect of the temperature on the VFA yield for stages #1 to #8.	64
Figure 40: Effect of the internal recirculation ratio on (a) TSS removal efficiency and (b) VFA yield for stages in steady state conditions.	65
Figure 41: Effect of the desired and actual SRT (a, c) TSS removal efficiency and (b, d) VFA yield, respectively, for stages in steady state conditions.	66
Figure 42: Effect of sodium bicarbonate addition on (a) TSS removal efficiency and (b) VFA yield for stages in steady state conditions.....	67

Figure 43: Extra days in steady state conditions versus (a) TSS removal efficiency and (b) VFA yield for stages in steady state conditions.	67
Figure 44: Effect of temperature on (a) TSS removal efficiency and (b) VFA yield for stages in steady state conditions.	68
Figure 45: Materials found in the recirculation line pump causing the clogging.	72
Figure 46: (a) Primary inlet y-strainers with different mesh sizes and (b) collected material on the y-strainer after 16 hours from cleaning.	73
Figure 47: Total COD concentration from lab measurements on composite samples (influent and outlet) and online probe located at the outlet (Stage #1).	74
Figure 48: Soluble COD concentration from lab measurements on composite samples (influent and outlet) and online probe located at the outlet (Stage #1).	75
Figure 49: TSS concentration from lab measurements on composite samples (influent and outlet) and online probe located at the outlet (Stage #1).	75
Figure 50: Ammonium concentration from lab measurements on composite samples (influent and outlet) and online probe located at the outlet (Stage #1).	76
Figure 51: Potassium concentration trend at the outlet (Stage #1).	76
Figure 52: pH trend at the outlet (Stage #1).	77
Figure 53: Temperature trend at the outlet (Stage #1).	77
Figure 54: Mass balance for Stage #1.	79
Figure 55: Total COD concentrations from lab measurements on composite samples (influent and outlet) and online probe located at the outlet (Stage #2).	80
Figure 56: Soluble COD concentrations from lab measurements on composite samples (influent and outlet) and online probe located at the outlet(Stage #2).	81
Figure 57: TSS concentrations from lab measurements on composite samples (influent and outlet) and online probe located at the outlet (Stage #2).	81
Figure 58: Ammonium concentrations from lab measurements on composite samples (influent and outlet) and online probe located at the outlet (Stage #2).	82
Figure 59: Potassium concentration trend at the outlet (Stage #2).	82
Figure 60: pH trend at the outlet (Stage #2).	83
Figure 61: Temperature trend at the outlet (Stage #2).	83
Figure 62: Mass balance for Stage #2.	84

Figure 63: TSS concentrations from lab measurements on composite samples (influent and outlet) and online probe located at the outlet (Stage #3).....	85
Figure 64: Temperature trend at the outlet (Stage #3).....	85
Figure 65: Mass balance Stage #3.	86
Figure 66: TSS concentrations from lab measurements on composite samples (influent and outlet) and online probe located at the outlet (Stage #4).....	87
Figure 67: Temperature trend at the outlet (Stage #4).....	88
Figure 68: TSS concentrations from lab measurements on composite samples (influent and outlet) and online probe located at the outlet (Stage #5).....	89
Figure 69: Temperature trend at the outlet (Stage #5).....	90
Figure 70: Mass balance Stage #5.	90
Figure 71: VFA concentration dynamics at the primary clarifier inlet and outlet on July 25 th and 26 th	92
Figure 72: Alkalinity concentration dynamics at the primary clarifier inlet and outlet on July 25 th and 26 th	92
Figure 73: Set-up of the basin for saturated sodium bicarbonate solution dosage.	93
Figure 74: Film on the clarifier’s surface after NaHCO ₃ dosage.....	93
Figure 75: VFA concentration dynamics at the primary clarifier inlet and outlet on Day 4 and 5.	94
Figure 76: Alkalinity concentration dynamics at the primary clarifier inlet and outlet on Day 4 and 5.....	95
Figure 77: TSS concentrations from lab measurements on composite samples (influent and outlet) and online probe located at the outlet (Stage #6).....	96
Figure 78: Temperature trend at the outlet (Stage #6).....	96
Figure 79: Mass balance Stage #6.	97
Figure 80: Jar test equipment.....	98
Figure 81: Jar test results for different FeCl ₃ dosages with dry weather (DWP) and wet weather (WWP) samples.	99
Figure 82: TSS concentrations from lab measurements on composite samples (influent and outlet) and online probes located at the inlet and outlet (Stage #7).	100

Figure 83: Total COD concentration from lab measurements on composite samples (influent and outlet) and online probe located at the outlet (Stage #7).	100
Figure 84: pH trend at the outlet and from lab measurements on composite samples (influent and outlet) (Stage #7).....	101
Figure 85: Temperature trend at the outlet for conductivity meter and ammonium probe (Stage #7).	101
Figure 86: Potassium concentration trend at the outlet (Stage #7).	102
Figure 87: Mass balance Stage #7.	103
Figure 88: TSS concentrations from lab measurements on composite samples (influent and outlet) and online probes located at the inlet and outlet (Stage #8).	104
Figure 89: Total COD concentration from lab measurements on composite samples (influent and outlet) and online probe located at the outlet (Stage #8).	105
Figure 90: pH trend at the outlet and from lab measurements on composite samples (influent and outlet) (Stage #8).....	105
Figure 91: Temperature trend at the outlet for conductivity meter and ammonium probe (Stage #8).	106
Figure 92: Potassium concentration trend at the outlet (Stage #8).	106
Figure 93: Mass balance Stage #8.	107
Figure 94: Effect of internal recirculation ratio on the TSS removal efficiency for stage #1 to #8.	108
Figure 95: Effect of sodium bicarbonate dosage on (a) TSS removal efficiency and (b) VFA yield for stage #1 to #8.....	108
Figure 96: Effect of the desired and actual SRT on (a, c) TSS removal efficiency and (b, d) VFA yield, respectively, for stage #1 to #8.	109
Figure 97: Effect of ferric chloride addition on (a) TSS removal efficiency and (b) VFA yield for stage #1 to #8.	110
Figure 98: Temperature effect on TSS removal efficiency for stage #1 to #8.	110
Figure 99: Effect of ferric chloride addition on (a) TSS removal efficiency and (b) VFA yield for stages in steady state conditions.	111

List of Appendices

A.1: One day SRT and no internal recirculation flow rate (Stage #1)	74
Probe values	74
Main parameters and mass balance.....	78
A.2: One day SRT and no internal recirculation flow rate (Stage #2)	80
Probe values	80
Main parameters and mass balance.....	84
A.3: One day SRT and high internal recirculation flow rate (Stage #3).....	85
Probe values	85
Mass balance	86
A.4: Three days SRT and high internal recirculation flow rate (Stage #4).....	87
Probe values	87
A.5: Three days SRT and low internal recirculation flow rate (Stage #5).....	89
Probe values	89
Mass balance	90
A.6: Three days SRT and low internal recirculation flow rate, and alkalinity dosing (Stage #6)	91
Alkalinity demand and NaHCO ₃ solution dosage	91
Probe values	95
Mass balance	97
A.7: Three days SRT, low internal recirculation flow rate, and FeCl ₃ dosing (Stage #7).....	98
Jar-tests for optimum FeCl ₃ dosage	98
Probe values	99
Main parameters and mass balance.....	102
A.8: Three days SRT, low internal recirculation flow rate, and alkalinity and FeCl ₃ dosing (Stage #8).....	104
Probe values	104

Main parameters and mass balance.....	107
A.9: Data Analysis – Plots	108
Steady state	111
A.10: R code and data	112
A.11: Conditions, Parameters, and Performance Values	113

Chapter 1: Introduction

The primary clarifier is a physical operation unit that aims to remove a large fraction of the settleable solids from wastewater. Since settleable solids include both inert and organic particles, optimizing the clarifier's efficiency can thus affect the carbon availability in the downstream biological nutrient removal processes (BNR). As a result, BNR plants characterized by low carbon (either amount or quality) usually result in failures to comply with nutrient discharge limits. Primary clarifiers can thus negatively influence the denitrification and biological phosphorus removal performance because they remove organic matter, useful for denitrifiers and phosphorus accumulating organisms (PAOs). On the other hand, the importance of removing inert particles is crucial. Indeed, biological processes adopted for nutrients removal require long sludge retention times (SRT). A low solids removal performance, or, more drastically, the removal of the primary clarifier from the treatment chain, usually leads to an increased portion of inert particles in the secondary treatment, which reduces the SRT, thus jeopardizing these biological processes. Therefore, the challenge of removing particles but at the same time preserving the organic matter, has led municipalities to supply external carbon source (such as, methanol, glycerin, and acetic acid) for biological carbon demand, and to add coagulants to increase the solids removal efficiency, also known as chemically enhanced primary treatment (CEPT).

However, while a lot of attention has been paid to physical and chemical (flocculation) operations in the primary clarifier, little has been done regarding the biological reactions that could occur there. In fact, recent studies suggest that hydrolysis (conversion of complex organic into soluble COD) occurs in the sludge blanket, and elutriation can be used to create an enhanced readily biodegradable chemical oxygen demand (rbCOD) concentration in the primary effluent, precious for the subsequent secondary process.

This thesis focuses on developing a reactive primary clarification process at pilot-scale as a mainline fermenter. The operating parameters studied are: SRT, internal recirculation rate, coagulant dosing, and pH conditioning. Those will be implemented one by one in the system, to understand their effect by itself and the synergies among them. The ultimate goal is indeed to reach the best process configuration in view of an enhancement of volatile fatty acids (VFA) in the primary effluent.

Chapter 2: Background and Literature Review

The production of wastewater is the direct consequence of the use of water in any type of human activity, whether residential or institutional, commercial and industrial (ICI). With a view to safeguarding the environment and its delicate natural balance, wastewater must be subjected to purification processes.

Especially in recent years, urban wastewater treatment plants are increasingly required to implement treatment process improvements to meet the stringent nutrient discharge limits while maintaining low operating costs. Therefore, a growing need for scientific research and greater investments in the urban purification sector are occurring, focused on the search for more efficient treatment processes.

Initially, wastewater treatment plants (WWTP) were built with the aim of targeting the removal of solids and organic contaminants only, placing load and concentration discharge limits on the total suspended solids (TSS) and biochemical oxygen demand (BOD), respectively. While the TSS represents the solid fraction present in the water (retained at 1.2 μ m filtration), the BOD represents the amount of oxygen required by the microorganisms to assimilate and degrade the organic substances present in the sewage. The higher the concentration of the organic substances present in the sewage, and the higher the rate at which they are degraded by microorganisms, the higher the oxygen demand.

Over the last few years, treatment plants were facing tremendous changes in regulatory requirements. Stringent limits were implemented to avoid, or at least to limit, the amount of nutrient loads discharged to water bodies. High loads of nitrogen and phosphorus can harmfully affect water quality and aquatic life leading to several issues, such as eutrophication (excessive nutrient availability), and thus harmful algal blooms. Algal blooms correspond to a very high level of algae that leads to green water surfaces. This phenomena happens mainly where the salinity is low, namely in lakes and rivers. Algae growth is reported to be a threat for aquatic life and human health [1]. By limiting the nutrient loads to water bodies, regulators thus aim to preserve the natural environment conditions.

The removal of nutrients (nitrogen and phosphorus) can be carried out through biological treatment processes that involve the use of microorganisms.

In the plant's influent, the nitrogen is mostly present as ammonia nitrogen ($\text{NH}_4\text{-N}$) and organic nitrogen, while the amounts of nitrous or nitric nitrogen are low or zero.

The classical biological removal of nitrogen (BNR) foresees a series of reactions that lead first to the oxidation of the ammonia up to nitrate (nitrification) and later to the reduction of this nitrate to elementary nitrogen (denitrification). Nitrification occurs mainly by chemoautotrophic bacteria whose carbon source for growth is represented by CO_2 or bicarbonates and energy derives from the oxidation of ammonia to nitrite and nitrite to nitrate. The denitrification takes place thanks to heterotrophic bacteria that use carbonaceous organic substrate for cellular reproduction and can use both molecular oxygen and oxidized compounds (nitrates, nitrites, sulphates, etc.), allowing the conversion of nitrate to nitrite and subsequently of nitrite into gaseous molecular nitrogen.

On the other hand, phosphorus is present in water in organic and inorganic form, can be soluble or particulate, in variable percentages depending on the origin and point of the plant where the analysis was carried out. With the regard to its origin, the presence of soluble inorganic phosphorus is due to the solubilization of the minerals crossed by the spring waters, while polyphosphates derive from the use of detergents and from metabolism. Organic phosphorus can go into solution and generate soluble inorganic orthophosphates or particulate phosphorus.

The biological removal of phosphorus from wastewater is known as enhanced biological phosphorus removal (EBPR). This is also referred to as "luxury uptake", because the removal method is based on stressing the operating conditions of the microorganisms to collect larger quantities of phosphorus than normal for their bacterial reproduction.

The phosphorus accumulating bacteria (PAO) use low molecular weight substrates (such as volatile fatty acids, ethanol, etc.) and can accumulate polyhydroxybutyrate (PHB) as an energy reserve. During anaerobic conditions, the bacteria use the energy released by the hydrolysis of the polyphosphates to accumulate these substrate in PHB. In aerobic conditions, they metabolize the PHB accumulated in the anaerobic phase to build new cells and replenish the polyphosphate pool, subtracting large quantities of phosphorus from the liquid phase. The heterotrophic biomass in the anaerobic zone performs a partial fermentation of the substrate increasing the concentration of the substrates available. This demolition is slower than the intake of low-molecular weight by PAO, thus limiting the process. The possibility of adding external or internal acetate sources makes it possible to limit the hydraulic retention time (HRT) of the anaerobic basin.

It is immediately evident that BNR and EBPR require significant amounts of carbonaceous organic substrate to perform their removal tasks, to meet the discharge limits. The carbon is externally supplied in the form of methanol, or acetic acid, but there is the possibility to produce it in situ and thus improve the sustainability of the treatment plant. This last option could be pursued even when the carbon is already present in the influent, but it is not enough.

The ability to recover energy and resources (i.e. nutrients) is indeed what is recently being pursued, as the WWTPs are now increasingly referred to as water resource recovery facilities (WRRF), within a circular economy context. In particular, the term circular economy refers to the ability of an economic system to be able to regenerate on its own, and guaranteeing its sustainability [2]. Wastewater facilities fit well in the circular economy. In fact, since wastewater is rich in energy and resources, treatment municipalities can avoid to use energy from utilities to perform all the required operational tasks, and external resources.

For example, fermenting the wastewater to produce volatile fatty acids (VFAs) and readily biodegradable chemical oxygen demand (rbCOD) to be used in subsequent biological nutrient removal (BNR) processes seems to be a sustainable process, having the additional advantage of decreasing secondary sludge quantities.

In this research, the fermentation of primary sludge is studied. Fermentation of primary sludge at WRRFs might eliminate the need for an external carbon source (acetic acid) for BNR and the energy required for producing it.

2.1 Primary Settler Tank

Within a conventional wastewater treatment plant (WWTP), two similar unit operations can be found at a different stage of treatment, primary and secondary treatment, sharing common task. These are known as settler, or clarifier, or sedimentation tanks.

Primary treatment has the objective to remove readily settleable solids and floating material, usually by means of sedimentation. Sedimentation, settler, or clarifier tanks are physical unit operations since they entail a physical force, i.e. gravity. By feeding the tank with wastewater, and providing a sufficient hydraulic retention time (HRT), particles present in the influent stream have the time to settle down to the bottom, and thus be removed.

Indeed, the settling tank aims to reduce the total solid suspended concentration (TSS). Primary settling tanks differ from the secondary ones in the different particles they aim to remove. However, both of them share common shape designs, namely circular or rectangular.

A raw or pre-treated discharge is characterized by a relatively low solids concentration, so that the sedimentation process takes place outside of the mass and compression sedimentation field, affecting instead the granular type of material. In the case of application in real installations, the design data obtained from a laboratory experience must be treated with a certain caution as the conditions that arise might be quite different from the theoretical.

In a real sedimentation tank due to the presence of the sewage inlet devices, it is never possible to distribute the inlet flow uniformly throughout the section, thus determining velocity differences.

Inlet velocity differences lead to necessary modifications of the design data based on the laboratory findings by adopting appropriate safety coefficients (indicatively an increase of 25-50% can be assumed for the tank volumes and surfaces). If a liquid containing solids is placed in a state of relative quiescence, the solids that have a greater specific weight than the liquid tend to settle, while solids with a lower specific weight tend to rise. These are the principles on which the design of primary sedimentation tanks is based: their purpose is the reduction of the solids content through the removal of the settling and floating solids.

The removal efficiency of the suspended solids is a function of the surface area of the tank, and the hydraulic retention time (HRT). The HRT, along with the surface loading area or overflow rate (OR), are the two main parameters to design a sedimentation tank. Typical design information for primary sedimentation tanks are reported in Table 1.

If the solid particles present in the wastewater had uniform size, density and shape, the removal efficiency would just depend on the surface of the sedimentation tank and on the retention time. The depth of the tank would have a limited influence, as long as the horizontal speed is smaller than that of the particles rising. In reality, the solids present are very heterogeneous and are susceptible to flocculation.

As shown in Table 1, primary sedimentation tanks are designed for retention times (HRT) between 1.5 and 2.5 hours, based on the inlet flow rate. Sedimentation tanks with lower retention times (0.5 - 1 hour) are generally used when this process is followed by biological treatment. In

the case of combined sewer system, it is advisable to check that a possible rainfall would not lower the hydraulic retention time below 30-40 minutes.

Table 1: Typical primary clarifier design information (Metcalf and Eddy, 2003).

Item	U.S. customary units			SI units		
	Unit	Range	Typical	Unit	Range	Typical
Primary sedimentation tanks followed by secondary treatment						
Detention time	h	1.5–2.5	2.0	h	1.5–2.5	2.0
Overflow rate						
Average flowrate	gal/ft ² ·d	800–1200	1000	m ³ /m ² ·d	30–50	40
Peak hourly flowrate	gal/ft ² ·d	2000–3000	2500	m ³ /m ² ·d	80–120	100
Weir loading rate	gal/ft·d	10,000–40,000	20,000	m ³ /m·d	125–500	250
Primary settling with waste activated sludge return						
Detention time	h	1.5–2.5	2.0	h	1.5–2.5	2.0
Overflow rate						
Average flowrate	gal/ft ² ·d	600–800	700	m ³ /m ² ·d	24–32	28
Peak hourly flowrate	gal/ft ² ·d	1200–1700	1500	m ³ /m ² ·d	48–70	60
Weir loading rate	gal/ft·d	10,000–40,000	20,000	m ³ /m·d	125–500	250

[†] Comparable data for secondary clarifiers are presented in Chap. 8.

The temperature influences the sedimentation process especially in cold climates, when, with the increase of the viscosity of the water, the solids removal efficiency of the clarifiers decreases as the sedimentation of the particles are delayed (Stockes' law).

Clarifiers can be classified depending on the mode with which the water moves in the tank. Therefore, settler tanks can either be:

- longitudinal or rectangular, movement of the flow from one end to the other in the sense from entry to exit;
- radial or circular, with the flow movement from the center to the periphery.

However, both categories fall within the horizontal flow sedimentation tanks. Selecting one type of clarifier, namely rectangular over circular, or vice versa, depends on several factors such as site conditions, plant size, and engineering valuation. The rectangular tanks are specifically suitable for solutions of “compact” plants, where there is a limited footprint availability. They suit

themselves well in small-medium plants. For large potentials, i.e. large plant size, circular tanks are generally cheaper and more convenient to build and operate. The symmetry that characterizes them makes it possible to obtain a very large overflow perimeter weir, without needing to adopt additional channels to contain the weir velocity, which is a normal practice in rectangular tanks.

Often, in wastewater treatment plants containing both primary and secondary treatment, primary tanks has rectangular shape, while secondary tanks are circular. The latter, which are characterized by low velocity to the weir, are necessary to ensure adequate efficiency in the removal of suspended solids, before discharging the effluent into the last disinfection basin. Moreover, as a rule of thumb, at least two primary tanks should be provided in order to guarantee a primary sedimentation treatment during possible maintenance periods [3].

2.2 Volatile Fatty Acids

VFAs are volatile fatty acids (carboxylic acids with an aliphatic chain) whose carbon chain is considered to be short (less than six carbon atoms). They are generally produced during the first stages of anaerobic degradation of organic matter. This degradation occurs mainly in anaerobic digesters (production of biogas) but also in natural metabolisms such as during digestion in ruminants. A measurement of the concentration of VFA in wastewater allows to know the degree of fermentation of the water. In anaerobic digestion, they are reaction intermediates and they can be inhibitors when reaching certain threshold concentrations. The main volatile fatty acids are:

- Acetic acid (CH₃-COOH)
- Propionic acid (CH₃-CH₂-COOH)
- Butyric acid (CH₃-(CH₂)₂-COOH)

Rarely, valeric acid and caproic acid and isomers (iso-butyric acid, iso-valeric acid) can be found. The importance of VFAs is recently raising in the market due to several applications in which they can be used. Those include the chemical, pharmaceutical and food industries [4]. In addition, VFAs can be potentially used as feedstock for the production of biogas, bioenergy and their by-product in general.

Although these acids were being mainly produced chemically, a biological way of producing them exist, and it involves waste stream sources such as food waste, and wastewater. The only biological process of converting organic waste to produce a valuable raw material, i.e. VFAs, is the anaerobic digestion, which will be explained in the next section.

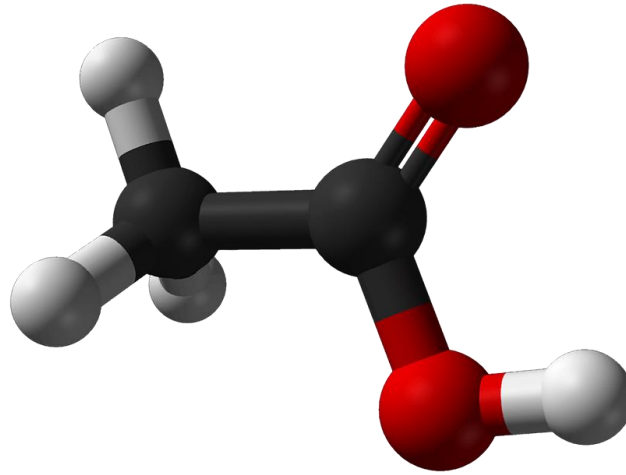


Figure 1: 3D molecular structure of the acetic acid (CH_3COOH).

The VFAs produced through the anaerobic digestion of wastewater is a valuable substrate for a variety of applications such as the production of biodegradable plastics, generation of bioenergy and biological nutrient removal [5]. This last VFA application strictly regards the topic of this study, since the aim of producing them on site from a waste stream (primary sludge) was to improve the biological nutrient removal performance.

2.3 Anaerobic Digestion

Anaerobic digestion (AD) is widely utilized to produce biogas from the decomposition of biological wastes by microorganisms in the absence of oxygen. The steps involved in the AD process are shown in Figure 2, and they can be optimized just for VFA production.

To enhance VFA production from primary sludge, the suspended organic matter present in it, such as carbohydrates, proteins, lipids, etc., should first be converted to soluble organic monomers (amino acids, sugars, fatty acids, glycerol, etc.) through hydrolysis reactions and then to VFA by acidogenesis. Due to the particulate form of the feedstock (primary sludge), the rate-limiting step in the fermentation process is the hydrolysis [6]. In particular, the difficulties that strictly or facultative anaerobic bacteria [7] face in hydrolyzing the primary sludge are related to its heterogeneous characteristics, and the presence of natural polymers with high molecular weight compounds, namely extracellular polymeric substances (EPS). Hence, increasing the hydrolysis

rate will be beneficial in terms of increased VFA production. In fact, the hydrolysis step degrades both insoluble organic materials and high molecular weight compounds such as lipids, polysaccharides, proteins and nucleic acids, into soluble organic substances (e.g. amino acids and fatty acids). These soluble organic components such as amino acids and fatty acids are then further converted in the second step, i.e. acidogenesis [6].

From literature, different studies [8] have been carried out to understand what are the crucial parameters and factors to speed-up hydrolysis. The main factors seem to be pH, temperature, hydraulic retention time, solids retention time, organic loading rate, particle size, type of substrates, microbial biomass, and additives. However, little has been done to see what it entails and what happens when those process parameters are implemented in a real treatment system fed continuously and aimed to work as a physical unit operation rather than as a biological operation, such a primary clarifier.

In the next paragraphs, the effects of the mentioned operating and environmental parameters affecting the VFAs production in a reactive primary clarifier are presented.

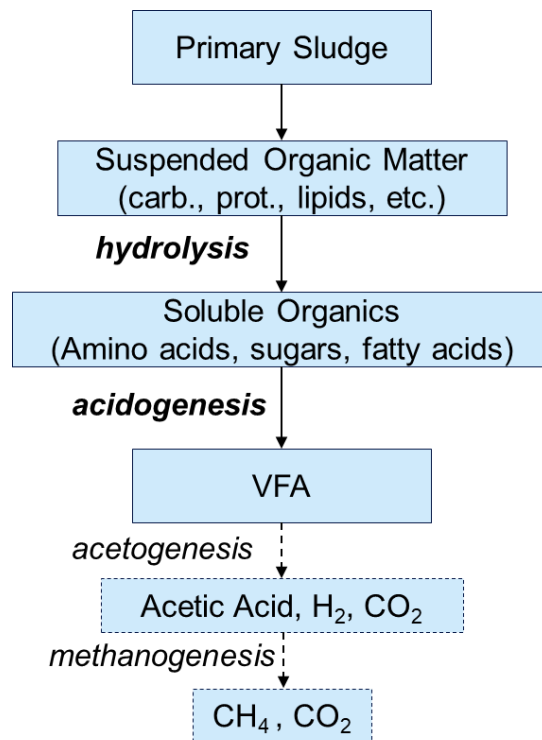


Figure 2: Biochemical reactions involved during the primary sludge anaerobic digestion.

2.4 Reactive Primary Clarifier

A reactive primary clarifier differentiate essentially from a conventional primary settler tanks both in its aims, and in its nature, but it maintains some common characteristic. First of all, it is important to highlight the fact that the conventional primary sedimentation tank is a physical unit operation, while a reactive or activated primary tank (APT) is a physico-biochemical reactor. In fact, in this latter case, there is not only the need for removing the settleable solids and so accomplish the physical treatment task, but there is also a biological purpose as well. The second and parallel aim of the reactive primary clarifier is to promote biochemical reaction within it.

For developing biological and chemical reactions, with high rates of reactions, elevated amount of biomass, or simply, solids is required. The fact that a sludge blanket is formed at the bottom of the settler tank due to particles sedimentation, it provides the right environment for developing such required conditions.

Under an operating point of view, the main difference between the conventional and the reactive primary clarifier is that the last one relies on creating a larger sludge blanket within the tank, and implementing an internal recirculation.

The sludge blanket height (SBH) can be defined as the height of the sludge from the bottom of the tank. In conventional primary settler tanks, the sludge blanket height is limited to avoid any possible particles resuspension.

An internal recirculation consist of pumping the sludge from the bottom of the primary settler tank back within it, but at a higher height than the bottom. In this way, the elutriation process can take place. The elutriation process consists in separating different type of particles, usually by means of an upward direct stream of gas or liquid [9].

In literature, only few studies report similar primary tank aimed at fermenting the sludge for a possible VFA production at a pilot-scale extent. Otherwise, most of the studies present in literature just focus on the optimum fermentation conditions to apply to the primary sludge, but not within the primary settler tank. The three most relevant studies are discussed below.

As shown in Figure 3, Chanona et al. [10] developed two type of schemes for producing VFA from primary clarifier. While one configuration foresees a side-fermenter located on the sludge line (Figure 3, b), the other set-up consists in the same 112L primary clarifier tank without

a fermenter, but with an internal recirculation for elutriation purpose. The tank was maintained at a constant temperature of $20 \pm 1^\circ\text{C}$ thanks to a glass-fiber cover, and fed with municipal raw wastewater.

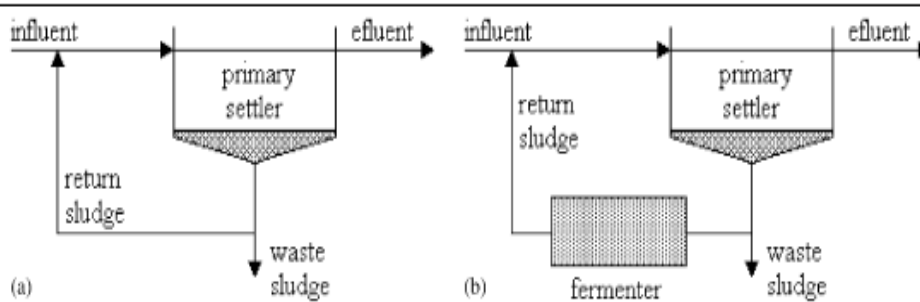


Figure 3: Reactive primary clarifier scheme (a), side-stream fermenter (b) (Chanona et al., 2006).

Since one of the main purpose of this study was to establish an algorithm able to find the optimum sludge recirculation and sludge waste flow rate based on effluent concentration of VFA, and sludge blanket height (SBH), they ran three experiments. The effluent VFA could indeed be compared to the influent VFA to see if any production has occurred or not, i.e. whether the reactive primary clarifier is enhancing the VFA production or not. The SBH instead could be associated with the amount of sludge present within the tank, thus it is associated with the SRT, and the amount of acidogenic bacteria present. They tracked the sludge blanket height, through a light transmission measurement.

During their experiments, they set two different SRTs (3.7d and 4.7d), and two different return flow rate ratios (3.75% and 5% of the influent flow rate). This study also explains how these two parameters (SRT and return flow rate), can be operationally changed. For example, a SRT decrease in such a reactive primary tank could simply be performed by increasing the flow rate of the sludge waste. In this way, less solids, thus less biomass, will be present within the reactive primary clarifier, thus a smaller SRT will be achieved.

In particular, they found out that when they generally reduce the SBH, or the SRT, to a certain extent, lower performance are reported in terms of VFA production. However, for low SBH, they report that by increasing the internal recirculation flow rate, higher concentration of VFA can be found in the effluent stream.

Besides, it is important to note that an SRT of less than five days, and low return flow rate ratio up to 5% the influent one were here adopted. The performance achieved are summarized in

Table 2, where the VFA production represents the difference between the effluent and the influent VFA concentration.

Table 2: Reactive primary clarifier performance, in terms of VFA production and solids removal efficiency (Chanona et al., 2006).

		Experiment 1	Experiment 2	Experiment 3
Operating conditions and influent characterization	Solid retention time (d)	3.8	3.7	4.7
	Influent flow rate (L/h)	40.0	40.0	40.0
	Return flow rate (L/h)	1.5	2.0	2.0
	Return flow rate ratio (% Q _{IN})	3.75%	5.0%	5.0%
	TSS (mg/L)	205.1	297.4	226.5
	VSS (mg/L)	139.1	197.4	137.5
	VSS/TSS	68%	65%	61%
	Soluble COD (mg/L)	74.1	113.6	114.9
	Total COD (mg/L)	342	463	382
	SCOD/TCOD	22%	25%	30%
	VFA (mgCOD/L)	9.1	17.3	6.2
	VFA/SCOD	12%	15%	5%
	pH	7.7	7.7	7.7
Performance parameters	VFA production (mgCOD/L)	12.0	20.4	25.4
	TSS removal efficiency (%)	35%	29%	35%

As Chanona et al. [10], even Bouzas et al. [11] used a very similar pilot-scale reactive primary clarifier with the same tank dimension size of 112L in a controlled temperature of 20°C. The configuration allows to operate the activated primary tanks showed in Figure 4 either with or without the side-stream fermenter. The in-line configuration is based on the same principle of elutriation mentioned earlier. The sludge settled at the bottom of the clarifier is in part recycled, i.e. it is mixed with the influent in order to elutriate the VFA out of the sludge. The influent was the raw municipal wastewater from the wastewater treatment plant of Valencia, and it had set flow rate of 40L/h.

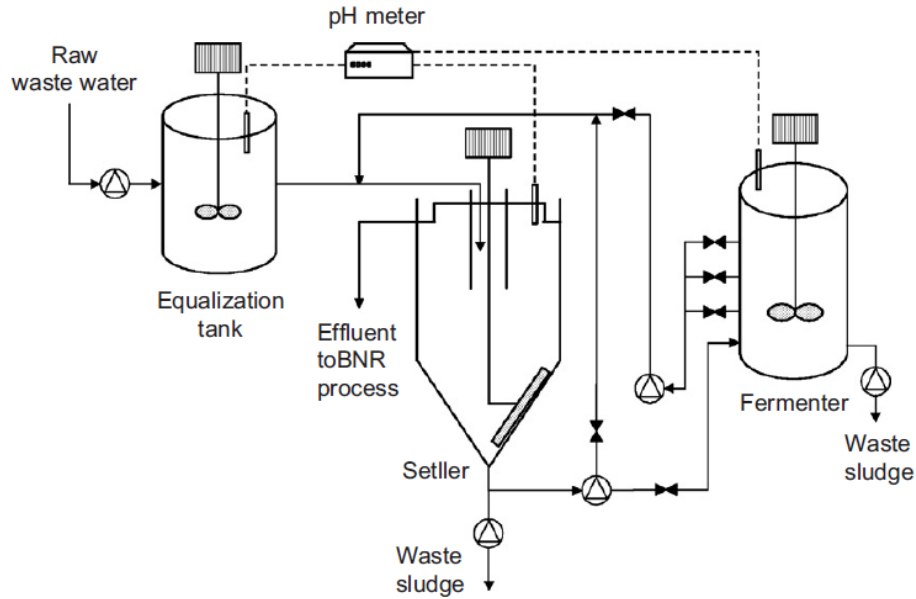


Figure 4: Reactive primary clarifier scheme equipped with complementary side stream fermenter (Bouzas et al., 2007)

Several experiments were carried out to find out the effects of the SRT in the process performance, which again involves the VFA production, or more specifically, the VFA yields. The VFA yield represented the difference between the effluent and outlet VFA amounts, normalized by the biomass present in the influent, which was indicated as volatile suspended solids (VSS).

In-line configuration at SRT of 7d, 7d, and 8d, resulted in VFA yields of 97.8, 110.3, and 165.9 mg/gVSS, respectively. However, at the same time low solids removal efficiency are found, namely around 30-35%. The latter is something similar to what reported previously for Chanona et al. study [10], but a value of at least 60% is expected if compared with conventional primary clarifier performance.

However, the low solids removal efficiency did not seem to be related to high sludge blanket height, but just to the solids retention time. In fact, the authors explained that a long retention time could deteriorate the settleability characteristics of the solid particles, leading to poor solids removal performance. In particular, it should be noted that the adopted SRT was up to eight days for “Experiment 3” (see Table 3).

Furthermore, Bouzas et al. also noticed that the long solid retention time did not seem to have any effect in the release of phosphorus and nitrogen. Also, they found very low pH variations.

Table 3: Main operational and performance parameters for the in-line reactive primary clarifier (Bouzas et al. 2007).

		Experiment 1	Experiment 2	Experiment 3
Operating conditions and influent characterization	Solid retention time (d)	7	7	8
	Influent flow rate (L/h)	40.0	40.0	40.0
	Return flow rate (L/h)	1.5	2.0	2.0
	Return flow rate ratio (% Q _{IN})	3.75%	5.0%	5.0%
	TSS (mg/L)	205	298	227
	VSS (mg/L)	139	203	138
	VSS/TSS	68%	68%	61%
	Soluble COD (mg/L)	74	114	115
	Total COD (mg/L)	342	473	382
	SCOD/TCOD	22%	24%	30%
	VFA (mgHAc/L)	8.5	16.2	5.8
	VFA/SCOD	12%	14%	5%
	pH	7.7	7.7	7.7
Performance parameters	VFA production (mgHAc/L)	13.6	22.4	22.9
	VFA yield (mgHAc/g VSS)	97.8	110.3	165.9
	TSS removal efficiency (%)	31%	31%	35%

Jin et al. designed a pilot scale reactive primary clarifier fed with municipal raw wastewater at a flow rate of 0.5m³/h. Figure 5 shows the scheme, where two different compartments can be clearly distinguished. The elutriation unit is separated from the sedimentation one. The elutriation unit is indeed located upfront the sedimentation part and it is equipped with a stirrer that could further break into smaller particles (more degradable) the large organic particles present in the sludge. In fact, this unit aims to mix the two influent streams, namely the influent and the recirculated primary sludge, and maximize the VFA production. The total volume of the described reactive primary clarifier is 0.95m³.

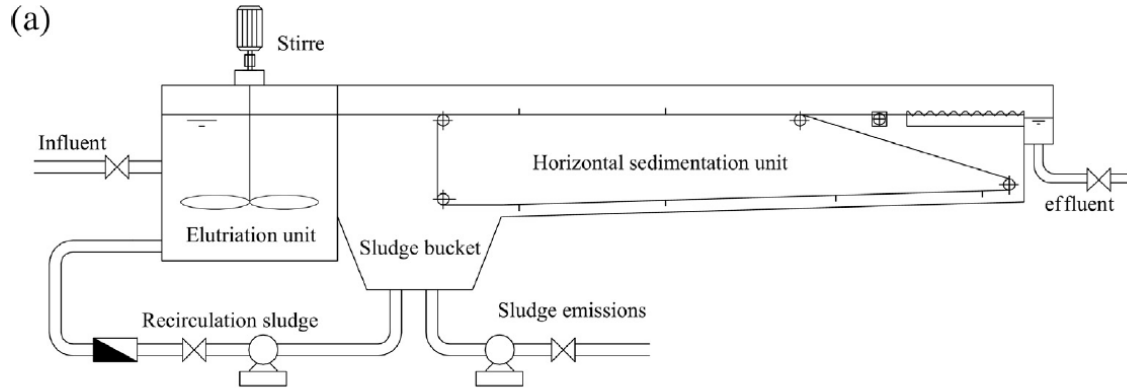


Figure 5: Activated primary tank scheme (Jin et al., 2016).

Five different SRT were tested, namely 1, 3, 5 and 7d. While during the lowest SRT of one day almost no VFAs were produced, they reported that increasing the SRT from 3d to 5d the VFA production were greatly enhanced (up to 50%). However, a SRT of 7d might be excessive since no further increase was reported, and the VFA production showed very similar value of the 5d experiment. In particular, for SRT of 3d and 5d, the measured VFA production was 12.3mg/L and 18.8mg/L, respectively. In particular, the optimal conditions in terms of an enhanced effluent VFA concentration for this specific reactive primary clarifier equipped with an upstream mixing section, were found to be SRT=5d, $G=152s^{-1}$, RSR=10%.

Table 4: Influent wastewater characteristics (Jin et al. 2016).

	TSS (mg/L)	TCOD (mg/L)	SCOD (mg/L)	SCOD/TCOD
Influent characterization	241 ± 43	342 ± 32	149 ± 24	44%

Retention Time: The retention time is one of the most important parameters in the production of VFA, as reported by many authors ([11], [12]). A relatively low retention time can avoid the growth of methanogens [13], thus preventing any VFA consumption for methane generation. In fact, once a certain (a minimum) retention time is reached, acidogenic microorganisms start to hydrolyze the particulate organic matter present in the sludge matrix. However, an excessive SRT increase could lead to short-chain fatty acid consumption, by acetogenesis and methanogenesis. The parameters found in literature vary widely depending on the type of substrate and reactor used.

Ahn and Speece [14] indicated an optimal retention time of five days for batch and semi-continuous systems. The same sludge retention time of five days was also reported to be optimal for a continuous system (pilot-scale clarifier) by Jin et al [12]. On the other hand, a solids retention time larger than five days leads to a VFA production up to 23mg HAc/L and a low solids removal efficiency of only 35% [11]. This can be explained by considering the high sludge blanket height accumulated within the clarifier. Similarly, Jin et al. [12] also noticed that an SRT larger than seven days does not improve soluble COD and VFA production.

The way of manipulating the SRT in such a reactive primary clarifier is to simply increase or decrease the waste sludge flow rate, which allows to retain more or less solids in the settler tank. It should be noted that as the SRT increases, the sludge blanket height (SBH) increases too. As previously mentioned, an excessive sludge accumulation in the primary clarifier removes room for particle sedimentation and solids can be dragged directly to the effluent. To ensure a minimum VFA concentration in the effluent, a certain sludge blanket height has to be achieved. If the sludge blanket is too low, a higher recirculation flow rate is probably required to maintain the same elutriation performance [10].

Recirculation Sludge Flow: An internal recirculation sludge flow within a primary clarifier has recently been investigated at pilot- and bench-scale ([11], [12]). Such implementation, with a flow rate that is a low percentage of the influent flow rate, seems to provide a good way for elutriating the fermentation products (i.e. readily biodegradable COD) out of the sludge blanket to the effluent.

Jin et al. [12] and Bouzas et al. [11] reported optimum recirculation flow rates of 10% and 12% (of the influent). This leads to an increase for VFA or SCOD produced, and no side effects were observed in terms of settling. At the same time, an excessive flow rate may turn into excessive turbulence that can re-suspend the settled particles. However, this is true only when the return line pipe ends within the sedimentation basin. Also the pumping costs build up.

pH: The pH value is an important parameter to consider when referring to fermentation since it directly and substantially affects a multitude of aspects of the process. pH can be adjusted by means of chemical addition of bases or acids, and most of the authors ([7],[14],[15],[16]) agree that

increasing the pH is preferred for an increased hydrolysis rate of primary (PS) and waste activated sludge (WAS) feedstock. An alkaline environment can indeed enhance sludge solubilisation and potentially inhibit methanogens, which work at a pH range 6.8-7.2 [3].

However, Cokgor et al. [17] showed that alkaline pH control may have negative effects on VFA production, and they instead experienced a maximum VFAs yield of 127.5 mgCOD/g VSS for uncontrolled pH in a stirred reactor at 22°C. In fact, while an alkaline environment favoured hydrolysis (42.9% at pH 9.9, [16]), acidogenesis was not always enhanced [18]. Besides, the VFAs produced, due to their acidic nature, tend to reduce the pH (5.0-6.0).

Table 5: VFA yield for different substrates and operational conditions.

Feedstock	Conditions	Yield (mgCOD/g VSS)	Author
PS	pH 11, stirred batch, five days SRT, 25°C	312.9 (SCFAs yield)	[15]
WAS	pH 10, stirred batch, 35°C	235.46 (VFAs yield)	[18]
PS + WAS	pH 8.9, stirred semi-continuous batch, seven days SRT, 55°C	423.22 (VFAs yield)	[16]

Temperature: Temperature affects sedimentation performance in primary sedimentation tanks due to the change in viscosity, but most important of all, temperature affects bacterial activities and biological and chemical reaction rates. In particular, for anaerobic digestion processes, VFA production shows a significant increase as the temperature rises [13], [14]. In fact, the hydrolysis rate and the solubility of proteins and carbohydrates can be enhanced through heat source application. Fermentation is usually operated at different temperatures: mesophilic (30-45°C) and thermophilic (50-65°C). However, while an increased temperature environment seems to be preferred for sludge fermentation goals, no clear conclusions can be drawn on which temperature range is optimal for sludge fermentation [7]. On the other hand, applying heating on fermentation reactors is a high-energy demand, and thus it requires a careful cost-benefit analysis.

Chemically Enhanced Primary Treatment and Chemical Primary Sludge: Since CEPT is a well-established method for increasing the efficiency of solids (TSS) and organic removal (BOD)

in a primary treatment unit, it is interesting to see the effect of such a primary sludge (which contains chemical) related to the anaerobic digestion, and thus to the VFA production. This enhanced primary treatment is widely adopted because it has the benefit to be easy to retrofit in existing facility and it does not have a high capital cost, but just operational cost due to the use of chemicals. Due to the higher removal of organic amount, the organic matter that reaches the downstream biological compartment will be lower, thus resulting in less aeration energy being required. Besides, the primary sludge will contain higher COD concentrations that can be transformed to biogas through anaerobic digestion, or in fermentation products as it will be highlighted in this research.

Coagulant addition is a common practice for increasing solids removal efficiency at a primary treatment level. Municipalities use metal salts to remove non-settleable particles such as colloidal particles. These particles are characterized by small particle size (less than $1.0\ \mu\text{m}$) and negatively charged surfaces. Due to the repulsive forces among them, and to the high retention time required to settle small particles, they are difficult to remove. By means of metal salts addition, and proper mixing steps, the negative charges can be neutralized leading those particles to aggregate and settle (flocculation). In particular, the primary sludge present in a treatment plant that uses metal salts will thus contain these chemicals, i.e. metals such as Fe, Al. Furthermore, iron and aluminum salts have the additional advantage that they can also be used for phosphorus control since it can be removed from the water stream through a chemical precipitation reaction.

Considering an anaerobic digestion process for a chemically enhanced primary treatment sludge, it is reported that it has a poorer degradability compared to simple primary sedimentation sludge [19]. This is because the chemical sludge flocs may create a sort of barrier effect, which makes them even more difficult to hydrolyze.

However, the use of iron versus aluminum salts entails different operational issues. In fact, Lin et al. [19] showed that, while Al-sludge forms strong bonds with particles and phosphorus, during anaerobic conditions, the Fe-sludge particles dissolve since ferric (Fe^{3+}) is transformed to ferrous (Fe^{2+}). Thus, the settled particles can be hydrolysed at the same rate as simple primary sludge. On the other hand, a higher soluble phosphorus release is expected for Fe enhanced sludge.

Therefore, for a CEPT, which has the goal, in addition to enhanced solid removal, to have high VFA production, the best coagulant is FeCl_3 .

In addition, regarding the ideal pH value for a CEPT sludge, different authors ([19], [20]) reported that for Fe-sludge an alkali treatment (pH of 10) can decrease the iron solubility and control phosphorus re-release by 50%, but the VFA yield will be lowered by 20% due to a decreased sludge degradability [21].

To summarize, pre-treatment steps were found to be crucial to accelerate the hydrolysis of a complex and heterogeneous material such as primary sludge, which then may lead to an increased rbCOD (ideally VFA) concentration in the primary effluent. Although these pre-treatments might be easy to implement at bench scale, difficulties might arise for pilot- or even full-scale plants. In particular, from the three analyzed literature studies, it could be noticed that the ways of enhancing VFA amount in the primary effluent usually consist in adjusting both operating and environmental parameters. For example, the retention time is adjusted by controlling the system SRT through the waste valve. Or, in view of elutriating the fermentation product out of the sludge matrix, introducing an internal recirculation line or a mixing unit were used. Also, the return line, due to the higher chance for sludge particles to get in contact with each other, favours the hydrolysis. Furthermore, while for a temperature control a sophisticated heating coil or cover would be required, adding chemicals to change pH or to improve solids removal performance would be operationally easy.

Chapter 3: Materials and Methods

Pilot-scale experiments were conducted at the pilEAUte facility (Université Laval) to determine the effect of different factors, such as retention time, elutriation, and chemical addition on the fermentation process in a primary clarifier in order to increase the hydrolysis rate of organic matter and thus to enhance COD solubilisation.

The plant is continuously fed by domestic wastewater coming from the adjacent university's campus. The plant configuration reported in Figure 6 consists of a pumping station, a storage tank, a primary settler and two parallel biological treatment lines followed by secondary clarifiers. Each biological line has five reactors: the first two anoxic and the last three aerobic.

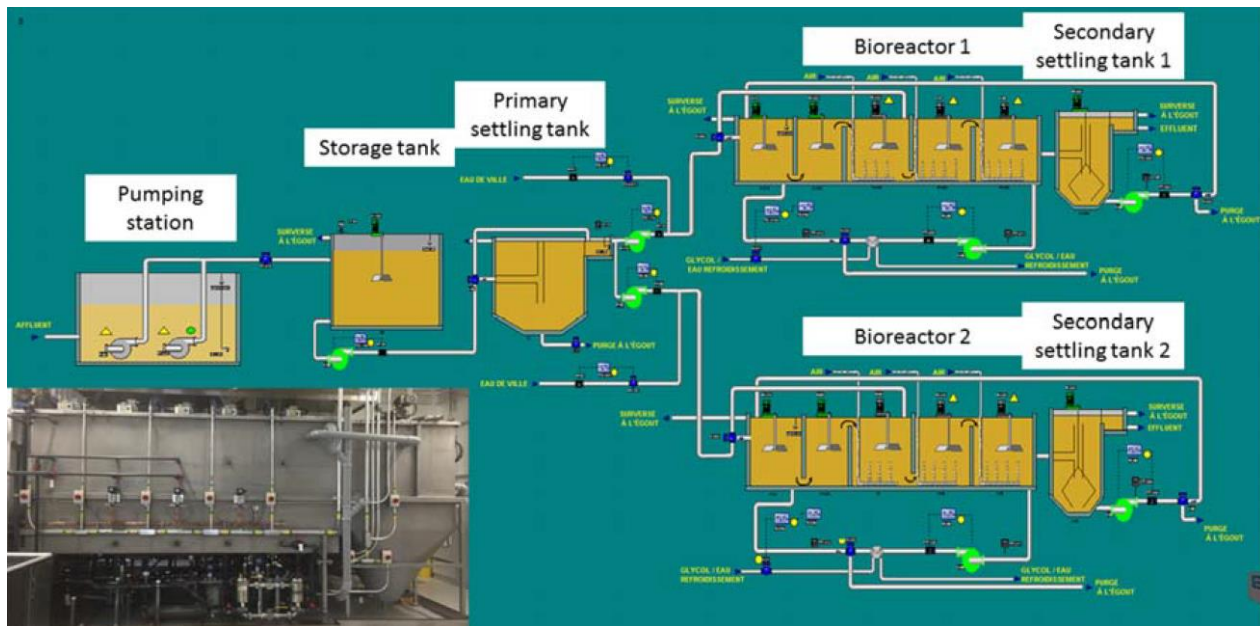


Figure 6: Scheme of the pilEAUte facility.

Beside the high process flexibility of the plant, the pilEAUte is online monitored with sensors at different locations: primary outlet, biological reactors, biological recycle stream and secondary outlet. Furthermore, refrigerated autosamplers can be used to grab samples.

Information about the pilEAUte's online monitoring system at the primary effluent is given in Table 6.

Table 6: Online sensors and monitored parameters located at the primary effluent.

Sensor	Monitored Parameters	Principle
spectro::lyser	T-COD, S-COD, TSS	UV-VIS spectrophotometry
ammo::lyser	NH ₄ -N, K, Temperature, pH	Ion selective electrode
Varion	NH ₄ -N, K, Temperature	Ion selective electrode
Conductivity meter	Conductivity, Temperature	Potentiometric

There are five different main parameters that were found (see References) to affect the solubilisation process and that will be investigated. Those are the sludge retention time (SRT), internal recirculation flow rate, a flocculant addition (FeCl₃), pH, and temperature.

Figure 7 shows the detailed set-up of the reactive primary clarifier where the influent is represented by the outlet of the storage tank (that is used as an equalization tank), and two possible outlet. One, on the right, is the primary clarifier effluent, while the other one is the waste stream regulated by an automatic back valve. The internal line recirculates the waste stream from the bottom of the tank to the sludge blanket zone at a fixed height (0.50m from the tank's bottom). It also should be noted that a different ending pipe height might have affected the results. In addition, Figure 7 shows the dosage points for chemicals, i.e. within the Clifford cylinder.

The parameters and their studied values are listed below:

- SRT 1d, 3d
- Internal Recirculation (Q_R) 0%, 14%, 50% of Q_{IN}
- NaHCO₃ dosage 0mgHCO₃/L, 100mgHCO₃/L
- FeCl₃ dosage 0mg/L, 20mg/L
- Temperature uncontrolled (seasonal changes)

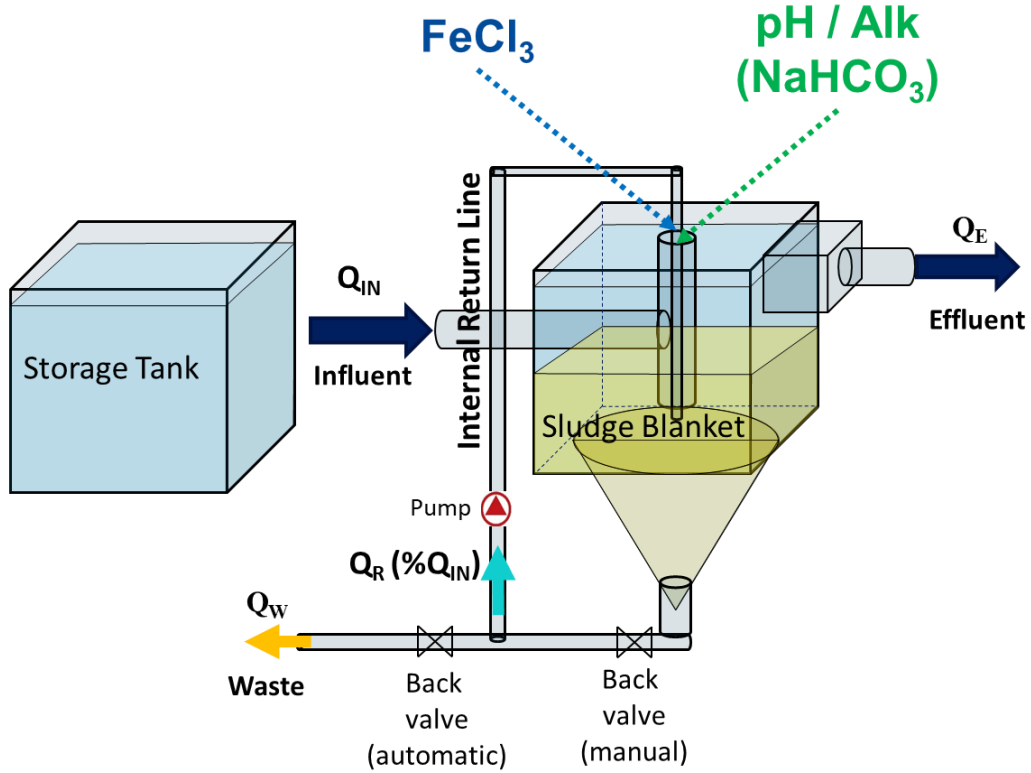


Figure 7: Process scheme of the modified primary clarifier.

Eight experimental stages have been carried out, and the main operating parameters are summarized in Table 7.

Table 7: Summary of the operating and environmental conditions for stages #1 to #8.

Stage	Flow rates			HRT	SRT		Chemical Dosages		Time for steady-state	Start-up Period
	Q_{IN}	Q_R	Q_W	HRT_{EFF}	$SRT_{DESIRED}$	SRT_{ACTUAL}	$NaHCO_3$	$FeCl_3$		
#	m^3/d	$\%Q_{IN}$	m^3/d	h	d	d	$mgHCO_3/L$	mg/L	d	d
1	26.4	0%	0.096	2.0	1	0.74	0	0	3	6
2	38.4	0%	0.04	1.4	1	1.51	0	0	3	3
3	16.8	50%	0.04	2.1	1	1.51	0	0	3	4
4	16.8	50%	0.02	2.1	3	1.83	0	0	9	7
5	16.8	14%	0.02	2.8	3	0.80	0	0	9	18
6	16.8	14%	0.02	2.8	3	0.74	100	0	9	8
7	16.8	14%	0.02	2.8	3	1.16	0	20	9	7
8	16.8	14%	0.02	2.8	3	1.00	100	20	9	14

To reach steady state conditions, it was assumed that a minimum of 3 times the SRT must elapse before starting the sampling activity. The SRT of a system is commonly defined as the mass of biomass in the reactor divided by the mass of wasted biomass per unit time.

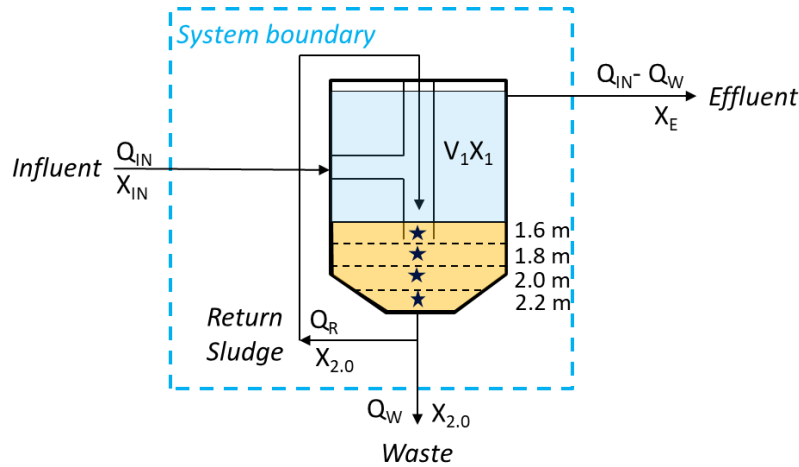


Figure 8: Schematic mass balance representation of the primary clarifier.

In fact, Equation 1 is derived from the biomass mass balance of the studied system showed in Figure 8, which can be generally worded as [3]:

Rate of accumulation of microorganisms within the system boundary	=	Rate of flow of microorganisms into the system boundary	-	Rate of flow of microorganism out of the system boundary	+	Net growth of microorganism within the boundary
---	---	--	---	---	---	--

which leads to:

$$SRT = \frac{V_1 X_1 + \sum V_i X_i}{Q_W X_{2.0} + (Q_{IN} - Q_W) X_E} \quad \text{Equation 1}$$

Where:

- V_1 = volume of the supernatant. L^3
- X_1 = TSS concentration in the supernatant M/L^3
- $\sum V_i X_i$ mass of sludge in the settler. Function of the sludge blanket height (SBH) M
- Q_W = waste sludge flow rate L^3/T
- $X_{2.0}$ = TSS concentration at 2.0m of immersion M/L^3

- X_R = TSS concentration in the waste sludge flow M/L^3
- X_E = TSS concentration in the effluent M/L^3

Furthermore, Equation 1 is based on the biomass balance with the following assumptions:

- X is a TSS concentration, rather than VSS (biomass). This is because the VSS/TSS ratio was observed to be close to 100% (see Table 9, Table 10, Table 12, Table 15, Table 18, Table 21, Table 24, and Table 27).
- No biomass from the inlet;
- X_1 could be considered equal to the TSS concentration in the effluent ($X_1=X_E$);
- If available, the TSS concentration of the waste stream is equal to the TSS value at 2.00 m of immersion ($X_{2.0}$), or it is equal to the TSS waste value from a composite sample measurement.

Sampling locations

Primary influent, effluent and waste from the pilEAUte facility in Université Laval, Quebec City, were used for these experiments. Composite samples of 50 mL collected each 15 min during a full day were collected by refrigerated autosamplers located at the three different locations illustrated in Figure 9.

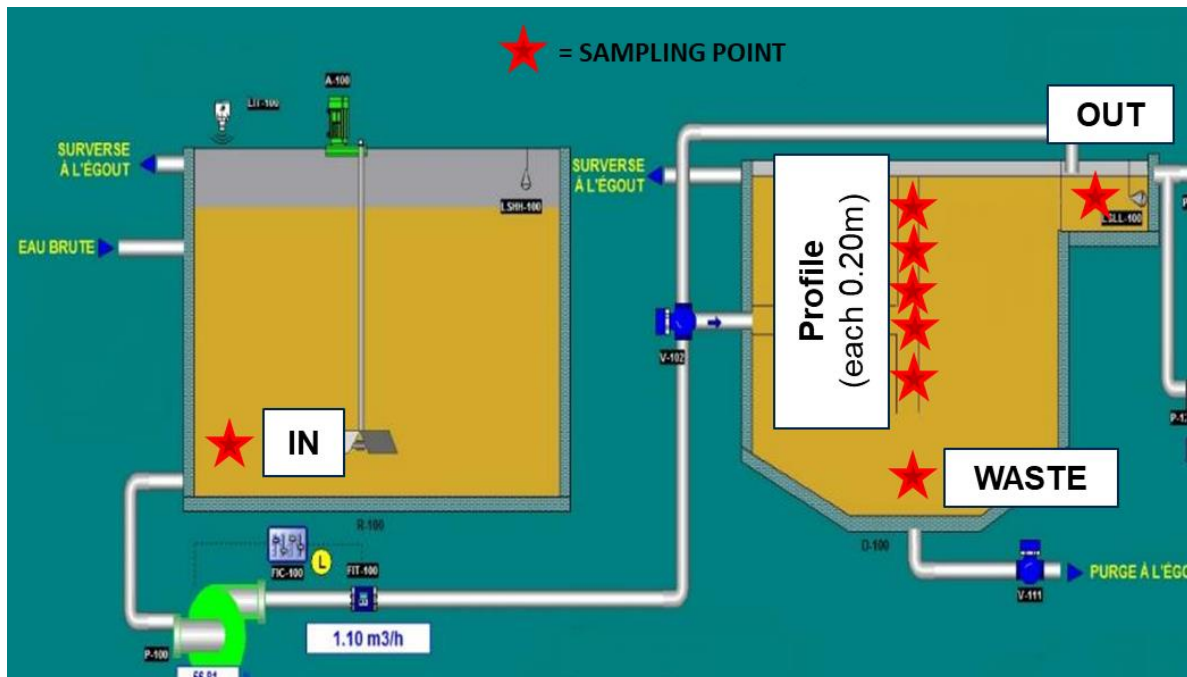


Figure 9: Overview of the storage tank and primary clarifier and the sampling locations.

During the experiments, a turbidity meter or manual sampling along the settler's height (each 0.20m) were used to track the sludge blanket behaviour, i.e. height and TSS concentration. TSS concentration profiles were used as a way to track the behaviour of the sludge blanket. In addition, from the samples taken at different heights, other important parameters can be obtained as well. These include VFA and alkalinity concentrations, and pH values. Also, it should be added that the wastage is done by an automatic valve opening for a fixed time period. In order to have a real idea of the SBH, the TSS concentration profile is precautionarily measured just before the valve opens.

It should be noted that the sample points located at 2.29 m of immersion, (equivalent to 0.00 m height and represented by the sampling point; see Figure 7) and 2.20 m of immersion will not be shown on the profile plots in the following sections. This is because of the presence of the return flow rate, which could result in local mixing conditions, and thus leading to unrepresentative values.

Table 8 shows the target parameters measured. The lab measurements were carried out on the overall composite sample of the one-day sampling activity.

Table 8: Investigated parameters of the pilot experiments.

	TARGET	SOURCE	METHOD	Replicates
SOLIDS	TSS	In, Out	Probes	-
	TSS, VSS	In, Out, Waste	Lab	3
	TSS profile	Primary clarifier	Probe (Turbidity meter), samples each 0.20m	
CARBON	T-COD, S-COD	In, Out, Waste	Lab (Hach kit)	3 for total, 2 for soluble
	T-COD, S-COD	Out	Probe (spectro::lyser)	
	VFA	In, Out, Waste	Lab (Titrimetric)	1
NUTRIENTS	Total-TN, Soluble-TN, NH ₄ -N	In, Out, Waste	Lab (Hach kit)	3 for total, 2 for soluble

	NH ₄ –N	Out	Probe (ammo::lyser)	-
	TP, PO ₄ -P	In, Out	Lab (Hach kit)	3 for total, 2 for soluble
Other physical-chemical properties	pH, T, K	Out	Probes	
	Bicarbonate Alkalinity	In, Out, Waste	Lab (Titrimetric)	1

Analytical methods

Total suspended solids and VFA measurements were conducted following the established SOPs (Université Laval). For the lower layers of the TSS profiles, and for the Waste samples, a TS% was carried out, instead of a TSS. This was due to the thickness of the sludge, and it was then converted into mg/L by assuming a sludge density of 1000 kg/m³. The procedure consisted in placing a certain amount of sludge on an aluminum dish, which was then inserted in the oven at 105°C overnight, and recorded the weight before and after the oven step. For the remaining lab measurements, the procedures provided by Hach were followed.

Performance parameters

The selected performance parameters are related to the fermentation and hydrolysis processes, since the goal is to have a primary clarifier that can act as a mainline fermenter. Indeed, the main aim of hydrolysis is the solubilisation of the solid organic fraction in the sludge.

The “COD solubilisation” and the “VFA production” are the concentration differences between the values at the outlet and inlet. Hence, a negative value indicates a consumption instead of a production.

The hydrolysis and VFAs yields are measures for the degree of fermentation, and they represent the amount of solubilized matter converted to soluble COD or VFAs [22].

$$\text{Hydrolysis yield} = \frac{SCOD_{OUT} - SCOD_{IN}}{TCOD_{IN}} \cdot 100 \quad \text{Equation 2}$$

$$VFAs\ yield = \frac{VFA_{OUT} - VFA_{IN}}{VSS_{IN}} \quad \text{Equation 3}$$

- VFA_{OUT} , VFA_{IN} , and VSS_{IN} are mass loads (M/T)
- VFA_{OUT} is only the effluent mass load; it does not consider the waste stream.

In addition, it should be noted that E% (removal efficiency) calculations for TSS, T-COD, S-COD, P-COD, VFAs, T-TN, S-TN, and NH_3-N are based on concentrations values, not on mass loads since it is assumed that the waste stream is negligible.

Data Analysis

The four investigated treatments or factors had a mixed number of two and three levels. In particular:

- Factor A: SRT – 2 levels (1d, 3d)
- Factor B: Q_R – 3 levels (0%, 14%, 50% Q_{IN})
- Factor C: $FeCl_3$ – 2 levels (0, 20mg/L)
- Factor D: $NaHCO_3$ – 2 levels (0, 100mg/L)

However, as could be seen in Table 7, the collected data did not follow a rigorous method to be used for a detailed statistical analysis. Although two or three levels for each factors were set, the gathered data did not follow any of a two or three factorial designs normally used in statistical analysis. In fact, three-, and in particular two-level factorial and fractional factorial designs are usually used due to their usefulness [23].

In this case, the analysis was then more complicated, but the data could be still analyzed as undesigned or historical data. However, it was important to be aware of possible correlations that would affect the conclusions. In particular, the temperature and the achievement of steady-state (SS) conditions probably affected the results. Because temperature might have stimulate bacterial activity, and a steady state condition guaranteed that, any conclusions drawn from the observed system, performance were time independent.

When analyzing undesigned data is indeed important to firstly understand the question that has to be answered through a statistical analysis of such an undesigned dataset. In accordance with the research objective, the question was to determine the effects of the four factors, and (possibly) the interactions among them that lead to an enhancement in the VFA yield (and/or on the solids removal efficiency, E%TSS). In other words, what was/were the most important factor/s affecting the VFA yield (and E%TSS). Also if any interactions between those factors existed or not.

Secondly, before drawing any conclusions, data had to be cleaned up. To obtain a preliminary impression of the relationship among the factors, the data were then plotted. Each factor was plotted against the two performance parameters, namely the solids removal efficiency, and the VFA yield.

Thirdly, the significance of effects was then determined by using an analysis of variance (ANOVA) approach. Linear models through R software were determined to identify any significant effects (both main effects and interactions), distinguishing between two cases: achievement of steady state conditions or not.

Chapter 4: Results

Table 7 shows the different scenarios applied to the pileAUte primary clarifier in order to understand the best conditions for fermentation. As described in the materials and methods section, five main parameters were investigated in this study to see the individual and combined effects on VFA enhancement, solubilisation, and hydrolysis. For each of them two or three levels/values were implemented, and the level that has provided the better performance was set before implementing the next design parameters.

4.1 The Effects of SRT and Internal Recirculation Flow Rate

In this section, the effect of different sludge retention times, and the influence of an internal return line operating at different flow rates, on the fermentation performance of the reactive primary clarifier were investigated. Different authors carried out research on elutriation of primary sludge on reactive primary clarifier context, in particular:

1. Bouzas et al. [11] reported a VFA yield of around 100 mg/g VSS for a SRT of 7 days, but with low solids removal performance, i.e. 30%.
2. Jin et al. [12] reported a VFA yield of 12.3, 18.8, and 19.9 mg/L for 3, 5, 7 days of SRT.

4.1.1 One day SRT and no internal recirculation flow rate

Aiming to reach a sludge retention time of one day, two campaigns were carried out, namely Stage #1 and #2, both without recirculation (Table 7). By providing a minimum sludge retention time of around one day to the primary clarifier, the aim was to see if this was enough to have any VFA production or solubilisation.

TSS concentration profiles were used to track the behaviour of the sludge blanket. By means of the sludge blanket height (SBH), the achievement, or not, of the steady state condition could be easily deduced.

Looking at the two TSS profiles from Stage #1 (Figure 10), measured on two consecutive days during the sampling (1.1 beginning, 1.2 end), the sludge blanket height (SBH) showed a value of 0.80 ± 0.10 m. For Stage #2 instead, the SBH value was higher than in Stage#1. Although the TSS concentration profiles differed a lot between the two days (2.1 and 2.2), the sludge blanket height showed a stable value of around 1.0m. The higher height is probably because the loading

rate to the system was increased from 1.1 to 1.6 m³/h, while the waste flow rate was decreased from 96 to 40 L/d.

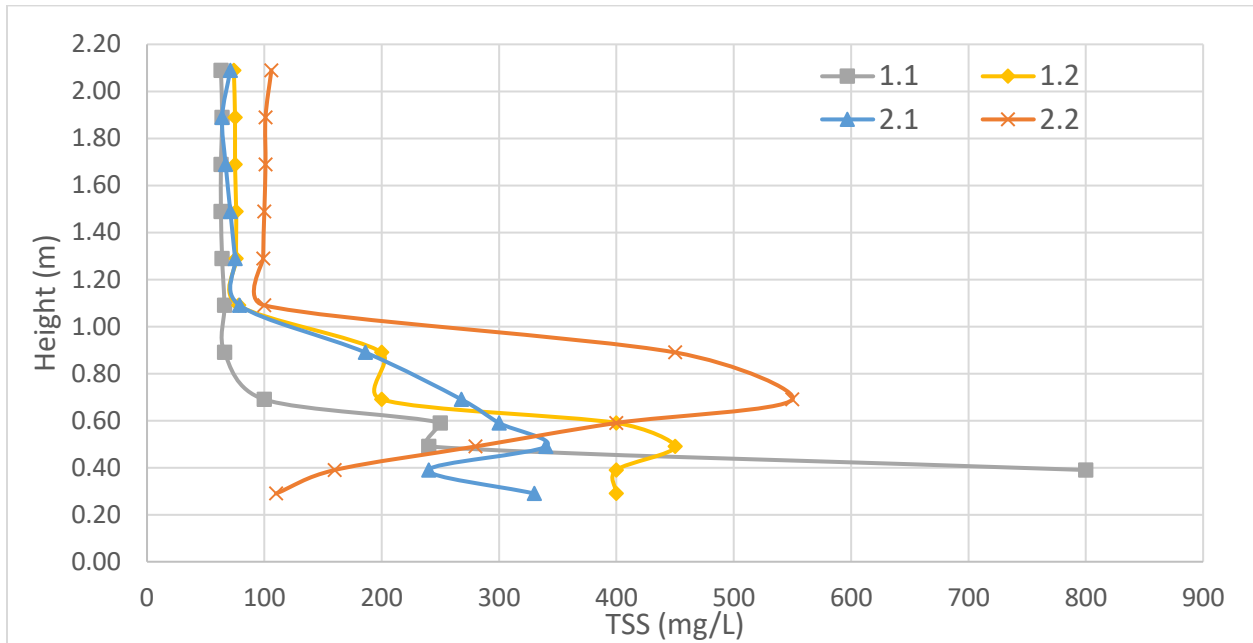


Figure 10: TSS concentration profile in primary clarifier by means of turbidity meter (Stage #1 and #2).

Important to note is that the turbidity meter used was not able to provide accurate values, and its use was limited to locating the sludge blanket. Lab measurements were carried out to measure the real TSS concentration. However, the lab measurements were only carried out for the bottom part of the primary clarifier and not for the whole height. This has affected the SRT estimation, since the solids concentration at the bottom was not representative of the complete sludge blanket. Referring to the TSS profile in Figure 10 it can be seen that there is a concentration gradient due to sedimentation.

A summary of the lab measurements carried out on the 24h composite samples from all three sampling locations, along with the removal efficiency (E %), can be found in Table 9 for Stage #1 and Table 10 for Stage #2.

The solids sludge concentration showed a value far above what was expected from the turbidity measurements, especially for Stage #2 where the loading rate was higher. In particular, the measured TSS value was around 10,800 mg/L. A value of around 60% of TSS removal efficiency, found for both stages, is in line with common primary clarifier performance.

In addition, low particulate nitrogen are measured for the waste, i.e. 1.55 gN/gCOD. Common values for municipal wastewater are instead in the range 6-10% of gN/gCOD. However,

these low values are due to analytical errors. In fact, as established from a later lab analysis (Li and Tohidi, 2019), the total TKN digestion was incomplete during this campaign.

Table 9: Lab measurement and removal efficiency based on triplicates for total and duplicates for soluble concentrations (Stage #1).

		SOURCE			
		IN	OUT	WASTE	E%
TSS	mg/L	232 ± 9	99 ± 9	4515 ± 994	58 ± 5%
VSS	mg/L	223 ± 3	93 ± 2	4436 ± 945	58 ± 5%
VSS/TSS		96 ± 4%	94 ± 10%	98 ± 31%	
T-COD	mg/L	495 ± 10	289 ± 5	6955 ± 829	42 ± 3%
S-COD	mg/L	93 ± 5	80 ± 2	665 ± 9	14 ± 6%
P-COD	mg/L	402 ± 11	209 ± 5	6290 ± 829	48 ± 3%
VFA	mgCH ₃ COOH/L	18.0	17.5	49.0	3%
T-TN	mg/L	54.8 ± 2.4	53.1 ± 5.5	108.5 ± 9.0	3 ± 7%
S-TN	mg/L	44.1 ± 1.3	43.6 ± 3.0	39.1 ± 1.7	1 ± 5%
NH₃-N	mg/L	27.7 ± 0.9	27.1 ± 0.8	24.3 ± 0.1	2 ± 4%
TP	mg/L	16.0 ± 1.0	15.5 ± 0.3	65 ± 3.4	3 ± 7%
PO₄-P	mg/L	10.5 ± 0.12	9.6 ± 0.06	28.3 ± 0.45	9 ± 1%
PO₄-P/TP		66 ± 6%	62 ± 2%	43 ± 5%	

Table 10: Lab measurements and removal efficiency based on triplicates and duplicates for total and soluble concentrations, respectively (Stage #2).

		SOURCE			
		IN	OUT	WASTE	E%
TSS	mg/L	283 ± 7	121 ± 4	10826 ± 225	57 ± 3%
VSS	mg/L	266 ± 8	113 ± 1	10538 ± 186	58 ± 4%
VSS/TSS		94 ± 4%	93 ± 3%	97 ± 3%	
T-COD	mg/L	554 ± 12	305 ± 4	16150 ± 1129	45 ± 3%
S-COD	mg/L	107 ± 6	77 ± 2	428 ± 2	28 ± 6%
P-COD	mg/L	447	228	15700	49 ± 4%
VFA	mgCH ₃ COOH/L	25.1 ± 1.6	11.3 ± 0.4	183.8 ± 5.6	55 ± 8%
T-TN	mg/L	41.2 ± 2.5	39.3 ± 1.6	148.0 ± 4.2	5 ± 7%
S-TN	mg/L	32.5 ± 1.2	31.3 ± 0.6	24.4 ± 2.9	4 ± 4%
NH₃-N	mg/L	30.5 ± 0.4	27.6 ± 0.6	26.3 ± 0.1	9 ± 2%
TP	mg/L	18.6 ± 0.9	15.9 ± 0.2	89.1 ± 9.9	14 ± 6%
PO₄-P	mg/L	13.5 ± 0.3	10.2 ± 0.2	30.2 ± 0.7	25 ± 2%
PO₄-P/TP		73 ± 5%	64 ± 2%	34 ± 11%	
Alkalinity	mgHCO ₃ /L	151 ± 2	149 ± 4	140 ± 5	
pH		7.32	7.46	6.24	

Table 11: Process performance parameters (Stage #1 and #2).

	STAGE #1			STAGE #2		
	IN	OUT	WASTE	IN	OUT	WASTE
S-COD/T-COD	19%	28%	10%	19%	25%	3%
VFAs/S-COD	19%	22%	7%	23%	15%	43%
COD solubilization (mg/L)		-13.0			-30.3	
Hydrolysis yield		-3%			-5%	
VFA production (as mgCH ₃ COOH/L)		-0.5			-13.8	
VFA yield (as mgCH ₃ COOH/g VSS)		-2.5			-51.9	

The *COD solubilisation* and the *VFA production* (Table 11) are the concentration differences between the values at the outlet and inlet. Even if they are both negative, which means that no solubilisation or VFA production has occurred with the set SRT of one day, it can be noted that the *S-COD/T-COD* ratio increases from 19% to 28%, due to sedimentation for Stage #1, and similarly for Stage #2 from 19% to 25%.

Furthermore, for Stage #2, if compared to Stage #1, the amount of VFAs present in the sludge blanket and the *VFAs/SCOD* ratio increased from 49.0 mg/L to 183.8 mg/L, and from 7% to 43%, respectively. Thus, with the higher loading rate and the lower waste flow rate, a higher VFA concentration can be achieved in the sludge blanket, but the *VFAs yield* still shows a negative value. This means that fermentation conditions are achieved with a SRT of one day, but these produced VFAs cannot reach the effluent, which could enable the *VFAs yield* to become positive.

However, the reason of the negative *VFAs yield* value is uncertain. Even when considering the total *VFAs yield*, which also includes the VFA in the waste in the VFA_{OUT} term (Equation 3), a value of -51.1 mgCH₃COOH/L is calculated. It is hypothesized that some microbial communities consume VFAs which coincides with ammonia and phosphates removal percentages of 9% and 25%, respectively (Table 10). Still, such removal processes are unlikely in anaerobic conditions as found within the sludge blanket.

Thanks to the increased Q_{IN} in Stage #2, a SRT of 1.51d was obtained compared to 0.75d of Stage#1 (see Appendi). However, probably the steady state conditions had not been met, and this can partially justify the uncommon nutrients removal mentioned earlier. In fact, the sampling campaign was carried out just after the minimum start-up period of three days, as reported in Table 7. Furthermore, the inconsistency of the TSS concentrations trend between profiles 2.1 and 2.2 shown in Figure 10 supports the dynamic conditions in place at the time of sampling.

4.1.2 One day SRT and high internal recirculation flow rate

While maintaining a SRT of around one day, in Stage #3, an internal recirculation was implemented in the primary clarifier. Since it was previously experienced that an enhancement of VFA production took place within the sludge blanket, the goal was to elutriate those fermentation products out of the sludge blanket, namely to bring them to the effluent stream. A high flow rate of $50\% Q_{IN}$ (Table 7) was provided to obtain better mixing conditions in the sludge blanket and in this way homogenize the concentrations within it.

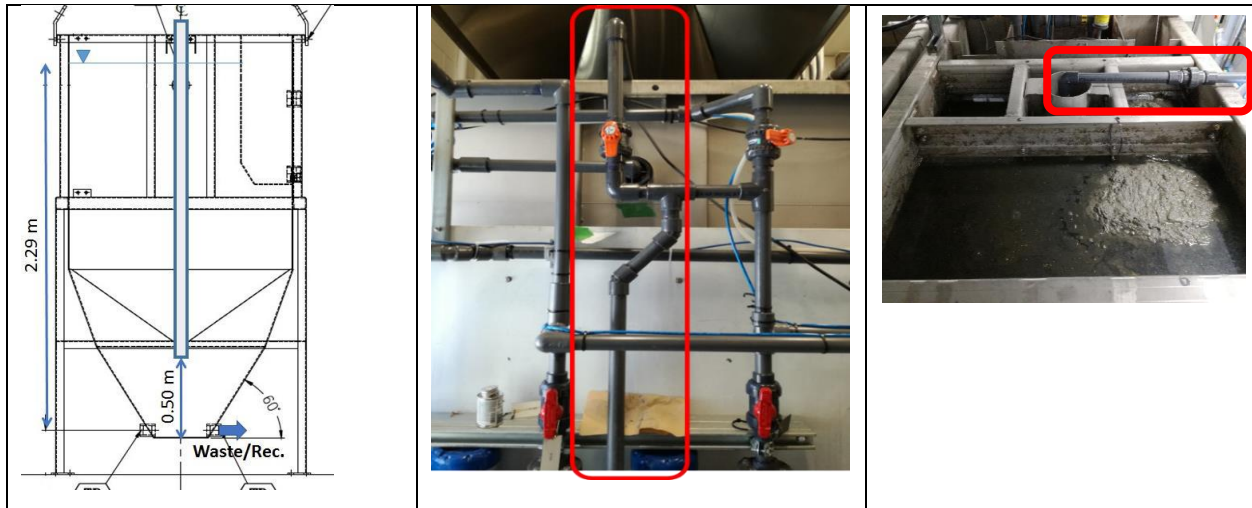


Figure 11: Internal recirculation line installed on the pilEAUte primary clarifier (marked in red) (left picture source: JOHN MEUNIER INC.).

The final part of the recirculation line is a flexible tube that ends at 0.5m from the bottom of the clarifier. The choice of staying 0.50 m above the bottom was made because ending further from the bottom would have negatively affected the solids removal efficiency, while a lower height, closer to the bottom, would have prevented a mixing zone.

From this stage on, a sample was taken each 0.20m along the primary clarifier height by means of an autosampler. In this way it was possible to have an accurate estimation of the SRT and to determine other important parameters such as pH, VFA, and alkalinity concentration profiles. Figure 12 illustrates the grab sample set-up. Moreover, as mentioned in the materials and methods section, the samples along the clarifier's height were precautionarily taken before the wastage valve opening, which is automatic and lasts for a fixed time.



Figure 12: Grabbing samples at different heights.

TSS measurements were carried out in triplicate for each sample (total 11). For the lower layers a TS% was carried out due to the thickness of the sludge, and then converted into mg/L by assuming a sludge density of 1000 kg/m^3 . In order to have an accurate sample for each layer, all pumped sludge that remained in the tube between each layer, was wasted before pumping the next sample. For the bottom part (i.e. 0m of height), the sample was pumped directly from the return loop sampling point (see Figure 7).

Figure 13 clearly indicates that the Solitax probe (turbidity meter) should only be used to estimate the location of the SBH. A blanket height of 1.30m was confirmed by the lab measurements. In fact, the values measured by the Solitax were around 400 mg/L, while the TSS measurements gave a value of 8,300 mg/L. Furthermore, the TSS started to increase at around 1.30m of height, reaching a maximum value of 23,300 mg/L at 0.5m, where the flexible tube used for the internal recirculation exactly ends. After that, the solids concentration decreases to 15,000 mg/L, due to the recirculation system.

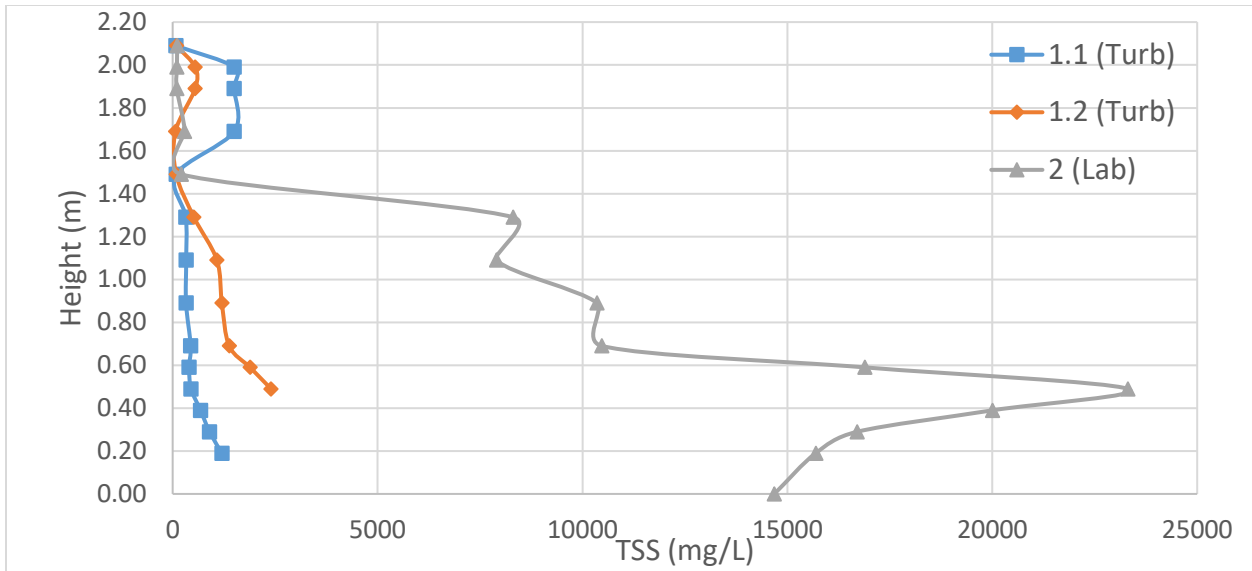


Figure 13: TSS concentration profile comparison between turbidity meter and lab measurements (Pre-Stage #3).

Besides the TSS concentration profile itself, the advantage of having grab samples at different heights is to assess the VFA, pH, and alkalinity profiles as well. Thus, these profiles can provide a better understanding of the environmental conditions inside the reactive primary clarifier.

From Figure 14 it can be noticed that the sludge blanket is located at around 0.50m. Furthermore, when going down from 0.50m, the TSS concentration rises, and reaches a concentration of 22,100 mg/L at 0.30m.

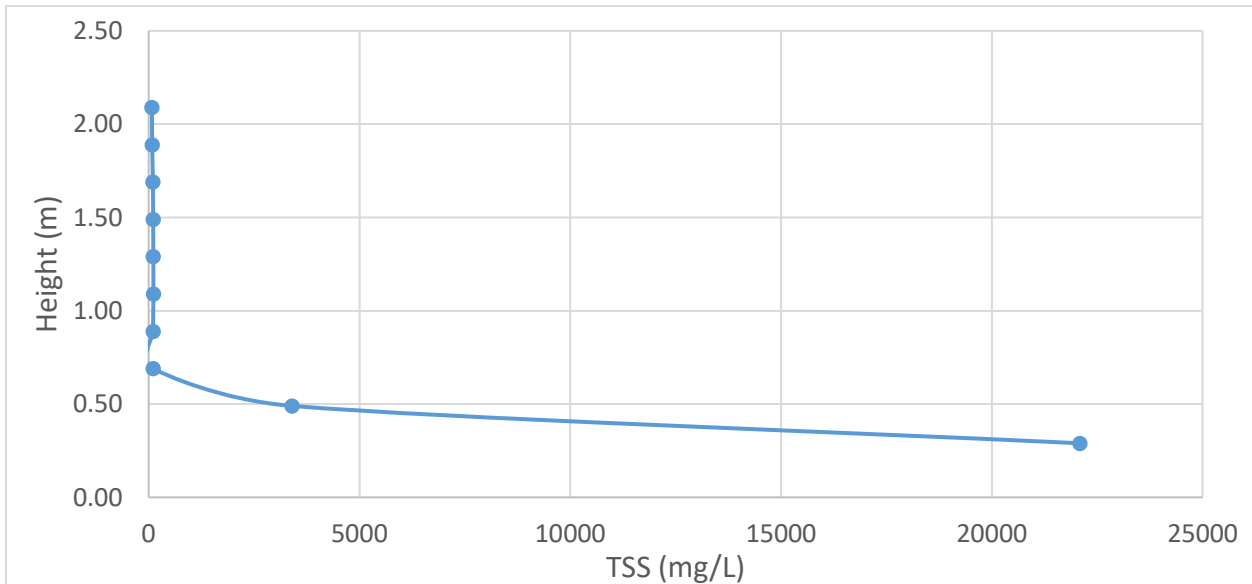


Figure 14: TSS concentration profile in primary clarifier (Stage #3).

As reported in in Figure 15, the VFA concentrations follow the same trend of the TSS, i.e. an increase from 0.50m and up to a value of 690 mg/L at lower heights. The acid pH values at the lower heights can be attributed to the acidification and VFA production within the sludge blanket. The three straight lines in Figure 15 represent the pH value, VFA, and alkalinity concentrations measured at the inlet (based on the composite sample). When comparing the lines *VFA_{in}* and the *VFA* in the upper part of the clarifier (higher heights), a difference of almost 20 mgCH₃COOH/L can be observed, which indicates a net VFA production. From the VFA data, it can thus be concluded that fermentation is occurring in the primary clarifier. This is also evident from the CO₂ gas bubbles observed at the surface (Figure 16). This is due to both the fermentation process [13], and to the pH drop (acidification) that leads to a supplementary release, based on the following reaction (chemical equilibrium):

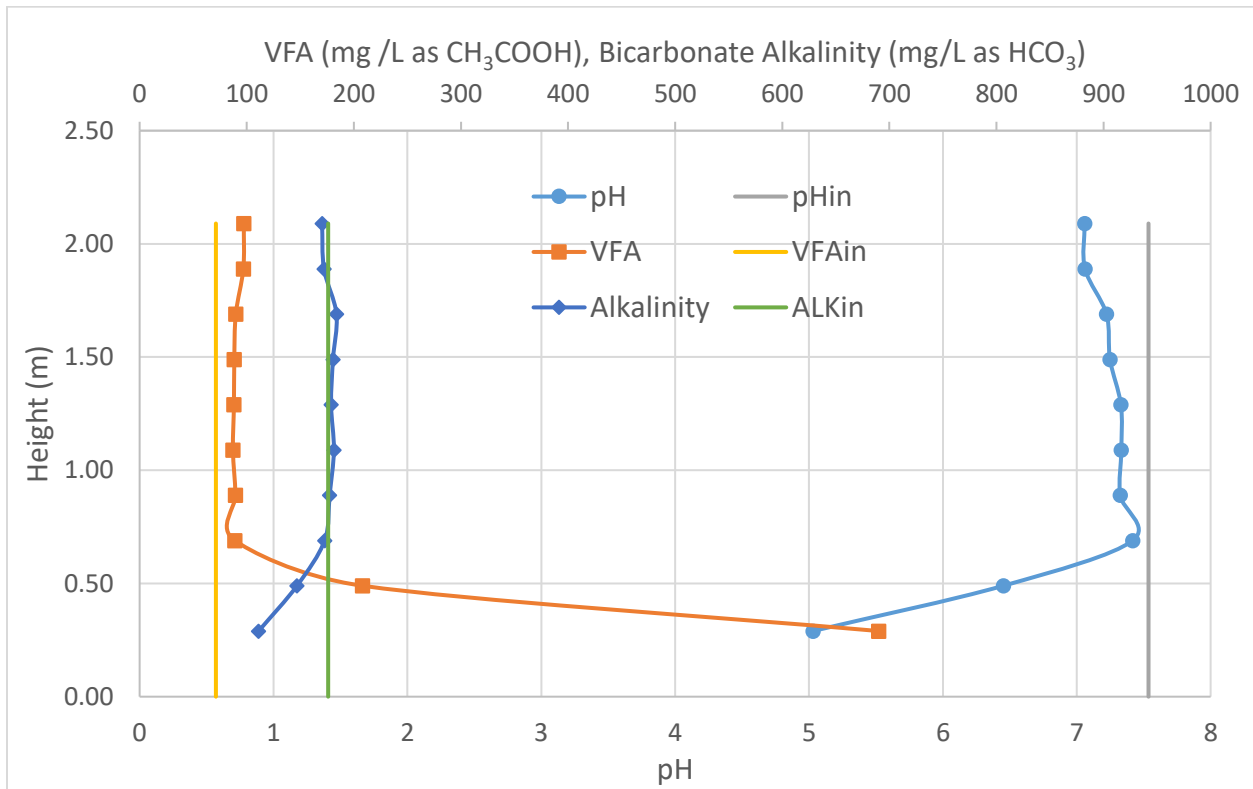


Figure 15: pH, VFA and alkalinity profiles for Stage #3.



Figure 16: Bubbles on the surface - a fermentation process is occurring.

Both the influent and the outlet soluble COD concentration are very close to each other (i.e. 218 mg/L and 210 mg/L, respectively), but solubilisation of organic matter is taking place.

In contrast to the previous set-up without return line, a positive value of the *VFA yield* of 18.9 mgCH₃COOH/L is reported here. As previously assumed from Figure 15 and Figure 16, fermentation is established and thanks to the recirculation line, the readily biodegradable carbon is now able to reach the outlet.

The high internal flow rate probably caused a poor value of the solid removal efficiency, i.e. 53% (Table 14). Indeed, due to the lower hydraulic retention time (see difference between HRT and HRT_{EFF}), the high return flow rate value of 50%Q_{IN} could negatively influence the sedimentation performance causing some solid material resuspension.

Table 12: Lab measurements and removal efficiency based on triplicates and duplicates for total and soluble concentrations, respectively (Stage #3).

		SOURCE			
		IN	OUT	WASTE	E%
TSS	mg/L	257 ± 4	129 ± 3	7960 ± 431	50 ± 2%
VSS	mg/L	240 ± 6	117 ± 4	7625 ± 415	51 ± 3%
VSS/TSS		93 ± 3%	90 ± 4%	96 ± 8%	
T-COD	mg/L	762 ± 39	530 ± 4	13777 ± 818	30 ± 6%
S-COD	mg/L	218 ± 8	210 ± 6	609 ± 3	4 ± 4%
P-COD	mg/L	544 ± 40	320 ± 7	13168 ± 818	41 ± 9%
VFA	mgCH ₃ COOH/L	71	76	335	-7%
T-TN	mg/L	47.8 ± 0.5	45.2 ± 2.1	183.7 ± 2.4	5 ± 2%
S-TN	mg/L	43.2	39.3 ± 1.0	32.4 ± 0.2	9 ± 1%
NH₃-N	mg/L	34.6 ± 0.4	33.9 ± 0.1	29.4 ± 0.4	2 ± 1%
TP	mg/L	16.7 ± 0.1	15.5 ± 0.2	54.7 ± 1.2	7 ± 1%
PO₄-P	mg/L	11.8 ± 0.2	11.9 ± 0.1	15.2 ± 0.0	0 ± 2%
PO₄-P/TP		71 ± 2%	76 ± 1%	28 ± 2%	
Alkalinity	mgHCO ₃ /L	176	160	74	
pH		7.54	7.64	5.57	

Table 13: Process performance parameters (Stage #3).

	IN	OUT	WASTE
S-COD/T-COD	29%	40%	4%
VFA/S-COD	33%	36%	55%
COD solubilization (mg/L)		-8.0	
Hydrolysis yield		-1%	
VFA production (as mgCH ₃ COOH/L)		4.7	
VFA yield (as mgCH ₃ COOH/g VSS)		18.9	

Table 14: Summary of the main parameters for Stage #3.

Set-Up condition summary - Main operating parameters											
Volumes			TSS concentrations			Flow rates			Retention Times		
V ₁	V ₂	V _{TOT}	X _{IN}	X _E	X _R	Q _{IN}	Q _W	Q _R	HRT	HRT _{EFF}	SRT
L	L	L	mg/L	mg/L	mg/L	m ³ /d	m ³ /d	m ³ /d	h	h	d
1968	232	2200	257	129	7960	16.8	0.04	8.4	3.1	2.1	1.51
Heights			Mass Loads			Mass		Removal Efficiency			
H _{TOT}	H ₁	SBH	L _{IN}	L _E	L _W	m _{BLANKET}	Accumulation	E%TSS			
m	m	m	g/d	g/d	g/d	g	g	%			
2.29	1.69	0.60	4312	2046	884	1848	2092	53%			

4.1.3 Three days SRT and high internal recirculation flow rate

In this stage, the waste flow rate was decreased from 40L/d to 20L/d to reach a desired SRT of three days, thus aiming to obtain higher VFAs yields.

Three different TSS profiles were assessed in this period, and they can be seen in Figure 17. The sludge blanket height seems to be stable and around 0.5m for the different days where the analyses were carried out.

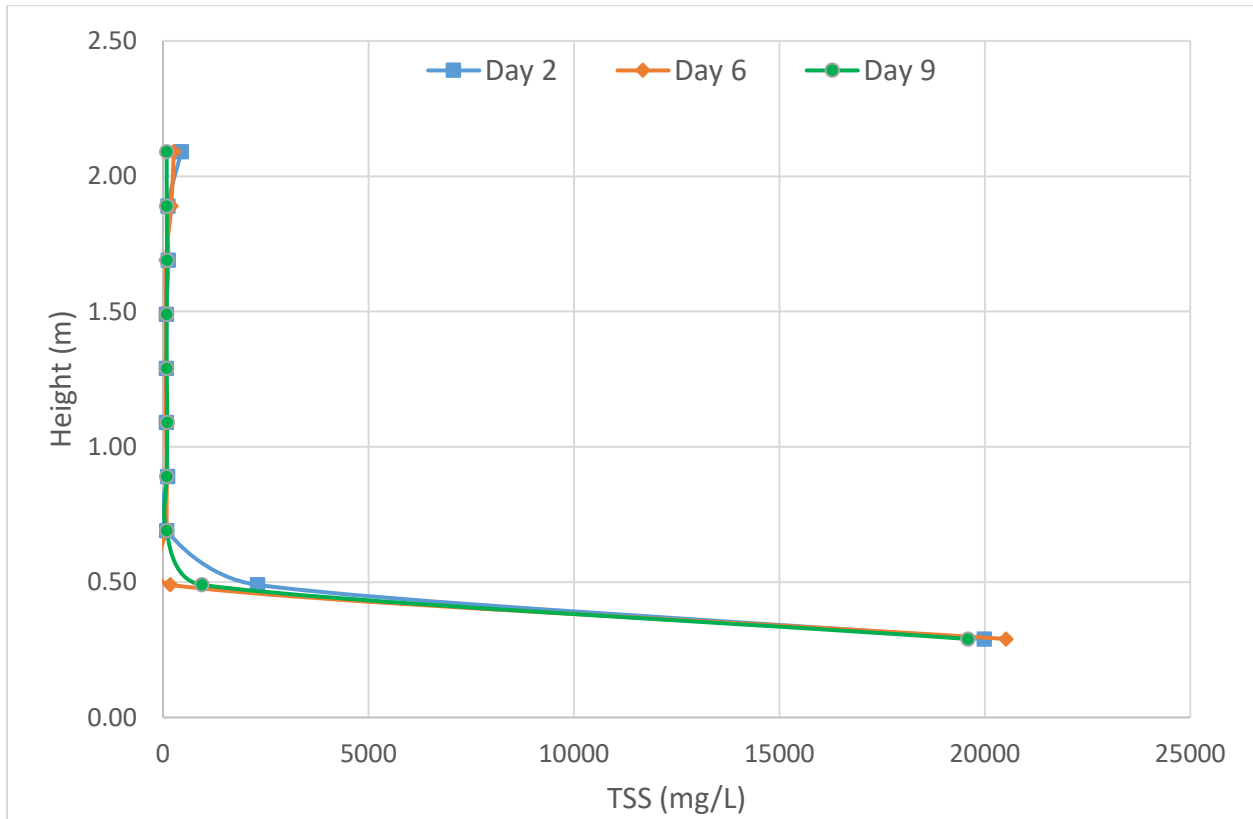


Figure 17: TSS concentration profile in primary clarifier (Stage #4).

Figure 18 and Figure 19 show the VFA, pH, and bicarbonate alkalinity values for Day 6 and 9, respectively. For Figure 19 the straight lines are based on composite sample measurements, and not on grabbed ones as for Figure 18. While the VFA and pH trends are very similar in shape and have almost the same values in both plots, the inlet bicarbonate alkalinity values at 0.30m height are different for the two periods. Day 9 shows a higher value of 240 mg/L, while on Day 6 it is equal to 155 mg/L. Moreover, regarding Day 9, after a little decrease at 0.5 m, from 190 to 170 mg/L, the bicarbonate alkalinity value rises to 240 mg/L in the lower sludge layer.

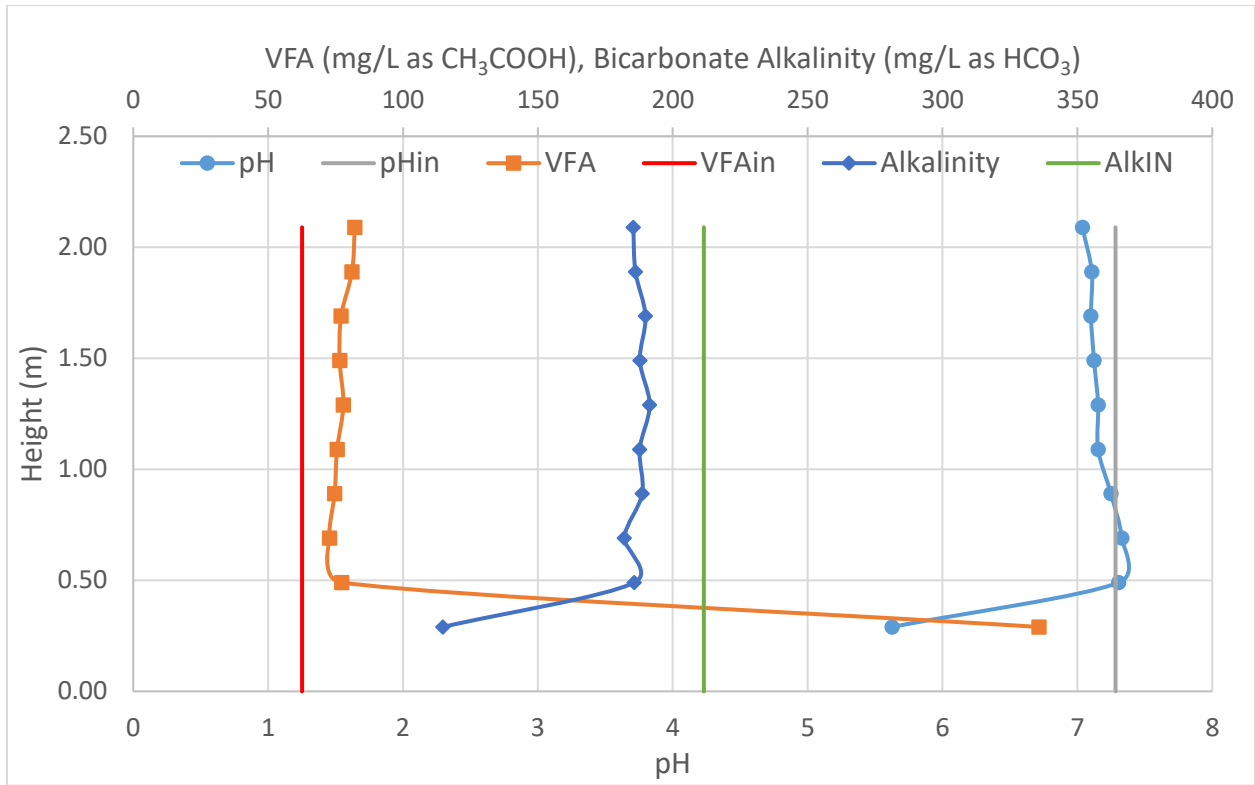


Figure 18: pH, VFA and bicarbonate alkalinity profiles for Day 6 based on grabbed samples (Stage #4).

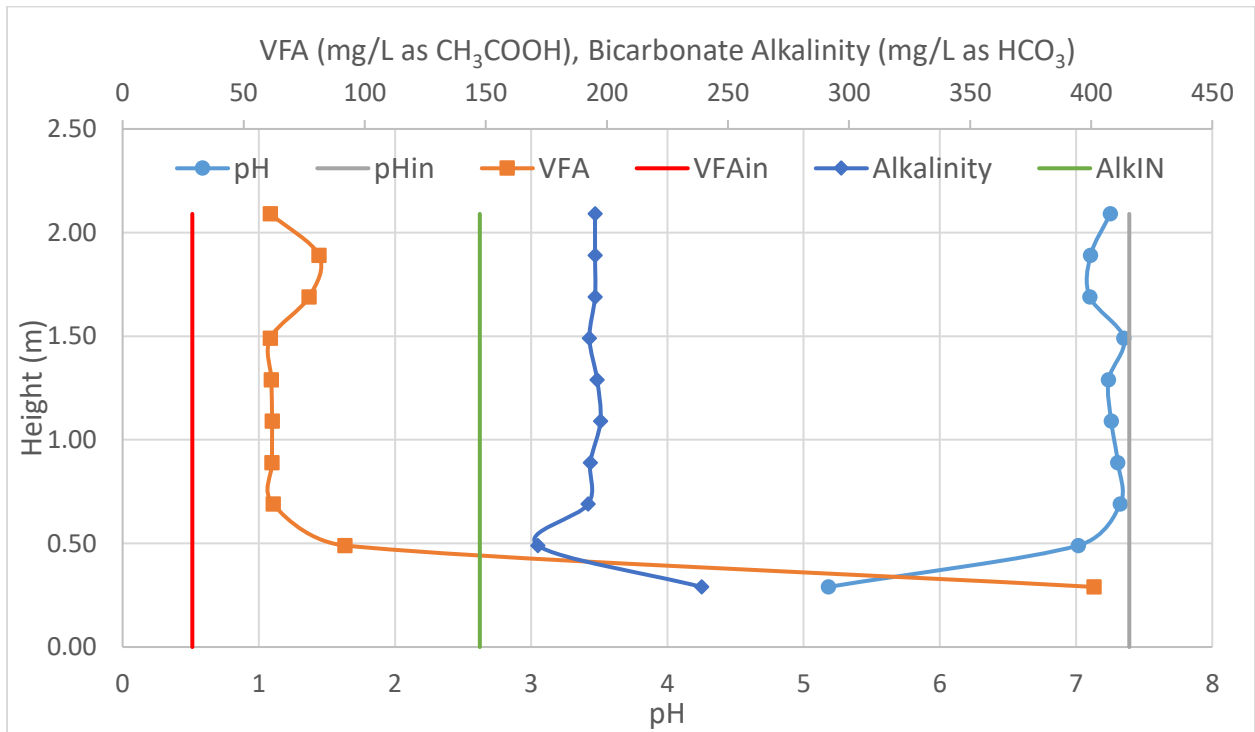


Figure 19: pH, VFA and bicarbonate alkalinity profiles for Day 9 based on composite samples (Stage #4).

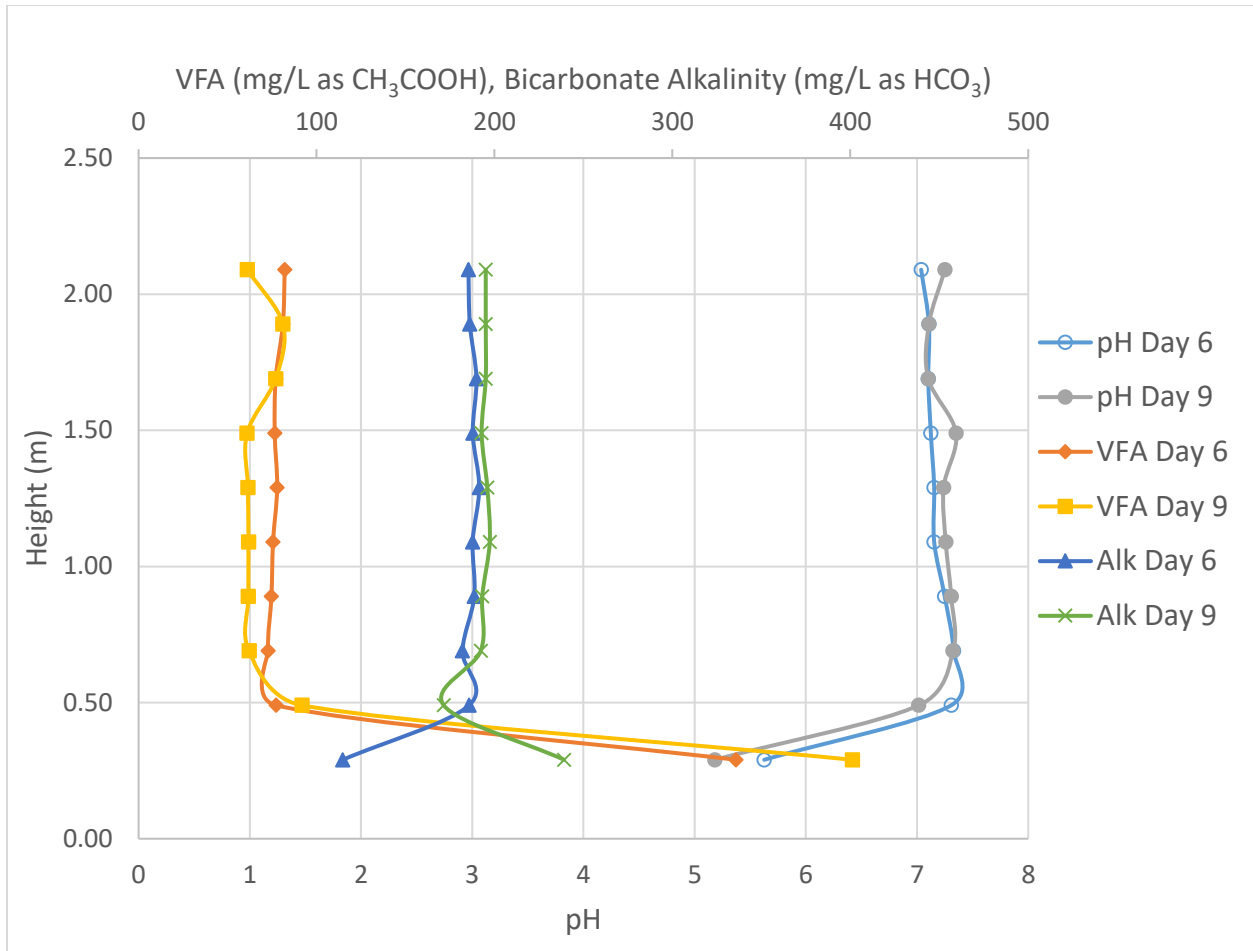


Figure 20: Comparison of pH, VFA and bicarbonate alkalinity profiles for Day 6 and 9 (Stage #4).

As can be inferred from Table 15 and Table 16, the fermentation and hydrolysis processes are firmly established and the higher SRT of three days seems to be beneficial. Indeed, the *VFA yield* is 61.4 mgCH₃COOH/g VSS and the *VFA production* is positive with a value of 12.0 mg/L. In addition, when we compare the amount of VFA over the soluble organic matter (*VFA/S-COD*) for SRT's of one day (Table 13) and three days (Table 16), the ratio increases from 36% to 42%, whereas the inlet and waste samples show almost the same percentages for both SRT's.

Compared to previous stages with sludge age of one day, a higher solids removal efficiency of 72% (Table 17), estimated on mass loads, is here reported. The temperature of 22.1 and 23.9 might have decreased the water viscosity, enhancing particle settling.

Table 15: Lab measurements and removal efficiency based on triplicates and duplicates for total and soluble concentrations, respectively (Stage #4).

		SOURCE			E%
		IN	OUT	WASTE	
TSS	mg/L	209 ± 13	61 ± 3	9481 ± 2010	71 ± 8%
VSS	mg/L	194 ± 9	56 ± 4	9056 ± 1924	71 ± 6%
VSS/TSS		93 ± 8%	92 ± 9%	96 ± 30%	
T-COD	mg/L	417 ± 4	252 ± 5	13033 ± 1534	40 ± 1%
S-COD	mg/L	89 ± 0	98 ± 4	431 ± 6	-10 ± 2%
P-COD	mg/L	328 ± 4	155 ± 6	12603 ± 1534	53 ± 2%
VFA	mgCH ₃ COOH/L	29	41	222	-41%
T-TN	mg/L	33.8 ± 1.2	31.6 ± 0.9	209.3 ± 5.0	6 ± 4%
S-TN	mg/L	29.7 ± 0.3	27.1 ± 1.6	22.3 ± 0.6	8 ± 3%
NH ₃ -N	mg/L	22.6 ± 0.2	21.9 ± 0.1	16.0 ± 0.1	3 ± 1%
TP	mg/L	10.7 ± 0.1	9.8 ± 0.1	65.7 ± 2.3	8 ± 1%
PO ₄ -P	mg/L	7.0 ± 0.0	7.2 ± 0.0	9.4 ± 0.1	-3 ± 1%
PO ₄ -P/TP		65 ± 1%	73 ± 1%	14 ± 4%	
Alkalinity	mgHCO ₃ /L	148	135	828	
pH		7.39	7.22	5.61	

Table 16: Process performance parameters (Stage #4).

	IN	OUT	WASTE
S-COD/T-COD	21%	39%	3%
VFA/S-COD	32%	42%	52%
COD solubilization (mg/L)		8.5	
Hydrolysis yield		2%	
VFA production (as mgCH ₃ COOH/L)		12.0	
VFA yield (as mgCH ₃ COOH/g VSS)		61.4	

Table 17: Summary of the main parameters for Stage #4.

Set-Up condition summary - Main operating parameters											
Volumes			TSS concentrations			Flow rates			Retention Times		
V ₁	V ₂	V _{TOT}	X _{IN}	X _E	X _R	Q _{IN}	Q _W	Q _R	HRT	HRT _{EFF}	SRT
L	L	L	mg/L	mg/L	mg/L	m ³ /d	m ³ /d	m ³ /d	h	h	d
1968	232	2200	209	61	9481	16.8	0.02	8.4	3.1	2.1	1.83
Heights			Mass Loads			Mass		Removal Efficiency			
H _{TOT}	H ₁	SBH	L _{IN}	L _E	L _W	m _{BLANKET}	Accumulation	E%TSS			
m	m	m	g/d	g/d	g/d	g	g	%			
2.29	1.69	0.60	3507	993	392	2201	3875	72%			

Although it was aimed to achieve a desired SRT of three days, a lower SRT of 1.83d was actually obtained. It should be noted that from the implementation of the return line on and/or once the fermentation conditions were established (i.e., from Stage #3), a layer of floating sludge was building up on the surface of the clarifier (see Figure 21). This rising sludge was almost daily removed, without considering it in the mass balance analysis. This undetermined load of wasted sludge is one reason of the lower SRT calculated throughout all the experimental campaign. This is evident when a mass balance of the system is performed. Indeed, by looking at Figure 22 a missing TSS mass load of 2297 g/d (that represents 65% of the inlet mass load) can be estimated. Even if some suspended organic matter is being hydrolyzed, and thus transformed into soluble organics (which can explain the reported negative values for S-COD and VFAs mass loads in Figure 22), only hydrolysis cannot justify the 65% TSS gap. In other words, the missing floating sludge leads to an underestimation of the waste load, which affects the sludge age value and the mass balances as well.



Figure 21: Rising sludge on the primary clarifier on June 11 (Stage #4).

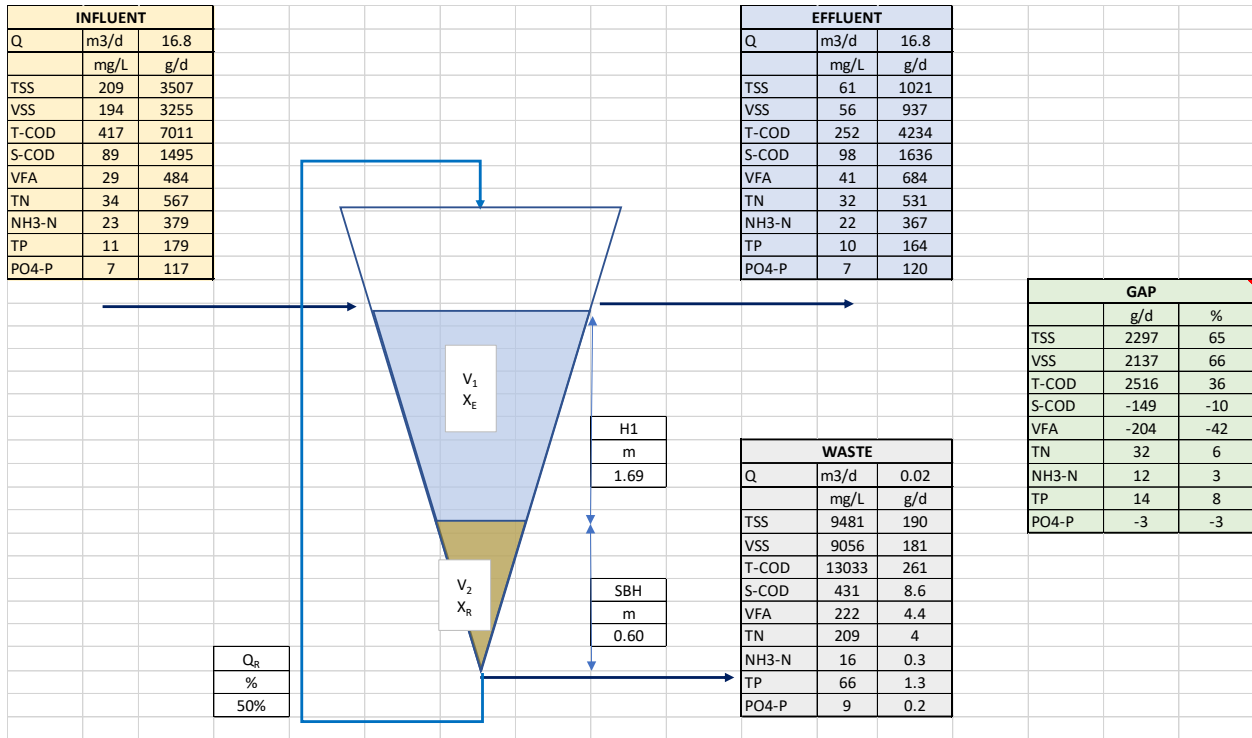


Figure 22: Mass balance for Stage #4.

4.1.4 Three days SRT and low internal recirculation flow rate

In order to remedy the poor E%TSS value obtained with a high recirculation flow rate (Table 12) and to avoid high pumping costs, the internal flow rate was decreased from 50% to about 15% of Q_{IN} , while keeping a sludge retention time of three days.

Two different TSS profiles were assessed in this period, and they can be seen in Figure 23 Figure 17.

The sludge blanket height seems to be stable and around 0.5m for Day 17 and 18, but on Day 18 the TSS concentration is a bit lower than the other day. This can be explained if the waste valve opening time is considered. In fact, the automatic waste valve opening happens each two days, to reach the desired SRT of three days. During this campaign (Stage #5), the waste valve opened while the 24h sampling was taking place. Whereas the profile for Day 17 was carried out before the opening, the profile for Day 18 was completed later. Therefore, the wasted sludge has caused the slightly lower sludge blanket height measured on Day 18.

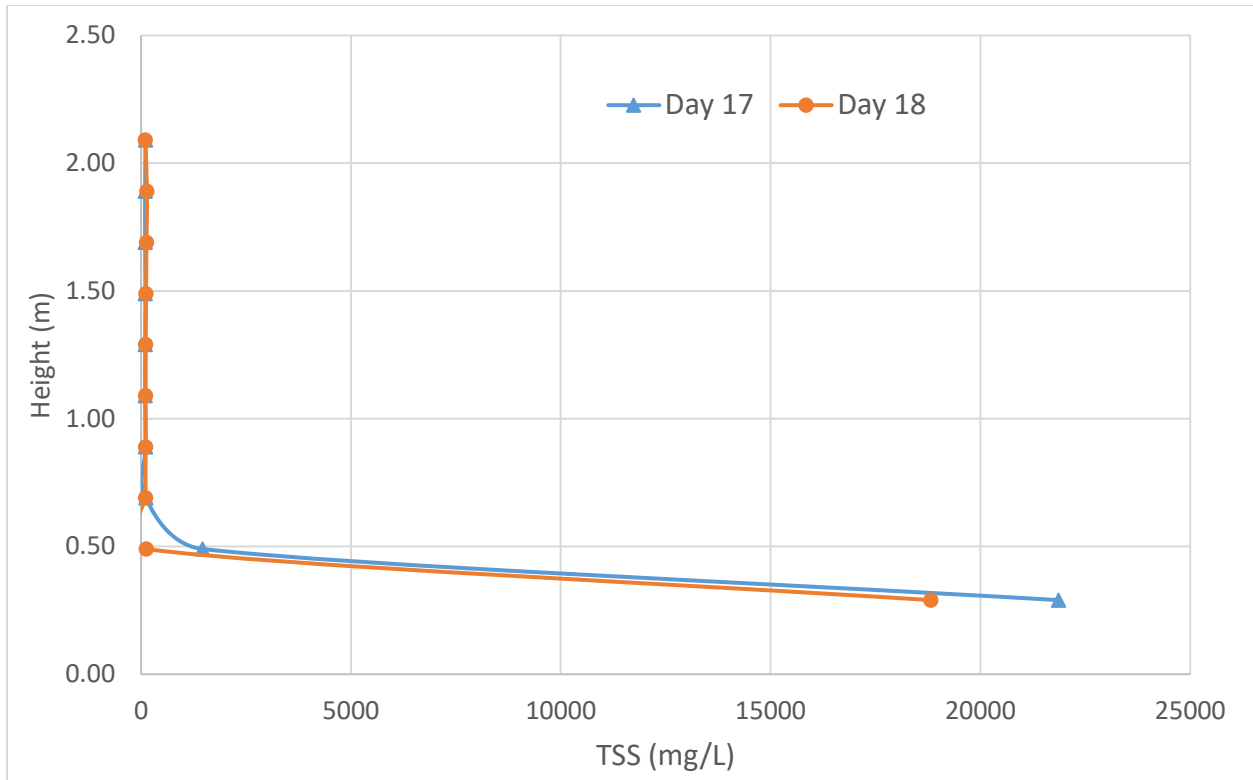


Figure 23: TSS concentration profile in primary clarifier (Stage #5).

Besides the waste valve opening, another important factor that may explain the decrease for both the TSS and VFA concentrations (see Figure 24) is that a rain event occurred overnight, as shown in Figure 25. Figure 24 clearly shows that as the VFA increases, the pH decreases especially for Day 17 when a higher solids concentration was present. The bicarbonate alkalinity concentration shows different trends for the lower heights between the two days, instead. While on Day 17 the measured bicarbonate alkalinity at 0.30m height was 207mgHCO₃/L, during Day 18 the bicarbonate alkalinity concentration had a lower value, i.e. 69mgHCO₃/L. This may still be associated with the dilution effect caused by the rain event.

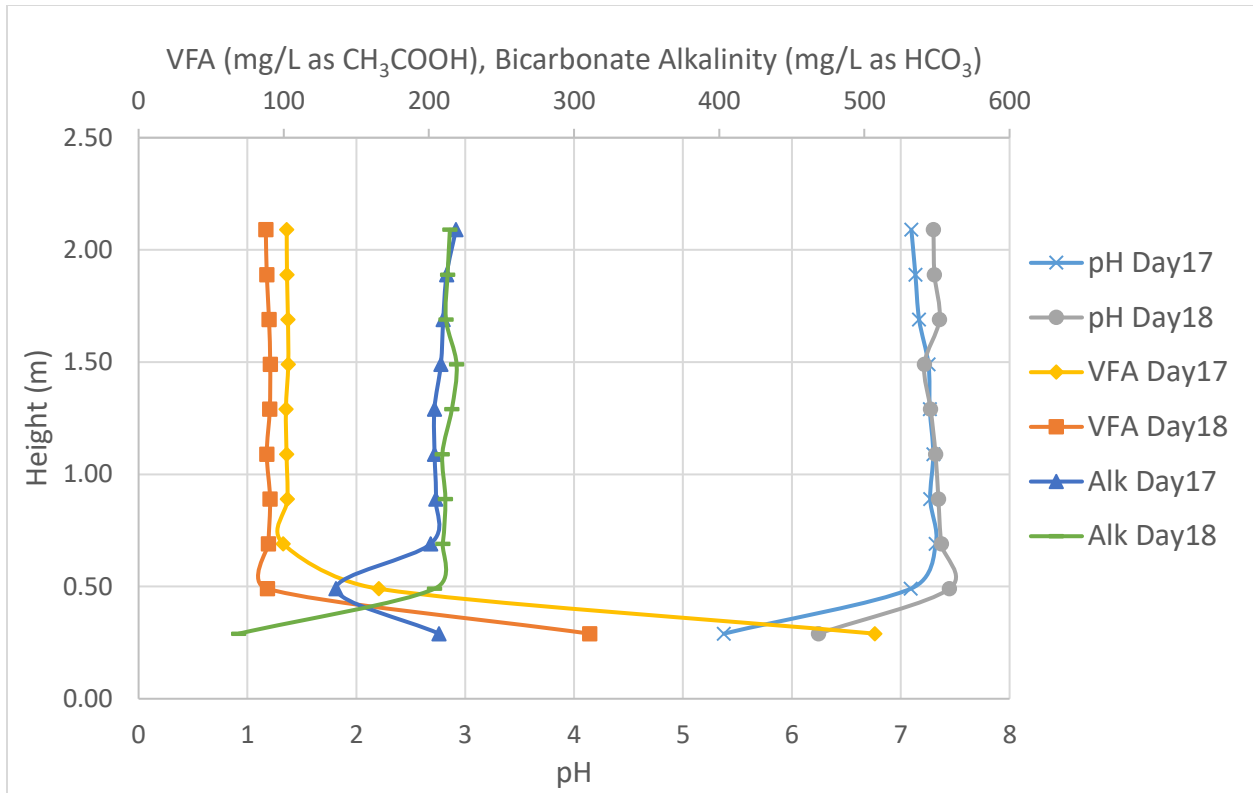


Figure 24: Comparison of pH, VFA and bicarbonate alkalinity profiles for Day 17 and 18 (Stage #5).

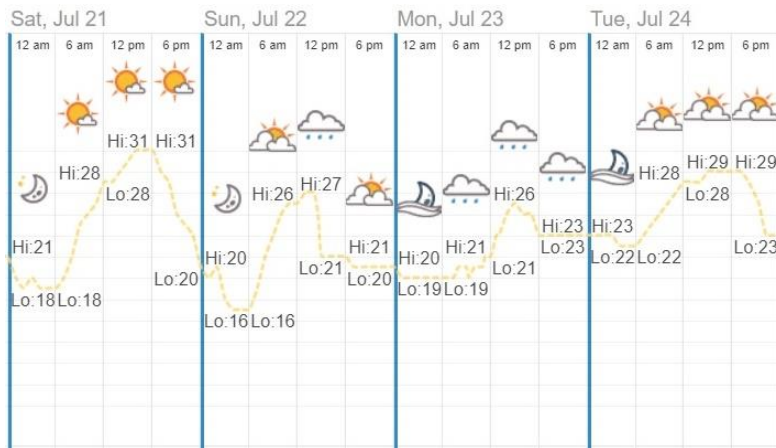


Figure 25: Weather in Quebec City from July 21 (Day 15) to 24 (Day 18). (Source: timeanddate.com)

The removal efficiency reported in Table 18 showed good performance on solids removal with a value of 71%. Regarding soluble matter, an overall fermentation with nutrient release can be observed. The ammonia and phosphate release are significant with an increase (from the inlet to the outlet) of 39.4 to 43.9 mg/L, and 13.4 to 15.3 mg/L, respectively. On the other hand, the

VFAs and S-COD showed a negative removal efficiency (i.e., a production) of -40%, and -19%, respectively.

Good hydrolysis performance can be noticed in Table 19 as well. The *COD solubilization* was 38.0 mg/L, and the *Hydrolysis yield* was 6%. Besides, the *VFA yield* reached a very high value of 90.1 mg/g VSS. The very high temperature (see Figure 69) may have enhanced the fermentation performance by speeding-up the chemical and biological reactions.

Table 18: Lab measurements and removal efficiency based on triplicates and duplicates for total and soluble concentrations, respectively (Stage #5).

		SOURCE			E%
		IN	OUT	WASTE	
TSS	mg/L	305 ± 14	89 ± 7	14235 ± 616	71 ± 6%
VSS	mg/L	286 ± 9	80 ± 5	13397 ± 563	72 ± 4%
VSS/TSS		94 ± 6%	89 ± 10%	94 ± 6%	
T-COD	mg/L	686 ± 15	457 ± 3	18933 ± 1472	33 ± 2%
S-COD	mg/L	195 ± 8	233 ± 1	529 ± 6	-19 ± 5%
P-COD	mg/L	491 ± 17	224 ± 3	18405 ± 1472	54 ± 4%
VFA	mgCH ₃ COOH/L	64	90	286	-40%
T-TN	mg/L	53.8 ± 1.0	52.8 ± 1.9	267.0 ± 21.2	2 ± 3%
S-TN	mg/L	44.6 ± 0.8	46.2 ± 0.8	42.8 ± 1.7	-4 ± 2%
NH₃-N	mg/L	39.4 ± 1.6	43.9 ± 0.7	37.9 ± 0.4	-12 ± 5%
TP	mg/L	19.3 ± 0.1	19.8 ± 0.3	93.5 ± 1.5	-3 ± 1%
PO₄-P	mg/L	13.4 ± 0.0	15.3 ± 0.0	18.8 ± 0.1	-14 ± 0%
PO₄-P/TP		70 ± 1%	77 ± 1%	20 ± 2%	
Alkalinity	mgHCO ₃ /L	199	203	77	
pH		7.47	7.28	6.08	

Table 19: Process performance parameters (Stage #5).

	IN	OUT	WASTE
S-COD/T-COD	28%	51%	3%
VFA/S-COD	33%	39%	54%
COD solubilization (mg/L)		38.0	
Hydrolysis yield		6%	
VFA production (as mgCH ₃ COOH/L)		25.9	
VFA yield (as mgCH ₃ COOH/g VSS)		90.1	

Regarding the good fermentation performance, which confirms the need of a SRT of three days and a low internal recycle flow rate, it should be noted that the start-up period for this stage was twice the required one of nine days. This long steady-state period probably has contributed to

establish a certain fermentative bacteria population within the system. Unfortunately, no microbial analysis can support this hypothesis.

As previously mentioned, the reasons for a very low SRT of 0.80d indicated in Table 20 (rather than a desired value of three days) are related to a combination of different aspects. One is the dilution effect caused by the rain event; the second one is the waste valve opening during the sampling; and the last one is the floating sludge that was removed on a daily basis. The sludge floating phenomenon was very well observed during a SVI (sludge volume index) test for a primary sludge. As can be seen on Figure 26, almost all sludge tended to rise up to the surface rather than to accumulate at the bottom of the Imhoff cone. This is mainly due to the gases (CO₂) produced by the on-going fermentation process [13]. The gases, while they are rising to the top, indeed drag the solids particles with them, leading to a build-up of a sludge layer on the clarifier's surface.

Table 20: Summary of the main parameters for Stage #5.

Set-Up condition summary - Main operating parameters											
Volumes			TSS concentrations			Flow rates			Retention Times		
V ₁	V ₂	V _{TOT}	X _{IN}	X _E	X _R	Q _{IN}	Q _W	Q _R	HRT	HRT _{EFF}	SRT
L	L	L	mg/L	mg/L	mg/L	m ³ /d	m ³ /d	m ³ /d	h	h	d
1968	232	2200	305	89	14235	16.8	0.02	2.4	3.1	2.8	0.80
Heights			Mass Loads			Mass		Removal Efficiency			
H _{TOT}	H ₁	SBH	L _{IN}	L _E	L _W	m _{BLANKET}	Accumulation	E%TSS			
m	m	m	g/d	g/d	g/d	g	g	%			
2.29	1.69	0.60	5117	1455	36	3305	2898	72%			



Figure 26: Primary sludge after 30 minutes of sedimentation in an Imhoff cone.

4.2 The Effect of Alkalinity

Wu et al [15] demonstrated that an alkaline pH is favorable for VFA enhancement, and prevents its conversion to methane. In addition, to fulfill the effluent alkalinity demand, a saturated concentration of sodium bicarbonate (NaHCO_3) was added to the primary clarifier. In fact, the studied pilot plant is characterized by effluent alkalinity values smaller than $200 \text{ mgCaCO}_3/\text{L}$, as reported in the Appendix. Instead, Metcalf and Eddy [3] indicate a general required value of $200 \text{ mgCaCO}_3/\text{L}$ for ensuring nitrification process. Furthermore, during their batch tests at room temperature (25°C), Wu et al [15] found a maximum VFAs yield of $312.9 \text{ mg COD/g VSS}$ at pH 10.0–11.0, and 5 days SRT.

In this scenario, the SRT was set at three days and the internal recirculation flow rate at around 15% of Q_{IN} .

For this particular case, the measurements were carried out down to 0.10m of height (Figure 27) since the sludge blanket seems to be located at a lower height than usual (around 0.40m instead of 0.60m, see Table 23).

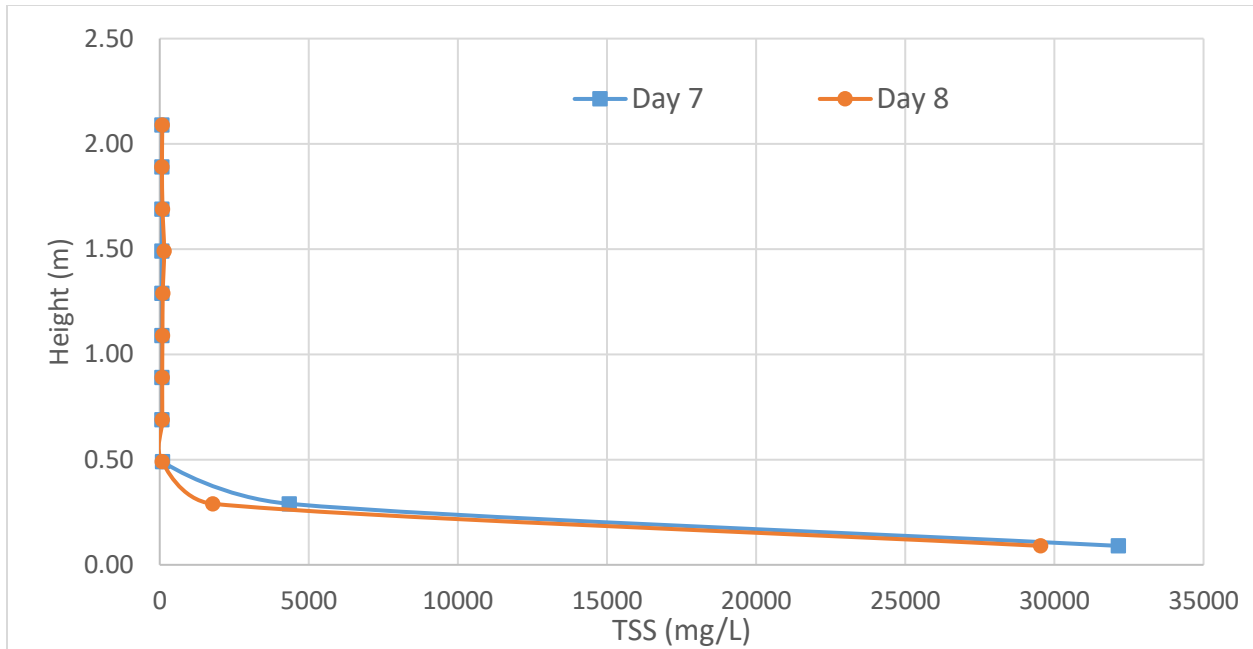


Figure 27: TSS concentration profile in primary clarifier (Stage #6).

Figure 28 shows higher VFA concentrations in the sludge blanket (i.e. 0.3m and 0.1m of immersion) for Day 7 compared to Day 8. This can be explained by looking at Figure 27 that indicates higher TSS concentrations as well on Day 7. A higher TSS concentration, at the same height, reflects a larger fermentative biomass present on Day 7 than on the day after.

The added sodium bicarbonate solution brought the primary settler in an almost alkaline environment with an outlet pH value of 7.63 and a bicarbonate alkalinity concentration of 368 mg/L as HCO_3 (Table 21). From Table 22, even if a lower performance was achieved compared to the period without sodium bicarbonate addition, fermentation seems still to occur, and a good VFA yield of 70.6 mg/g is reported. As opposed to previous stages without alkalinity addition, the sludge blanket shows here a neutral pH value, rather than an acidic pH. Although there is no nutrient release, the TSS removal performance (47%) might be negatively affected by the alkaline addition. However, further studies are required to support this relation.

When comparing the VFA/S-COD ratio from Table 22 with the ones of previous stages, namely #3, #4, and #5 (Table 13, Table 16, and Table 19, respectively) the water quality coming to the plant has a higher VFA fraction.

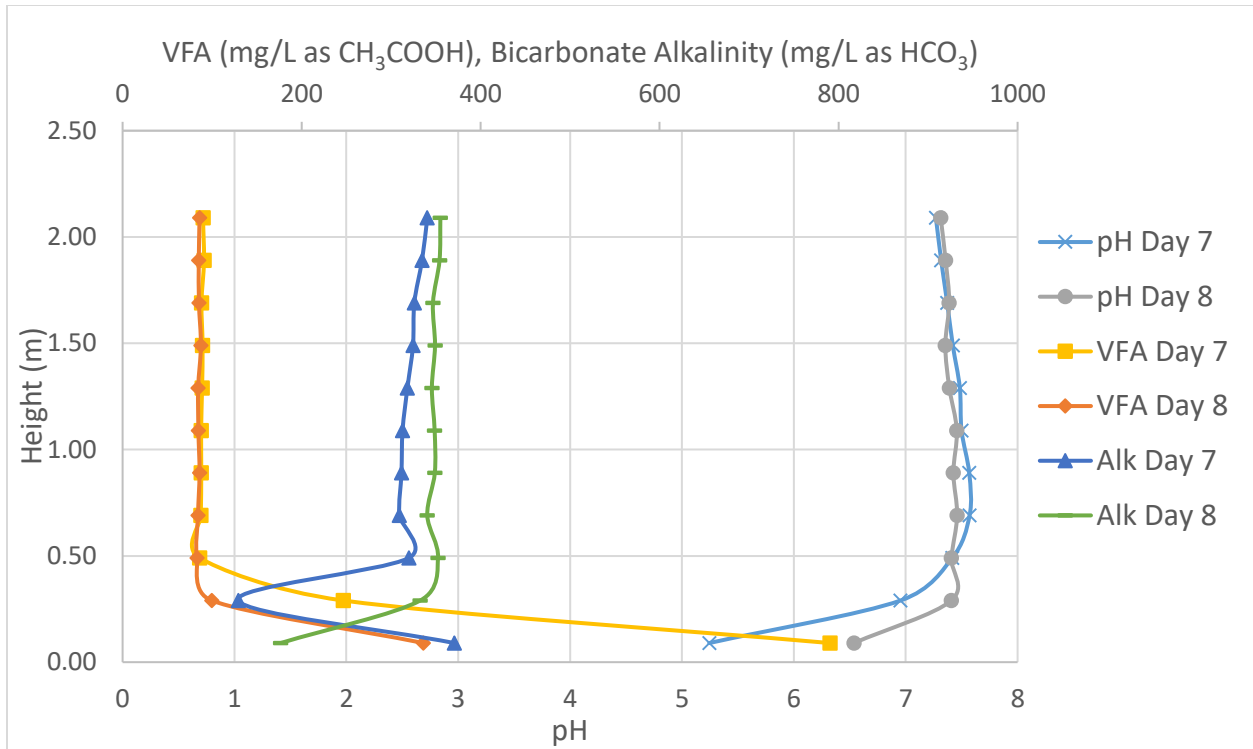


Figure 28: Comparison of pH, VFA and bicarbonate alkalinity profiles for Day 7 and 8 (Stage #6).

Table 21: Lab measurements and removal efficiency based on triplicates and duplicates for total and soluble concentrations, respectively (Stage #6).

		SOURCE			
		IN	OUT	WASTE	E%
TSS	mg/L	183 ± 6	98 ± 4	12083 ± 287	47 ± 4%
VSS	mg/L	168 ± 5	91 ± 3	11203 ± 286	46 ± 4%
VSS/TSS		92 ± 5%	93 ± 6%	93 ± 3%	
T-COD	mg/L	466 ± 9	372 ± 2	17727 ± 503	20 ± 2%
S-COD	mg/L	128 ± 4	135 ± 1	513 ± 1	-5 ± 3%
P-COD	mg/L	338 ± 9	237 ± 2	17214 ± 503	30 ± 3%
VFA	mgCH ₃ COOH/L	58	70	255	-21%
T-TN	mg/L	40.6 ± 1.8	39.5 ± 1.4	306.0 ± 11.1	3 ± 5%
S-TN	mg/L	33.6 ± 0.7	35.4 ± 4.0	29.5 ± 1.2	-5 ± 2%
NH₃-N	mg/L	29.5 ± 0.0	28.0 ± 0.2	23.6 ± 0.1	5 ± 0%
TP	mg/L	15.0 ± 0.2	14.2 ± 0.1	93.3 ± 6.5	5 ± 1%
PO₄-P	mg/L	10.5 ± 0.0	10.4 ± 0.0	9.4 ± 0.2	1 ± 0%
PO₄-P/TP		70 ± 1%	73 ± 1%	10 ± 7%	
Alkalinity	mgHCO ₃ /L	199	203	77	
pH		7.47	7.28	6.08	

Table 22: Process performance parameters (Stage #6).

	IN	OUT	WASTE
S-COD/T-COD	27%	36%	3%
VFA/S-COD	46%	52%	50%
COD solubilization (mg/L)		7.0	
Hydrolysis yield		2%	
VFA production (as mgCH ₃ COOH/L)		12.0	
VFA yield (as mgCH ₃ COOH/g VSS)		70.6	

As for the previous stages, the actual SRT of 0.74d (Table 23) is not close to the targeted one of three days. The floating sludge flocs may have had an effect in lowering the sludge age value. A further picture that shows the floating sludge is given in Figure 29.

Table 23: Summary of the main parameters for Stage #6.

Set-Up condition summary - Main operating parameters											
Volumes			TSS concentrations			Flow rates			Retention Times		
V ₁	V ₂	V _{TOT}	X _{IN}	X _E	X _R	Q _{IN}	Q _W	Q _R	HRT	HRT _{EFF}	SRT
L	L	L	mg/L	mg/L	mg/L	m ³ /d	m ³ /d	m ³ /d	h	h	d
2101	99	2200	183	98	12083	16.8	0.02	2.4	3.1	2.8	0.74
Heights			Mass Loads			Mass		Removal Efficiency			
H _{TOT}	H ₁	SBH	L _{IN}	L _E	L _W	m _{BLANKET}	Accumulation	E%TSS			
m	m	m	g/d	g/d	g/d	g	g	%			
2.29	1.89	0.40	3080	1591	36	1198	1078	48%			



Figure 29: Rising sludge on the primary clarifier on Day 4 (Stage #6).

4.3 Effect of Ferric Chloride

By means of a peristaltic pump (Figure 30) a ferric chloride 40% w/w solution was dosed to the top of the primary clarifier, within the Clifford cylinder. The optimal solution of 20mg/L was identified through jar-tests as discussed in the Appendix.

The ferric chloride is broadly used for chemical enhanced primary treatment (CEPT) to further increase the solids removal efficiency of a primary clarifier [21]. However, its interactions with the fermentation process are unknown, and in this section, the solids removal performance and the fermentation performance will be compared. Lin et al [21] suggested that for a CEPT which has as goal, in addition to enhanced solids removal, to enhance VFA production, the best coagulant should be FeCl_3 , instead of polyaluminum chloride. In fact, PACl is responsible for limiting the surface exposure for enzymatic hydrolysis (cage effect). Anaerobic conditions will make the ferric to become ferrous, which leads to floc disintegration, resulting in absence of cage effects against hydrolytic bacteria.

Given the good fermentation performance found with three days SRT and low internal flow rates, these conditions were maintained.

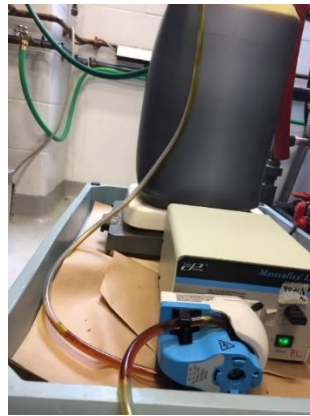


Figure 30: FeCl_3 solution pumped into the primary clarifier's Clifford cylinder by means of a peristaltic pump.

On Day 6 and 7, very different TSS profiles can be observed in Figure 31. The automatic waste valve opening between the two days can explain the sludge height drop from 0.7m to about 0.3m.

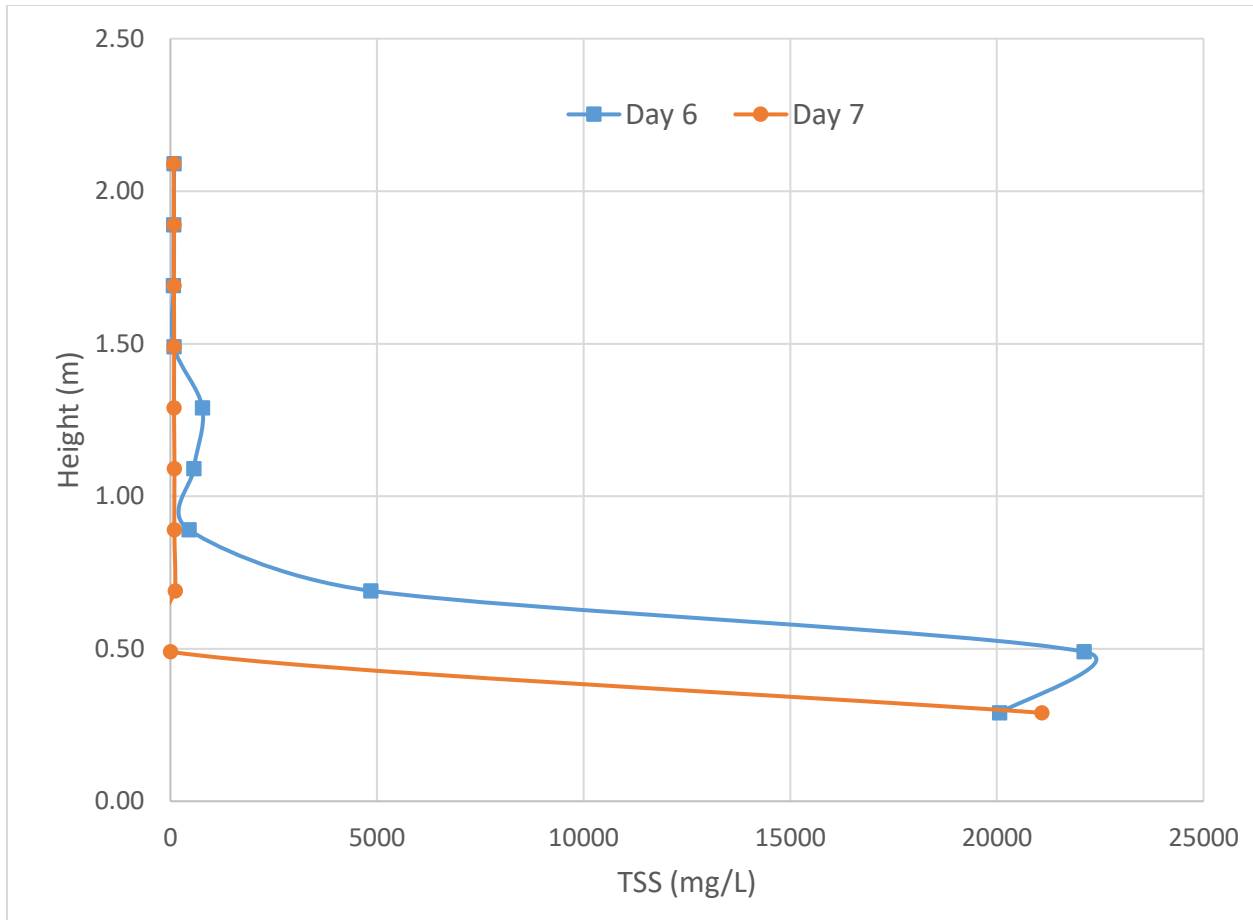


Figure 31: TSS concentration profile in primary clarifier (Stage #7).

As for the TSS concentrations, and also for the VFA, pH, and bicarbonate alkalinity profiles, the same differences in patterns can be observed in Figure 32, where overall lower values are measured during day 7. It can also be noticed that due to the FeCl_3 addition, a very acidic environment is found in the sludge blanket, with a lowest pH value of 4.68 on Day 6. The very high VFA concentration of 713mg/L (one of the highest) clearly contributes to lower the pH.

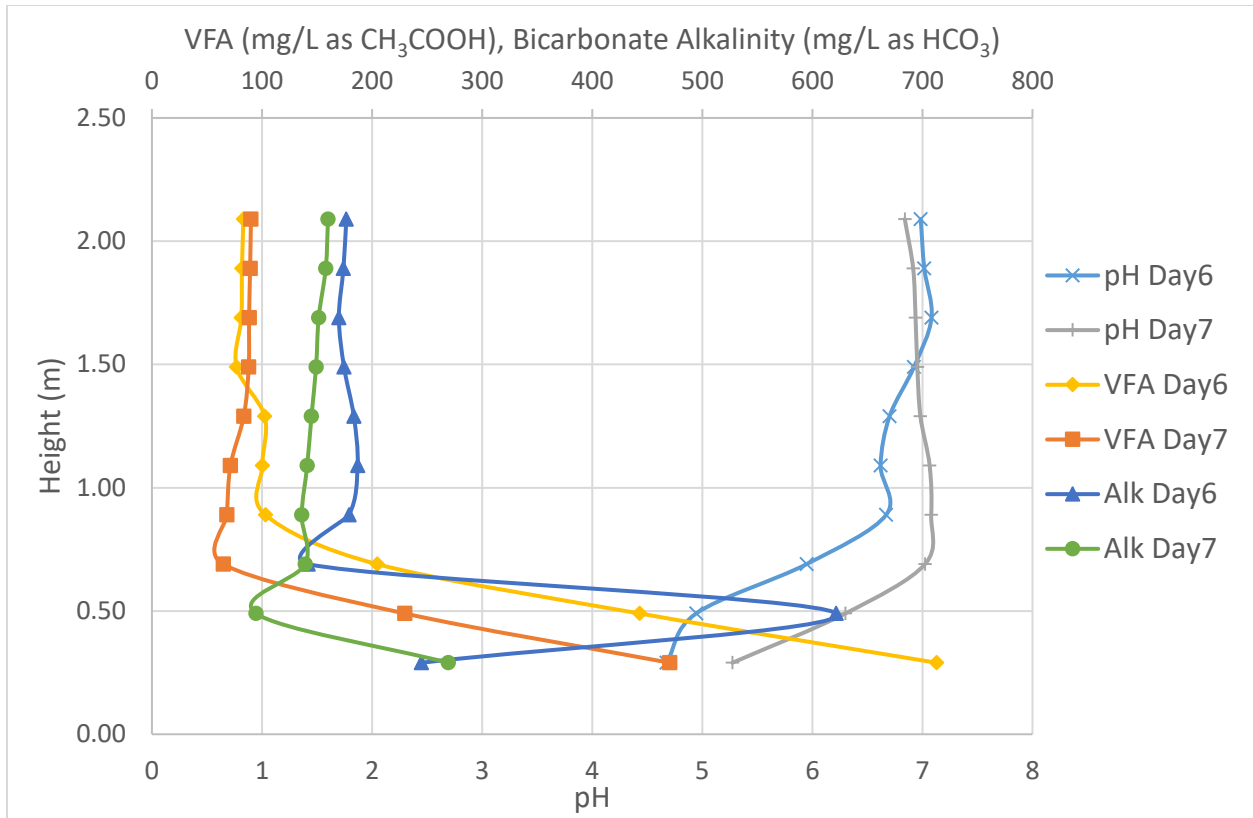


Figure 32: Comparison of pH, VFA and bicarbonate alkalinity profiles for Day 6 and 7 (Stage #7).

The solids removal efficiency was 63% (Table 24), which is in line with common primary clarifier performance, but it is too low compared to what is expected after coagulant addition. The poor solids removal performance could be due to the improper on-site mixing conditions since the FeCl_3 solution is simply added to the wastewater without applying any mixing before the sedimentation step.

However, in contrast to previous experiments without coagulant, a significant chemical phosphorus removal can be observed. In particular, the removal efficiency for phosphates is 23% and the chemical phosphorus precipitation as FePO_4 is the main reason. Below the chemical reactions involved in the chemical phosphorus precipitation are given:

- $\text{FeCl}_3 \rightarrow \text{Fe}^{3+} + \text{Cl}^{3-}$
- $\text{Fe}^{3+} + \text{PO}_4^{3-} \rightleftharpoons \text{Fe}(\text{PO}_4)_{(s)}$

Table 24: Lab measurements and removal efficiency based on triplicates and duplicates for total and soluble concentrations, respectively (Stage #7).

		SOURCE			
		IN	OUT	WASTE	E%
TSS	mg/L	441 ± 21	165 ± 4	15034 ± 426	63 ± 6%
VSS	mg/L	427 ± 10	148 ± 4	14519 ± 385	65 ± 3%
VSS/TSS		97 ± 5%	90 ± 4%	97 ± 4%	
T-COD	mg/L	837 ± 23	421 ± 5	21427 ± 1484	50 ± 3%
S-COD	mg/L	144 ± 0	126 ± 1	645 ± 52	13 ± 0%
P-COD	mg/L	693 ± 23	296 ± 5	20782 ± 1485	57 ± 4%
VFA	mgCH ₃ COOH/L	62	61	488	2%
T-TN	mg/L	49.6 ± 1.5	46.3 ± 0.2	266.7 ± 9.5	7 ± 4%
S-TN	mg/L	41.6 ± 0.6	36.3 ± 0.4	35.2 ± 0.4	13 ± 2%
NH₃-N	mg/L	35.3 ± 0.2	32.6 ± 0.1	26.2 ± 0.3	8 ± 1%
TP	mg/L	18.3 ± 0.2	16.7 ± 0.1	78.4 ± 0.7	8 ± 1%
PO₄-P	mg/L	12.4 ± 0.0	9.5 ± 0.0	19.2 ± 0.1	23 ± 0%
PO₄-P/TP		68 ± 1%	57 ± 1%	24 ± 1%	
Alkalinity	mgHCO ₃ /L	206	191	205	
pH		7.43	7.35	5.47	

One main effect of the ferric chloride is the increase of VFA present in the sludge blanket. In particular, Table 24 shows a VFA concentration in the waste of 488mg/L (almost double to what was measured in the previous stages), and a high VFA/S-COD of 76%, which means that almost all the soluble carbon is present as VFA. However, the *VFA yield* is negative, namely -3.3mg/L (Table 25). So, even if the fermentation process seemed to be strongly established within the sludge blanket, this abundant amount of soluble carbon could not be elutriated out, or simply, it is not able to reach the effluent stream. Probably, by letting the system run for a longer time better elutriation can be achieved. In fact, the start-up period was just seven days, compared to the minimum time of nine required days (see Table 7).

Table 25: Process performance parameters (Stage #7).

	IN	OUT	WASTE
S-COD/T-COD	17%	30%	3%
VFA/S-COD	43%	49%	76%
COD solubilisation (mg/L)		-18.5	
Hydrolysis yield		-2%	
VFA production (as mgCH ₃ COOH/L)		-1.3	
VFA yield (as mgCH ₃ COOH/g VSS)		-3.3	

4.4 Combined Effect of Alkalinity and Ferric Chloride

To see the combined effect of NaHCO_3 and FeCl_3 on the fermentation performance, they were simultaneously dosed to the primary clarifier. Wu et al [24] reported that on alkaline pH can accelerate the rate of organic hydrolysis, but at the same time it inhibits the further organic conversion to VFAs when applied to iron-enhanced primary sludge. Lin et al [20] reported as well that Fe-CEPT does not inhibit VFA production, but when there are anaerobic conditions and acid conditions (like during acidogenesis) ferric become ferrous and precipitated phosphorus is released again. This phosphorus release can be prevented by increasing pH. In fact, they showed that an alkaline environment leads to a decrease in iron solubility.

Table 26: pH, VFA and bicarbonate alkalinity values during NaHCO_3 and FeCl_3 dosages (Stage #8).

Day	Primary inlet (storage tank)			Primary outlet			Added NaHCO_3 solution		
	pH	VFA (mg/L as CH_3COOH)	Alkalinity (mg/L as HCO_3^-)	pH	VFA (mg/L as CH_3COOH)	Alkalinity (mg/L as HCO_3^-)	pH	VFA (mg/L as CH_3COOH)	Alkalinity (mg/L as HCO_3^-)
Day13	7.17	63	193	7.03	84	226	9.33	0	52,170
Day14	7.52	61	189	7.21	83	210	8.80	0	61,703

On Day 13 the waste valve automatically opened, which in turn led to a lower sludge mass present in the system. This is well illustrated on Figure 33 where the SBH is lower on Day 14 compared to the previous day.

Figure 34 shows that the VFA concentration is around 800 mg/L at 0.3m of height for Day13, which corresponds to a low alkalinity concentration of 137mg/L and a pH value of 4.70. On the other hand, Day 14 shows instead a higher value of alkalinity, i.e., 813mg/L, and a lower VFA concentration of 525mg/L. While the higher sodium bicarbonate addition on Day 14 of 61,703mg HCO_3^- /L (Table 26) is associated with a higher bicarbonate alkalinity concentration, the lower VFA could in part be explained by considering the waste valve opening.

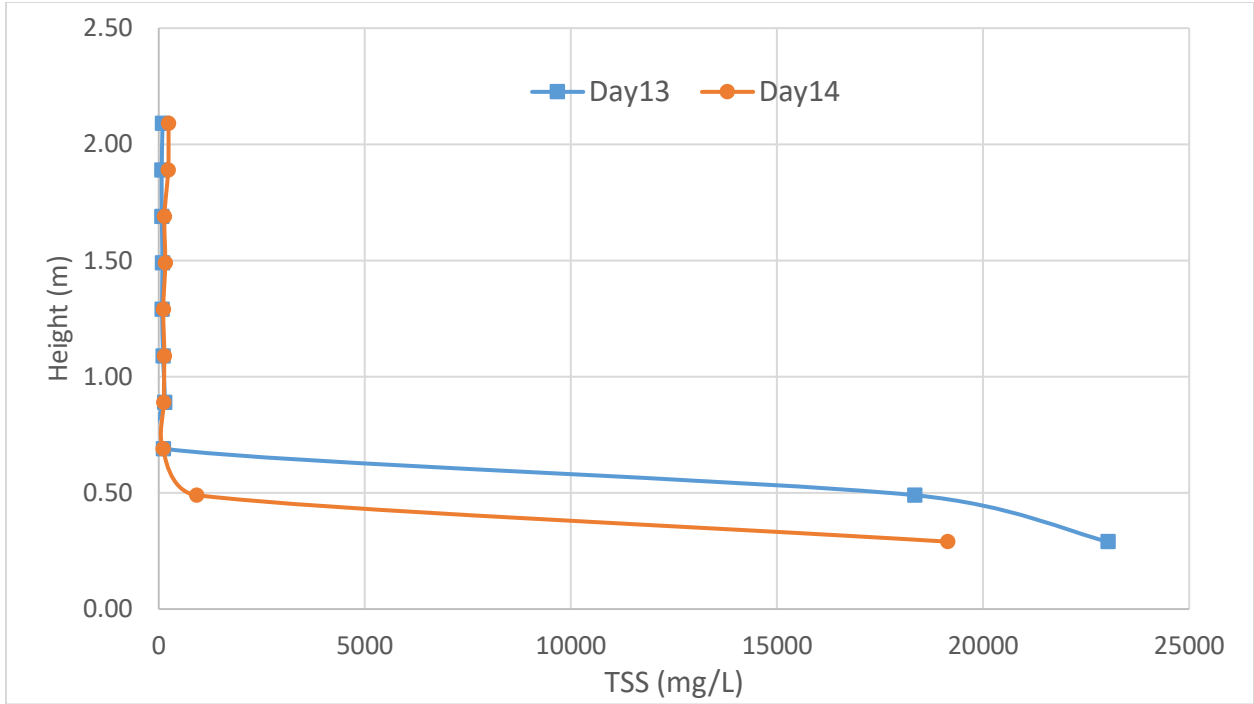


Figure 33: TSS concentration profile in primary clarifier (Stage #8).

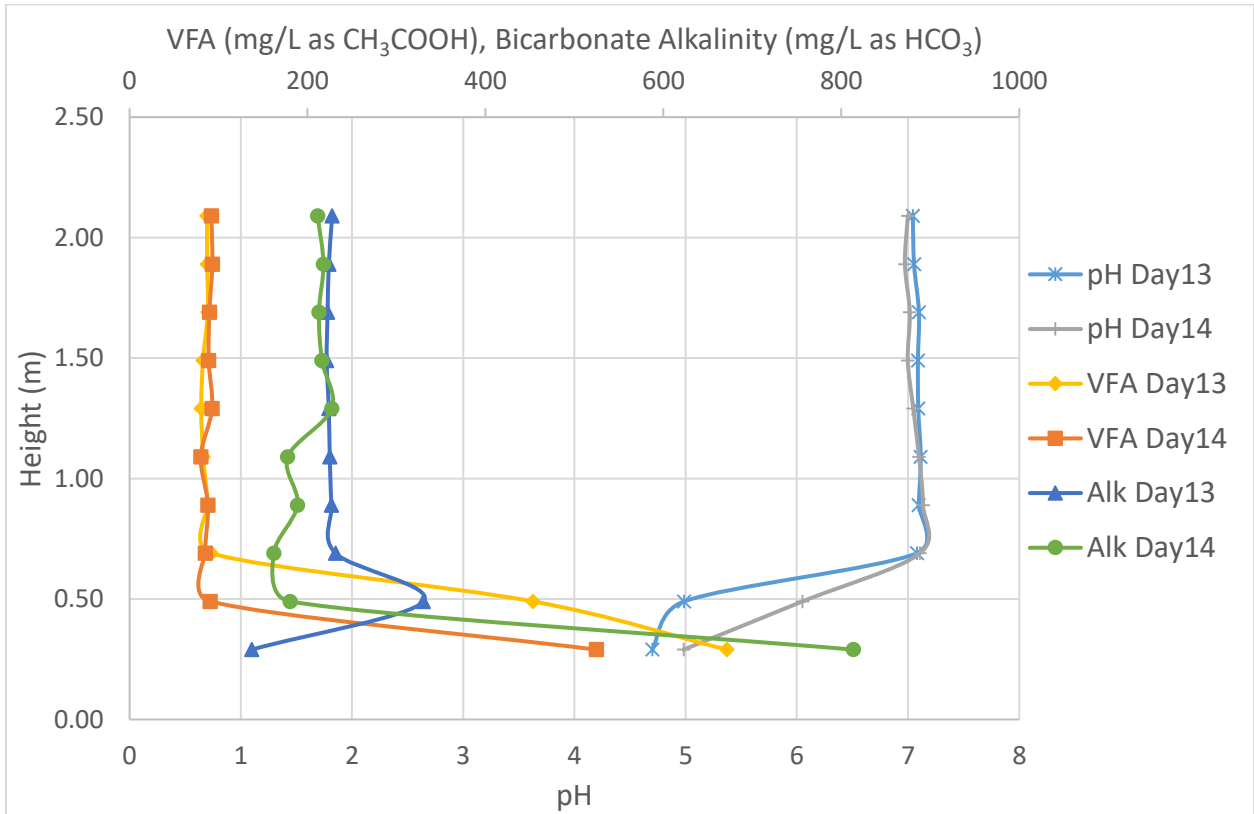


Figure 34: Comparison of pH, VFA and bicarbonate alkalinity profiles for Day 13 and 14 (Stage #8).

In case of FeCl₃ and NaHCO₃ addition, the solids removal efficiency is 65% (Table 27), which is in line with Stage #7, where a value of 63% was measured (Table 24).

As mentioned earlier, the coagulant dosage seems to be beneficial for VFA enhancement. In fact, in Stage#7 and #8, the VFA concentration in the sludge blanket showed higher values than the other stages. In particular, for Stage #8, Table 27 indicates 452 mg/L of VFA, while for Stage #7 the measured VFA concentration was 488 mg/L (Table 24).

Again, as seen for Stage #7, FeCl₃ addition has the additional advantage of removing the reactive phosphorus by chemical precipitation with a removal efficiency of 12%.

Although an outlet bicarbonate alkalinity concentration of 210 mg/L was measured, higher than the inlet (i.e., 189 mg/L), the pH value is 7.21, lower than the inlet one. It seems that, while the iron addition seems to lower the pH, the sodium bicarbonate dosage is beneficial for increasing the buffer capacity of the system. In particular, 1191 mg/L of bicarbonate alkalinity is reported for the waste location, and it seems to not negatively affect the fermentation performance.

Table 27: Lab measurements and removal efficiency based on triplicates and duplicates for total and soluble concentrations, respectively (Stage #8).

		SOURCE			E%
		IN	OUT	WASTE	
TSS	mg/L	382 ± 31	134 ± 12	16201 ± 2413	65 ± 10%
VSS	mg/L	363 ± 27	120 ± 12	15726 ± 2350	67 ± 10%
VSS/TSS		95 ± 11%	89 ± 13%	97 ± 21%	
T-COD	mg/L	806 ± 76	408 ± 3	24893 ± 151	49 ± 11%
S-COD	mg/L	127 ± 1	134 ± 2	922 ± 5	-6 ± 1%
P-COD	mg/L	680 ± 76	275 ± 3	24422 ± 152	60 ± 14%
VFA	mgCH ₃ COOH/L	61	83	452	-37%
T-TN	mg/L	47.5 ± 1.2	46.3 ± 1.1	292.7 ± 9.9	2 ± 3%
S-TN	mg/L	40.2 ± 0.8	39.1 ± 0.1	22.8 ± 0.2	3 ± 2%
NH₃-N	mg/L	34.5 ± 0.1	32.0 ± 0.4	14.8 ± 0.1	7 ± 1%
TP	mg/L	17.1 ± 0.0	15.2 ± 0.1	86.3 ± 0.6	11 ± 1%
PO₄-P	mg/L	11.8 ± 0.1	10.4 ± 0.0	14.5 ± 0.1	12 ± 1%
PO₄-P/TP		69 ± 1%	68 ± 1%	17 ± 1%	
Alkalinity	mgHCO ₃ /L	189	210	1191	
pH		7.52	7.21	5.16	

From Table 28 it can be deduced that a VFA production of 22.4 mg/L, and a VFA yield of 61.6 mg/g VSS is obtained, which indicates that overall VFA enhancement is occurring.

Table 28: Process performance parameters (Stage #8).

	IN	OUT	WASTE
S-COD/T-COD	16%	33%	4%
VFA/S-COD	48%	62%	49%
COD solubilisation (mg/L)		7.0	
Hydrolysis yield		1%	
VFA production (as mgCH ₃ COOH/L)		22.4	
VFA yield (as mgCH ₃ COOH/ g VSS)		61.6	

4.5 Effect of Temperature

Even if no heating coil or any other system was controlling the temperature, temperature data measured by the online probes throughout the different seasons were available. By comparing these data with the process performance during the different experiments, the effect of temperature on the fermentation and solubilisation processes can be assessed.

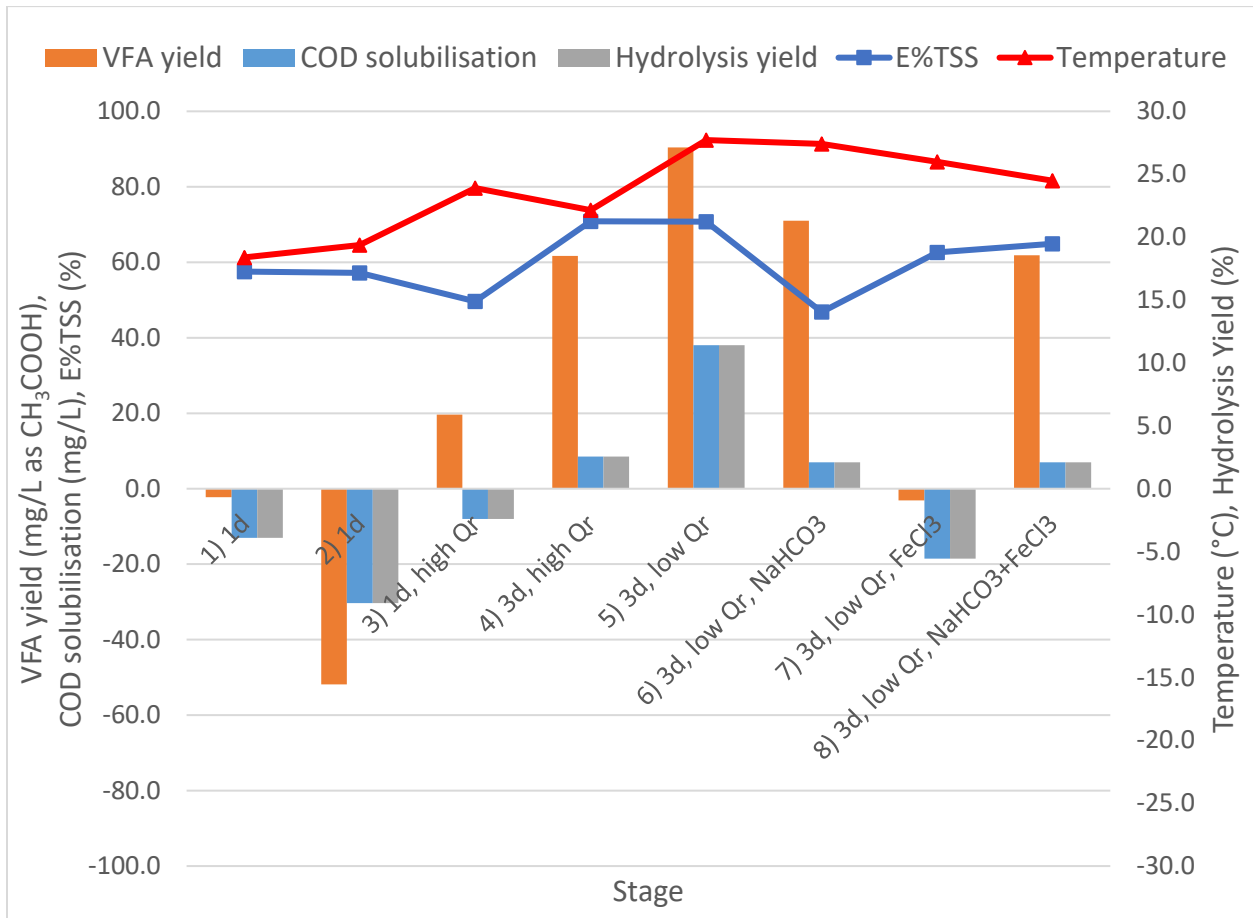


Figure 35: Temperature effect on VFAs yield, COD solubilisation, solids removal efficiency (E%TSS) and hydrolysis yield during the different stages.

Except for the stage (#7) where only the coagulant was dosed, when the water temperature was above 22°C and the internal return line was present, the *VFA yield* and the other parameters used for tracking the fermentation performance (namely, *COD solubilisation*, *hydrolysis yield*) showed positive values. In particular, as Figure 35 clearly shows, the highest performance was reached when the temperature peaks to values of about 28°C. In fact, the measured values in this case were:

- VFA yield = 90.5 mgCH₃COOH/L
- COD solubilisation = 38.0 mg/L
- Hydrolysis yield = 5.5%

4.6 Data Analysis and Statistical Analysis with R

For the following sections, the two tables below (Table 29 and Table 30) were used to produce plots and run the ANOVA analysis on *R*. Table 29 summarizes the main important findings of the study, divided in factors (operating conditions) and performance of the reactive primary clarifier. Table 29 differs from Table 30 due to the observations reported. In particular, in Table 30 just observations (Stages) that achieved the steady state conditions are reported.

Table 29: Summary of the operating conditions and performance for stages #1 to #8.

Stage	Conditions							Performance	
	Q _R	SRT desired	SRT actual	NaHCO ₃	FeCl ₃	T	Extra days in SS	E%TSS	VFA
	%Q _{IN}	d	d	mgHCO ₃ /L	mg/L	°C	d	%	mgCH ₃ COOH/L
1	0	1	0.74	0	0	18.4	3	58	-2.2
2	0	1	1.51	0	0	19.4	0	57	-51.8
3	50	1	1.51	0	0	23.9	1	50	19.7
4	50	3	1.83	0	0	22.1	-2	71	61.7
5	14	3	0.8	0	0	27.7	9	71	90.5
6	14	3	0.74	100	0	27.4	-1	47	71.1
7	14	3	1.16	0	20	26	-1	63	-3.1
8	14	3	1	100	20	24.5	6	65	61.8

Table 30: Summary of the operating conditions and performance for stages in steady state conditions.

Stage	Conditions							Performance	
	Q_R	SRT desired	SRT actual	NaHCO_3	FeCl_3	T	Extra days in SS	E% TSS	VFA yield
	% Q_{IN}	d	d	mg HCO_3/L	mg/L	$^\circ\text{C}$	d	%	mg $\text{CH}_3\text{COOH}/\text{L}$
1	0	1	0.74	0	0	18.4	3	58	-2.2
2	0	1	1.51	0	0	19.4	0	57	-51.8
3	50	1	1.51	0	0	23.9	1	50	19.7
5	14	3	0.8	0	0	27.7	9	71	90.5
8	14	3	1	100	20	24.5	6	65	61.8

4.6.1 Analysis of Plotted Data

Only significant and meaningful plots are reported in this section. Remaining graphs could be found in A.9 (Appendix).

From Figure 36 it can be seen that, except for Stage7 (FeCl_3 addition), for a positive recirculation ratio, i.e. from the implementation of the internal recirculation, a VFA enhancement in the effluent can be observed. Also, it seems that a lower recirculation ratio of 14% is better than 50%, since the VFA yield shows average values of 74.5 and 40.7 mg $\text{CH}_3\text{COOH}/\text{L}$, respectively.

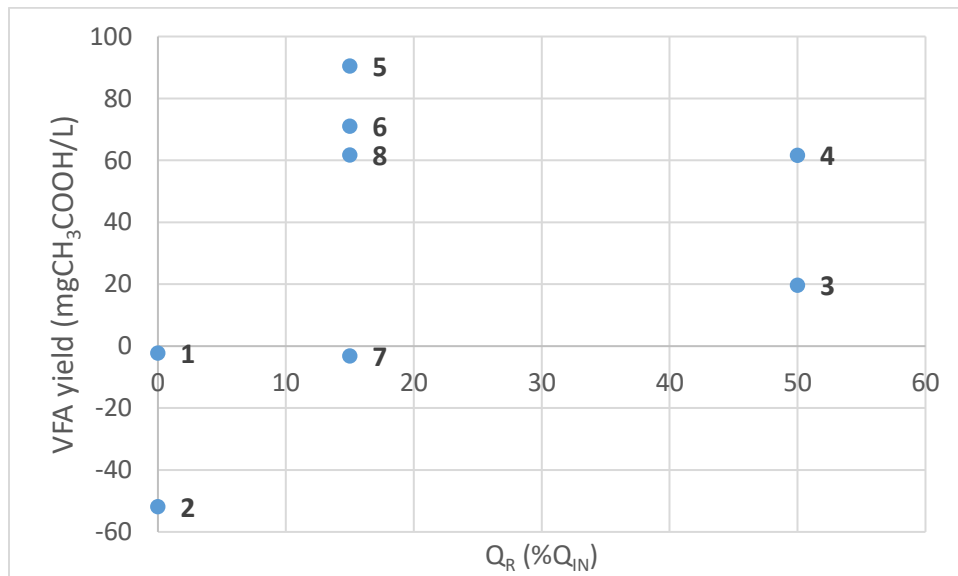


Figure 36: Effect of the internal recirculation ratio on the VFA yield for stages #1 to #8.

In Figure 37 and Figure 38, if just the positive x-axis values are considered (i.e. number of elapsed days are larger than the required ones), it seems that the more the reactive clarifier runs under steady-state conditions, the better the performance both for E%TSS, and VFA yield. However, it should be said that the extra days period might be also correlated with other factors, inducing then to a false relationship since the true effects might be confounded with other effects.

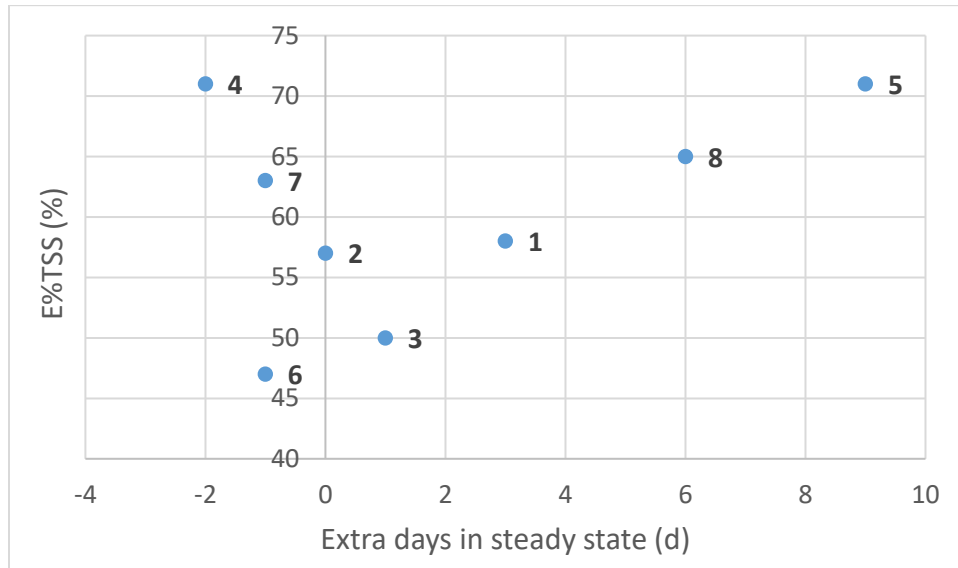


Figure 37: TSS removal efficiency versus extra days in steady state conditions for stages #1 to #8.

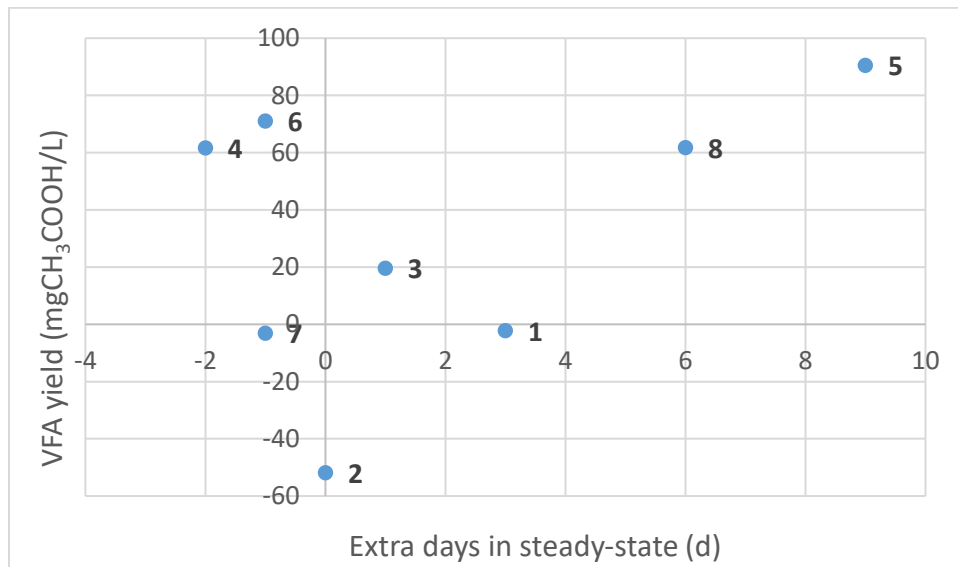


Figure 38: VFA yield versus extra days in steady state conditions for stages #1 to #8.

As can be noticed in Figure 39, higher temperatures generally have positive effect in terms of increasing the VFA yield. Also, it seems to be linearly correlation between temperature and VFA yield exist.

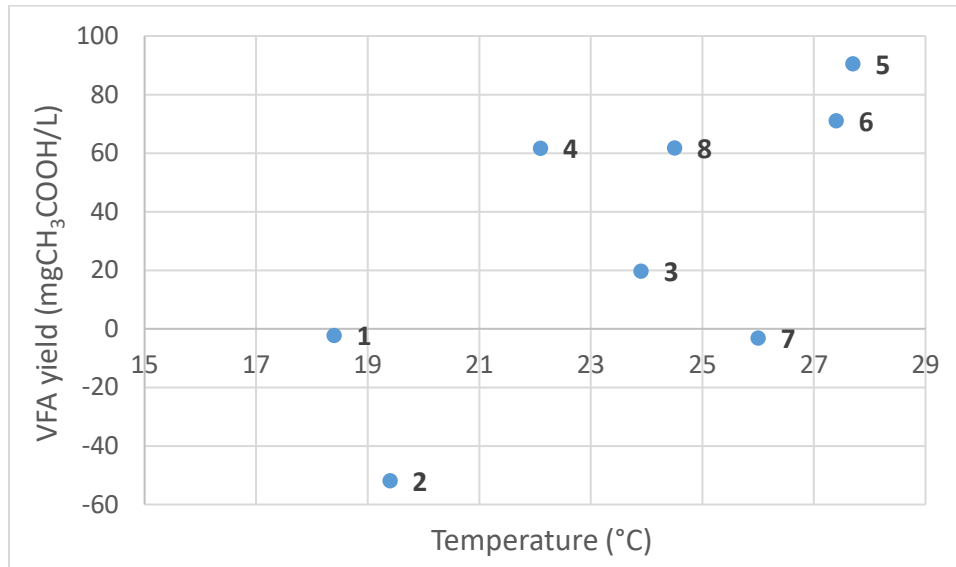


Figure 39: Effect of the temperature on the VFA yield for stages #1 to #8.

Steady state

In this section only observations that achieved steady state conditions are considered.

Plot (a) and (b) of Figure 40 shows that the highest values of solids removal efficiency and VFA yield, respectively, are achieved for a low recirculation ratio (14%). It is interesting to observe that the condition without any internal recirculation did not lead to any VFA enhancement, this was probably due to the absence of elutriation process happening. Also, a high recirculation ratio of 50% (Stage #3) had negative effect to solids removal because it might disturb the sedimentation process of the particles, or even re-suspend the settled one due to excessive turbulence in the sedimentation zone.

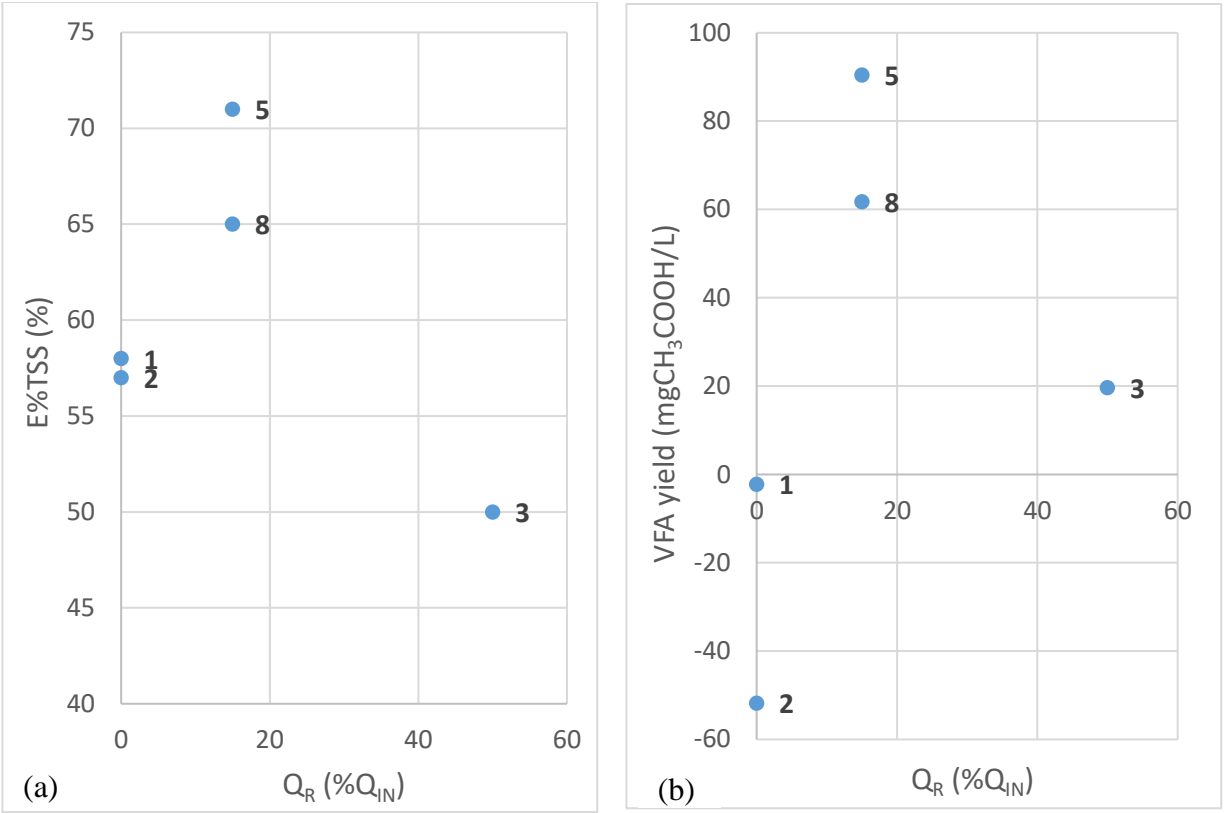


Figure 40: Effect of the internal recirculation ratio on (a) TSS removal efficiency and (b) VFA yield for stages in steady state conditions.

In Figure 41 for the desired SRT plots (a) and (b), a desired SRT of three days compared to one day, had a clear positive influence in both the investigated performance: it leads to higher solids removal and VFA yield. However, when considering the actual SRT (plot (c) and (d)), a SRT of less than one day seems to lead to better performance.

From Figure 42 a clear conclusion cannot be drawn from the obtained data since for 0mg/L of $NaHCO_3$ dosage, and, on the other side, for 100mg/L dosage, only one observation is available. Therefore, more data are needed to understand the effects of sodium bicarbonate dosage on the reactive clarifier's performance. Same as $NaHCO_3$ addition, no clear effects of $FeCl_3$ on the performance can be observed (see plots in the Appendix).

In Figure 43, the extra days in steady state conditions are plotted against the performance parameters. It seems that the more the primary clarifier run under the same operating conditions, the highest the particle removal, and the VFA yield as well. An increasing linear trend can be clearly seen in both graphs. In fact, if just the positive x-axis is considered, it seems that the more the system operates in steady-state conditions, the better the performance both for E%TSS, and VFA yield. However, it should be said that the start-up period might be correlated with other

factors such as temperature, leading then to false relationships since the true effects might be confounded with other effects.

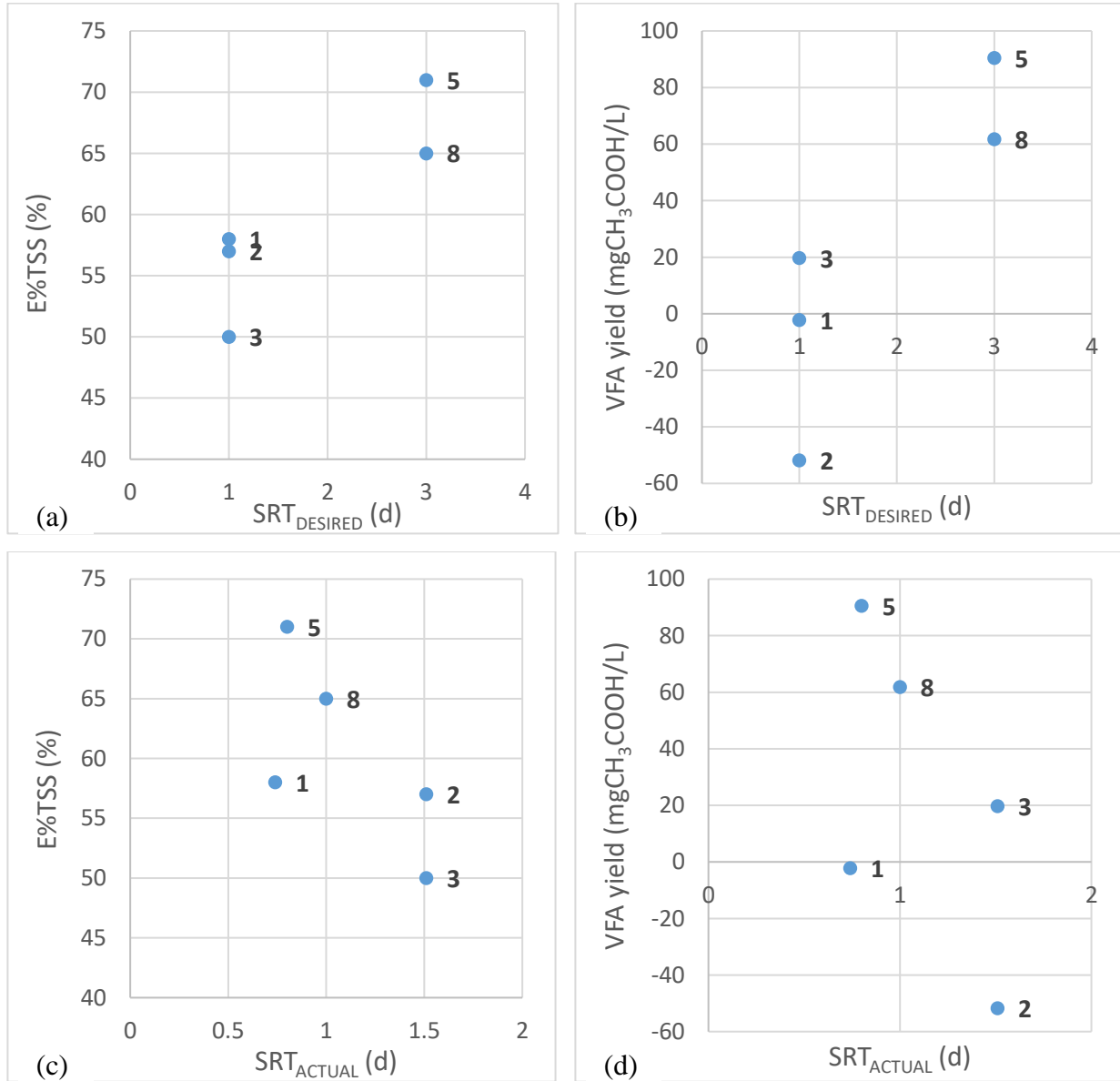


Figure 41: Effect of the desired and actual SRT (a, c) TSS removal efficiency and (b, d) VFA yield, respectively, for stages in steady state conditions.

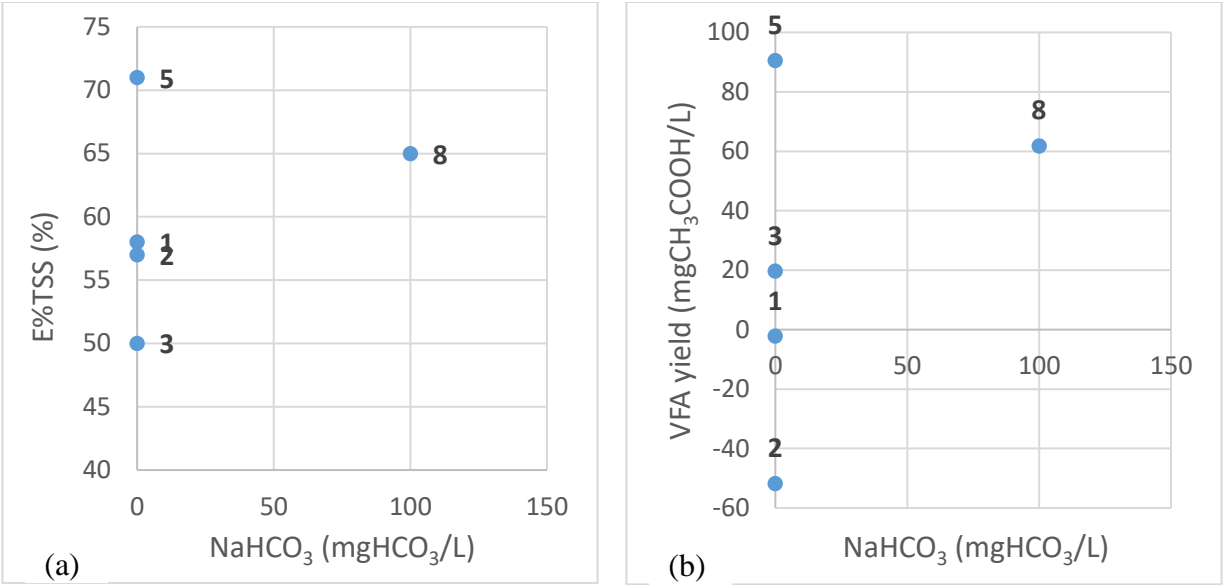


Figure 42: Effect of sodium bicarbonate addition on (a) TSS removal efficiency and (b) VFA yield for stages in steady state conditions.

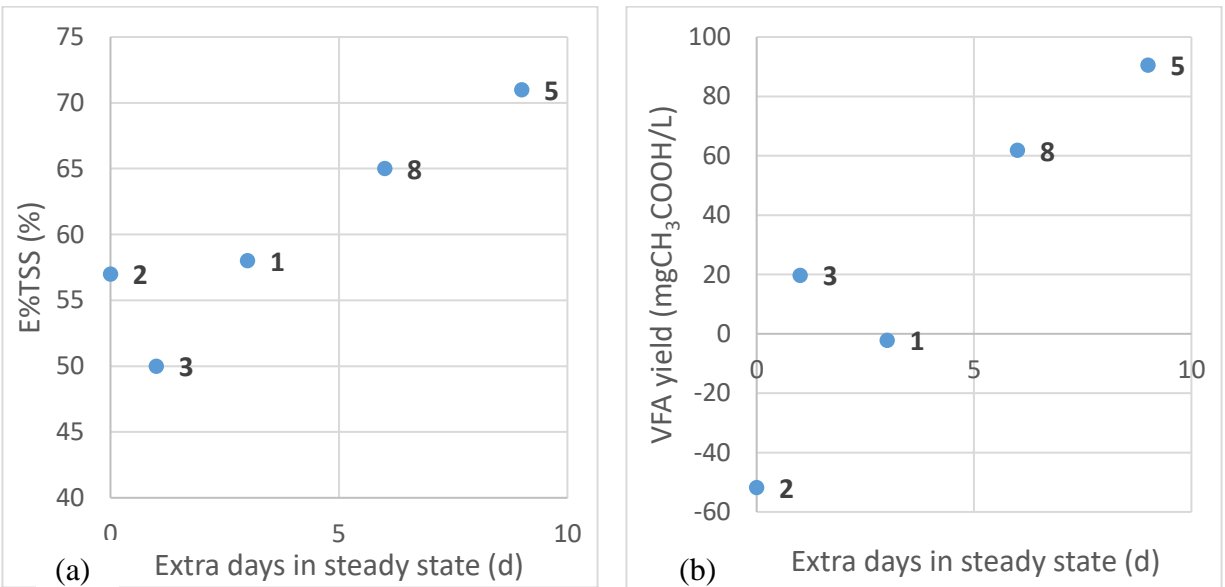


Figure 43: Extra days in steady state conditions versus (a) TSS removal efficiency and (b) VFA yield for stages in steady state conditions.

Figure 44 indicates that higher temperatures lead to higher performance, specially for the VFA production. This could be explained by considering the higher rate of biochemical reactions that occur in the sludge blanket. It is indeed evident from literature that hydrolysis rates could be enhanced through heat application. However, the temperature effect might be correlated with other factors.

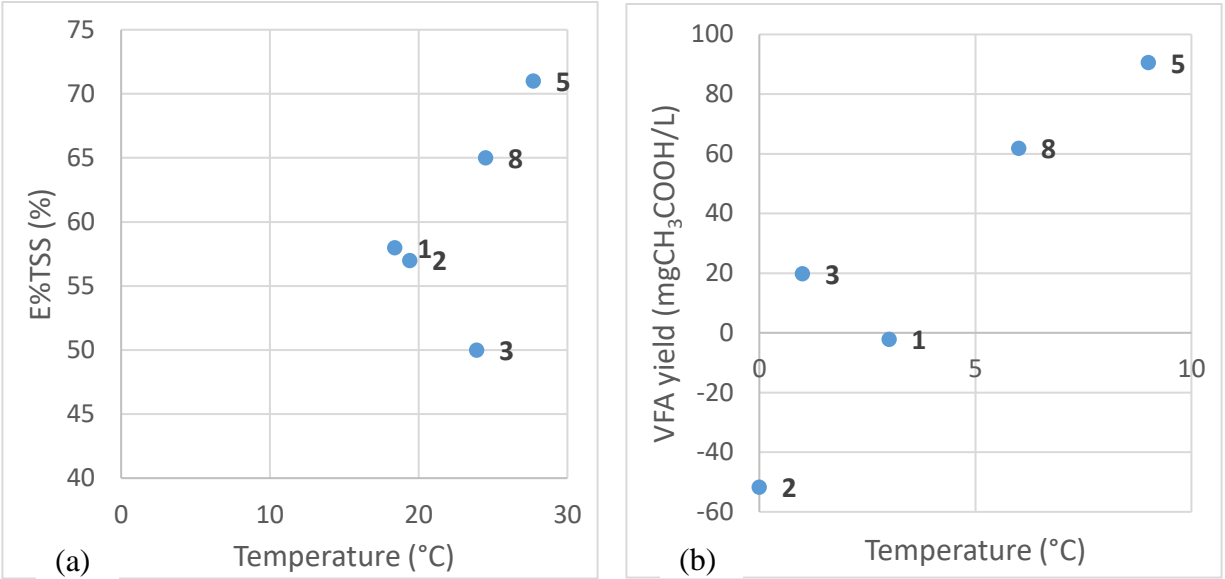


Figure 44: Effect of temperature on (a) TSS removal efficiency and (b) VFA yield for stages in steady state conditions.

4.6.2 ANOVA Analysis (R)

A statistical analysis on the obtained data was performed through R software, and the outputs are presented. Only desired SRTs are considered rather than actual ones, since the actual SRTs are not fixed, and they could not be treated as a factor with just two levels. In fact, if the ANOVA test is nevertheless performed, the following warning messages appear:

```

warning messages:
1: In anova.lm(model1) :
  ANOVA F-tests on an essentially perfect fit are unreliable
2: In anova.lm(model2) :
  ANOVA F-tests on an essentially perfect fit are unreliable

```

In fact, more than one observation per group has to be provided in order to perform an F-test, which is the ratio of the mean square of the selected factor per the mean square of the residuals. Since the ANOVA test, test precisely the variances, having just one observation per group would lead to a zero standard deviation (meaning that there is no variance in the sample), or an infinite t-value, which has no sense. In other words, the number of available observations (stages) are too limited to come up with any variance tests.

Table 31 shows the ANOVA table where the VFA yield was set as the experiment random variable. As it can be seen under the last column “Significance”, none of either the factors or their interactions resulted as significant effects in determining the outcome of the experiment.

Table 31: ANOVA table for VFA yield response.

Source	Degrees of Freedom	Sum of Square	Mean Sum of Square	F value	Pr (>F)	Significance
SRTdes	1	8628	8628	7.014	0.23	
Q _R	2	1489	745	0.605	0.673	
NaHCO ₃	1	518	518	0.421	0.634	
FeCl ₃	1	2647	2647	2.152	0.381	
NaHCO ₃ :FeCl ₃	1	1777	1777	1.444	0.442	
Residuals	1	1230	1230			

In Table 32 the TSS removal was set as the experiment response, instead. In this case, all the factors seemed to be more or less significant in the TSS removal efficiency with p-values smaller than 0.1 (“.” means $0.05 < p < 0.1$, “*” means $0.01 < p < 0.05$). In particular, significant factors with p-values less than 0.05 (*) were (in significance order): (i) “NaHCO₃:FeCl₃”, the interaction factor between the two dosed chemicals, (ii) “SRTdes”, the desired SRT, and (iii) “NaHCO₃”, sodium bicarbonate addition. The estimated coefficients for these factors are presented in Table 33. It can be seen that a higher SRT lead to better solids removal performance, because the coefficient estimate for “SRTdes” has a positive value. In contrast, due to their negative coefficient estimates, the internal recirculation and the chemical additions lead to lower solids removal performance.

Table 32: ANOVA table for TSS removal efficiency response.

Source	Degrees of Freedom	Sum of Square	Mean Sum of Square	F value	Pr (>F)	Significance
SRTdes	1	132.3	132.3	264.6	0.0391	*
Q _R	2	109.7	54.85	109.7	0.0674	.
NaHCO ₃	1	121	121	242	0.0409	*
FeCl ₃	1	25	25	50	0.0894	.
NaHCO ₃ :FeCl ₃	1	169	169	338	0.0346	*
Residuals	1	0.5	0.5			

Table 33: Coefficient estimates for TSS removal efficiency response.

Coefficient	Intercept	SRTdes	Q _R (14%)	Q _R (14%)	NaHCO ₃	FeCl ₃	NaHCO ₃ :FeCl ₃
Estimate	47.000	10.500	-7.500	-7.500	-0.240	-0.400	0.013

Chapter 5: Conclusions

Achieving fermentation and VFA production without affecting the solids removal efficiency seems to be a possible way for a primary clarifier, to become a reactive primary settler. Some fermentation reactions were established in the sludge blanket by providing just one day of sludge retention time. However, elutriation made through implementation of an internal recirculation line was key in the process. Just after its application, some extra VFA was being released in the effluent.

Coagulant addition affects the VFA yield, without increasing the solids removal efficiency of the case study's primary settler. However, its implementation is useful under a soluble phosphorus control strategy. In addition, when sodium bicarbonate is added as well, they are able to positively affect the soluble phosphorus removal.

The best configuration for VFA enhancement turned out to be an actual SRT of at least one day, and a low internal recirculation flow. Long start-up periods are needed, because higher VFA yields are reported after a longer period of running the operation in a certain way. Fermentation biomass needs a certain time before it can acclimatise and perform the fermentation. For advanced soluble phosphate control, the dosage of ferric chloride and sodium bicarbonate can play a positive role by avoiding the re-release.

A possible scale-up of this system in a real WWTP could be operationally easy, but issues may arise regarding the rising sludge phenomena. Through a scum skimmer, the rising sludge can be controlled.

Furthermore, regarding the carried out statistical analysis, the ANOVA approach was clearly limited and any conclusions is misleading. Limitations were mainly due to: (i) limited numbers of data points, (ii) undesigned data set, (iii) high variability of data.

Chapter 6: Recommendations and Suggestions for Further Research

Based on the experimental findings of this research, recommendations and suggestions for the implementation and enhancement of the experimental set-up or operation conditions are presented.

The flexible tube height was set at 0.50m from the bottom. However, a lower or higher height might actually have an impact on both the performance parameters. For example, a higher flexible tube's end might increase the VFAs in the primary effluent.

Moreover, during the implementation of the recirculation line several pipe clogging were faced due to the presence of rags and fibrous materials. Figure 45 shows the type of materials that were found at either the pump's rotor or inlet pipe, which caused its clogging. To limit the clogging, the mesh size of the y-strainer located at the primary inlet were reduced (from the third one to second one in Figure 46), and the strainer was kept cleaned following a two days cleaning schedule. However, a long-term solution would consider to implement a shredder or a grinder in order to destroy this fibrous material.



Figure 45: Materials found in the recirculation line pump causing the clogging.

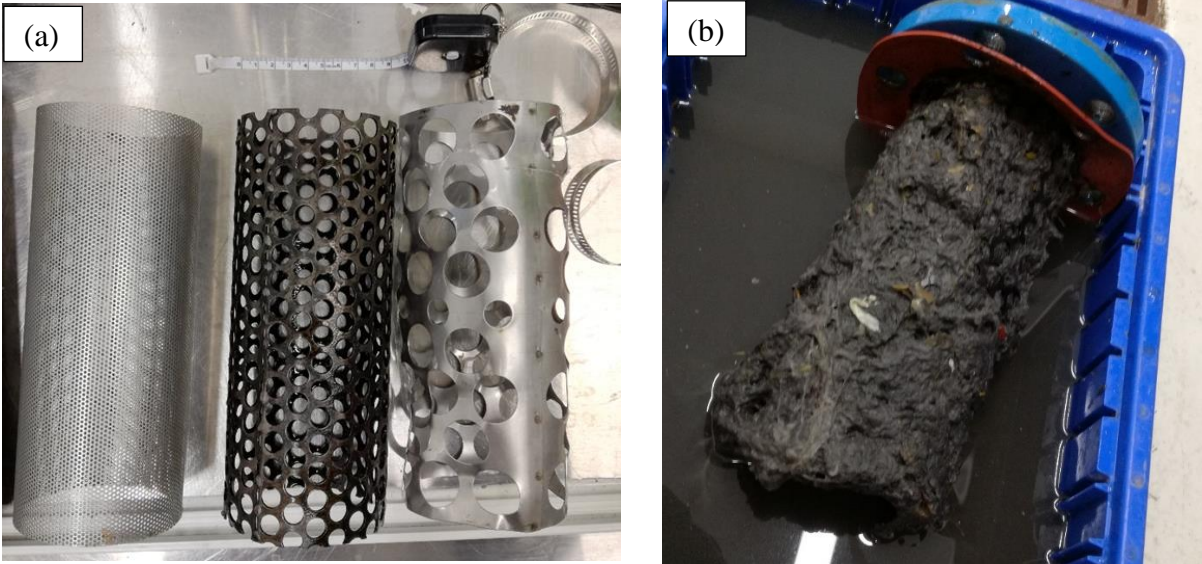


Figure 46: (a) Primary inlet y-strainers with different mesh sizes and (b) collected material on the y-strainer after 16 hours from cleaning.

In addition, since the study here involved four factors rather than one only, a factorial design with a two levels of treatment is generally recommended [23]. Indeed factorial design, due to their efficiency, are preferred over a one-factor-at-a-time experiment. Especially in a research study like this one, where interactions may exist, a factorial design is able to consider them as well. In fact, through a factorial design main effects and interactions and their significance are usually deduced. Furthermore, while a full factorial design consist in running all the possible combinations (both treatments and levels) of the experiment, a fractional factorial is just a part of it, instead. For this four factors experiment, a full factorial would require N experiments, where $N = 4 \times 2 \times 3 \times 2 \times 2 = 96$, which is a very large number of observations and time or resource constraint would be certainly faced. On the other hand, a fractional design allow running just a part of the experiment. In a second moment, it could be still implemented with the remaining fractional runs to get the full factorial matrix.

The next steps of the research may thus involve:

1. develop and calibrate a reactive primary clarifier model;
2. adjust the height of the internal recirculation tube;
3. perform a 2^k factorial experiment;
4. identify the microbial communities involved;
5. run a cost-benefit analysis (chemical, pumping cost).

Appendix

Equation 4: Mass accumulation of the sludge blanket.

$$Accumulation = SRT(L_{IN} + L_E + L_W)$$

A.1: One day SRT and no internal recirculation flow rate (Stage #1)

Probe values

Figure 47 to Figure 52 show the data collected by the online probes located at the primary effluent, some of them compared with the lab measurement values obtained from the composite samples (straight line).

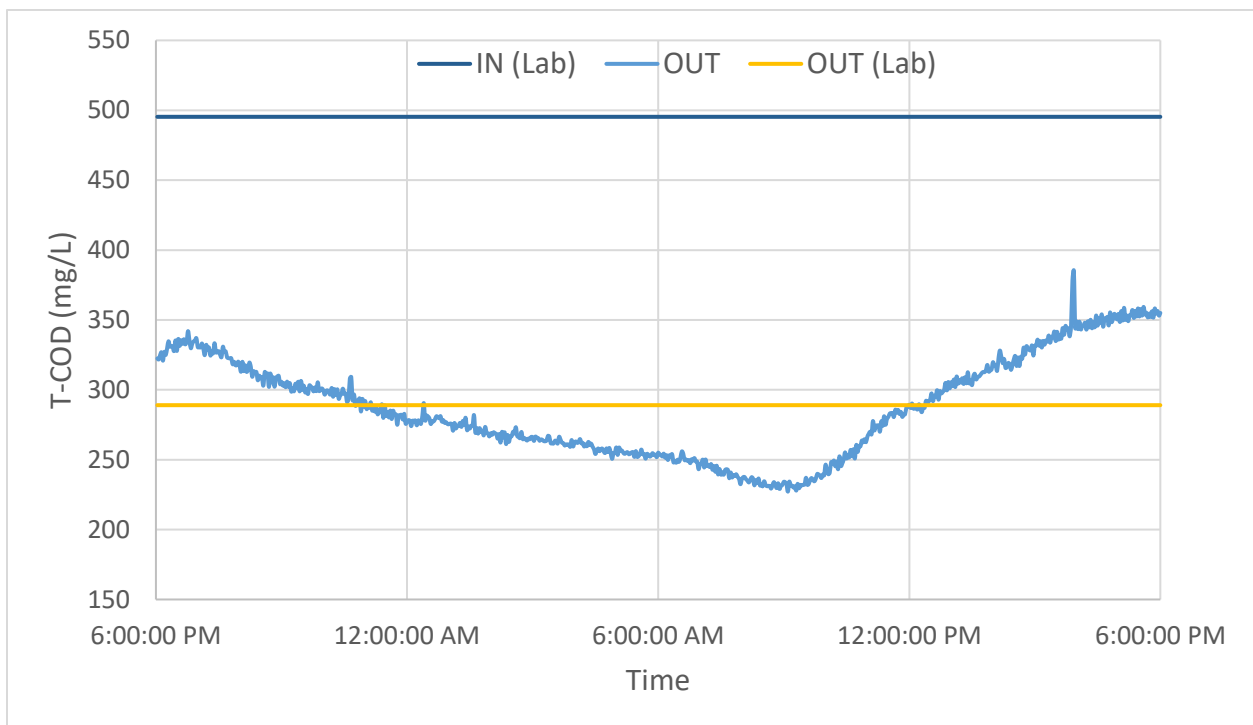


Figure 47: Total COD concentration from lab measurements on composite samples (influent and outlet) and online probe located at the outlet (Stage #1).

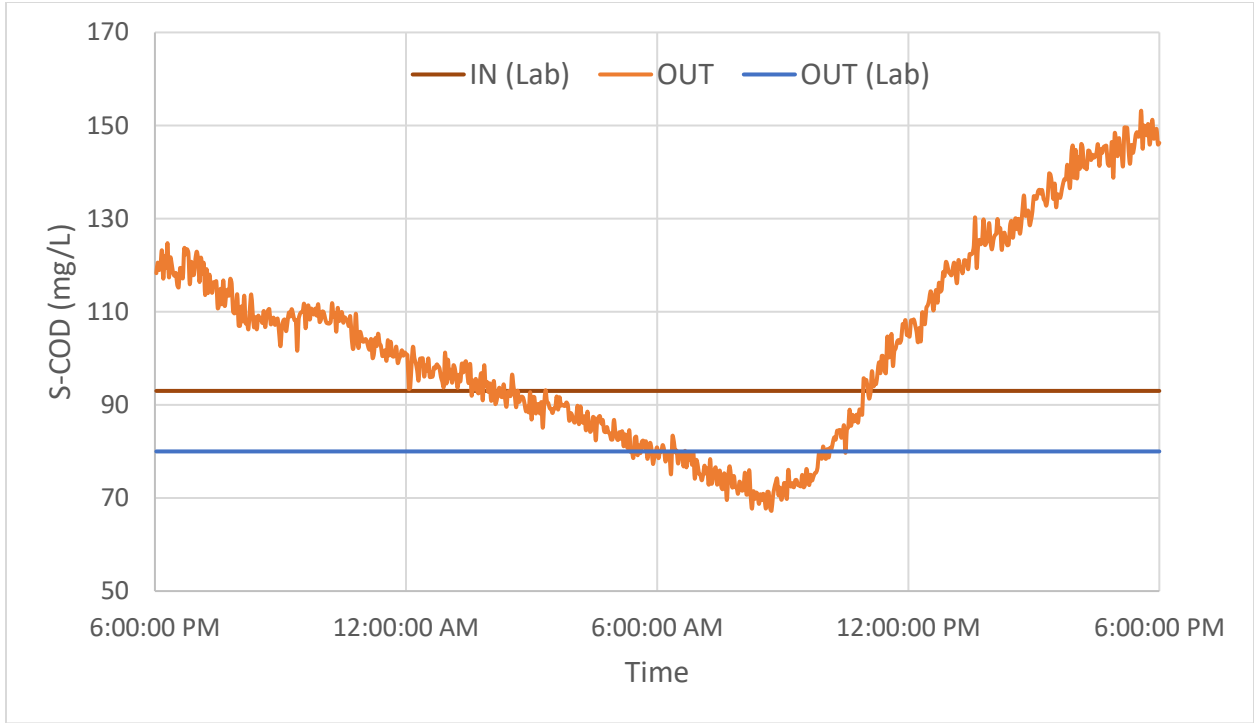


Figure 48: Soluble COD concentration from lab measurements on composite samples (influent and outlet) and online probe located at the outlet (Stage #1).

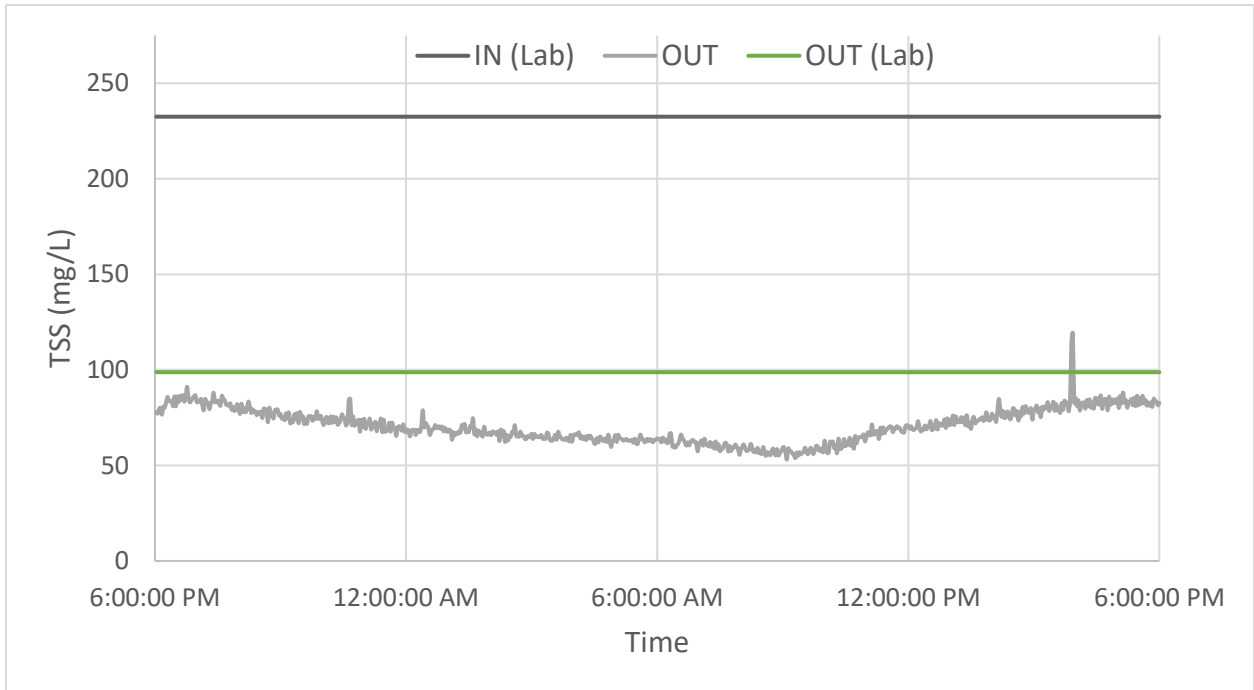


Figure 49: TSS concentration from lab measurements on composite samples (influent and outlet) and online probe located at the outlet (Stage #1).

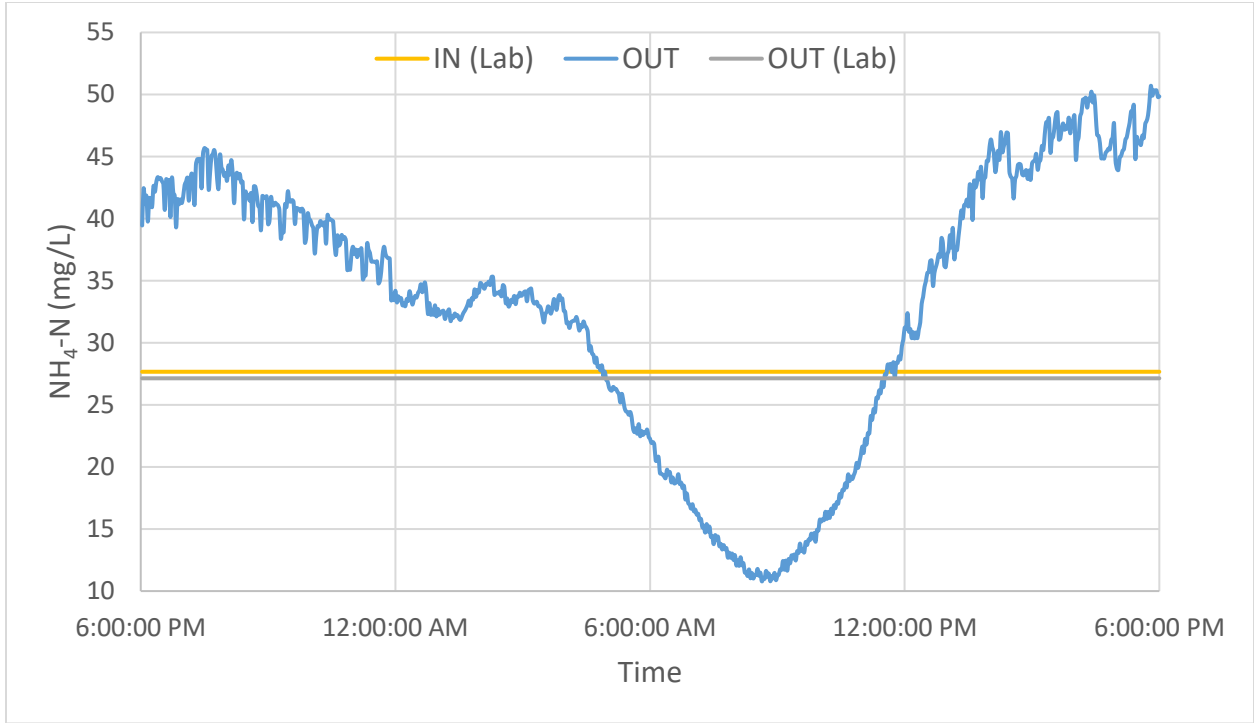


Figure 50: Ammonium concentration from lab measurements on composite samples (influent and outlet) and online probe located at the outlet (Stage #1).

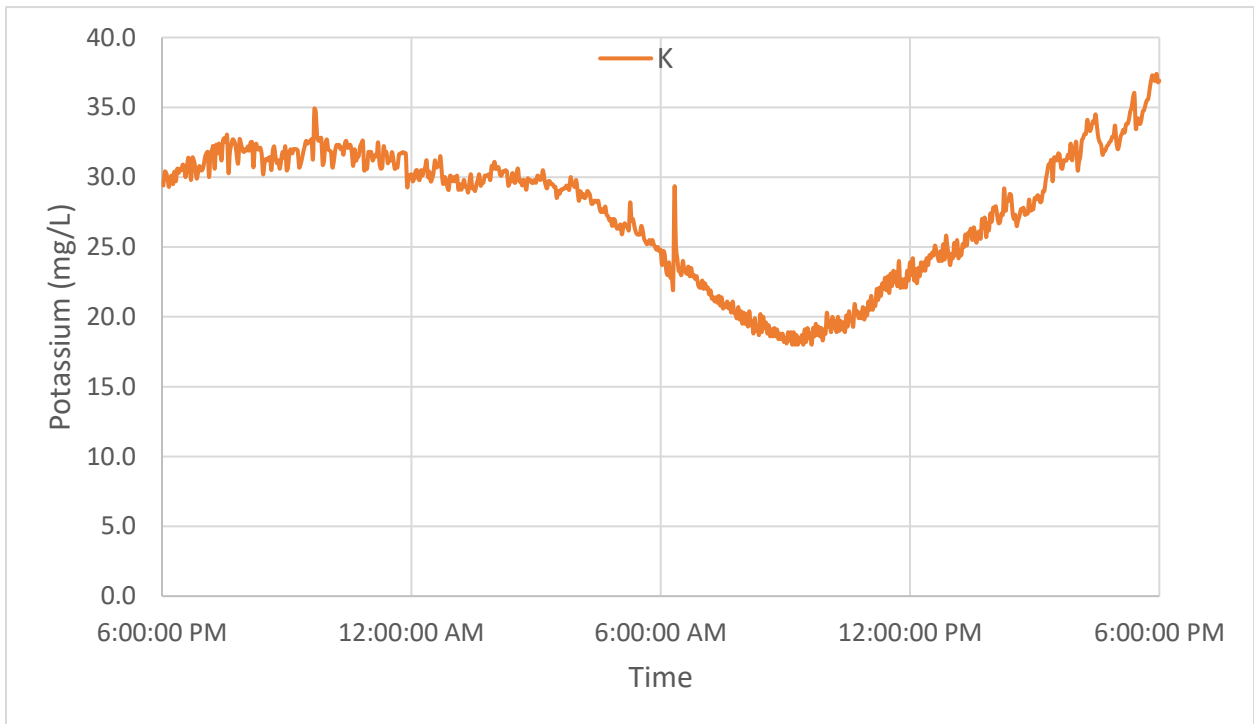


Figure 51: Potassium concentration trend at the outlet (Stage #1).

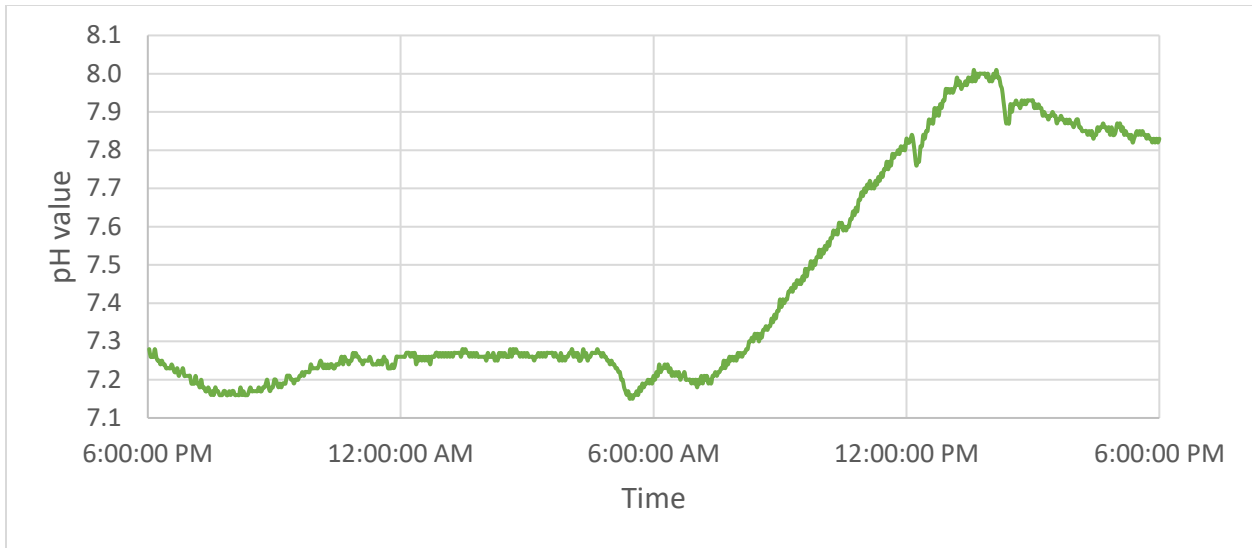


Figure 52: pH trend at the outlet (Stage #1).

Figure 52 shows that the pH profile is varying a lot during the day that remarks a low alkalinity capacity of the system. Furthermore, it can be seen how the pH has low value during the night (i.e. around 7.2) and then start to rise in the morning due to urea that arrives to the plant, which perfectly agrees with the ammonia trend (Figure 50).

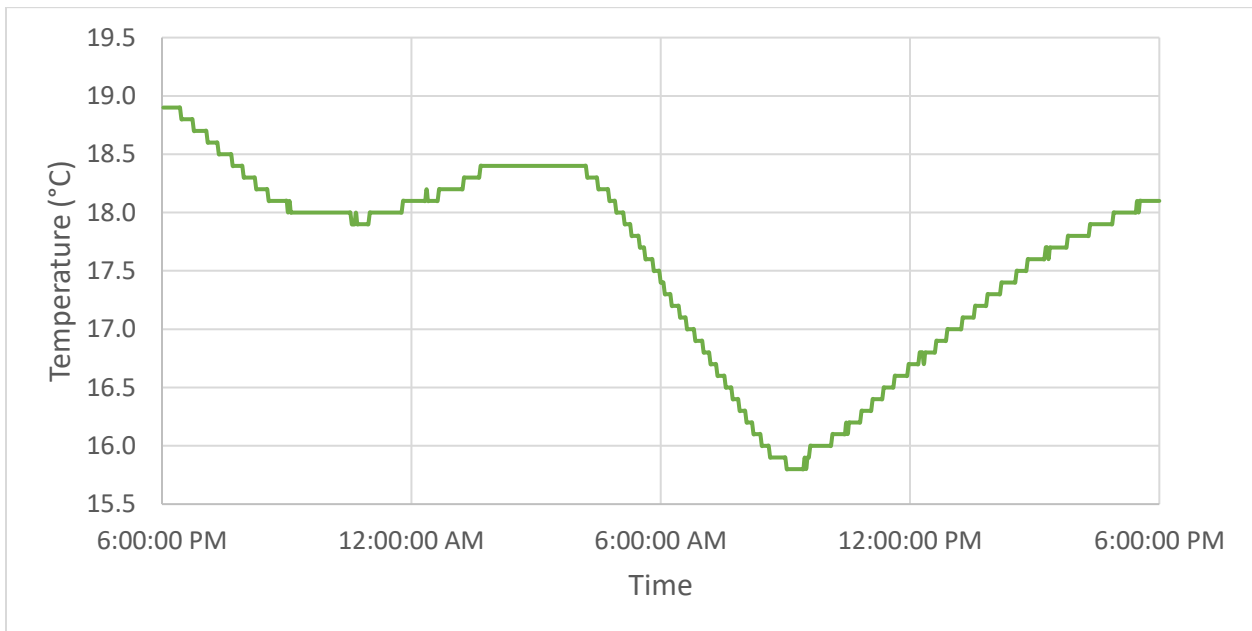


Figure 53: Temperature trend at the outlet (Stage #1).

From the online probes, it is easy to note how the concentrations drop during the night and start to rise again in the morning. This diurnal effect is mainly due to the feeding water characteristics, i.e. municipal wastewater from the nearby university campus.

Main parameters and mass balance

Table 34: Summary of the main parameters for Stage #1.

Set-Up condition summary - Main operating parameters											
Volumes			TSS concentrations			Flow rates			Retention Times		
V ₁	V ₂	V _{TOT}	X _{IN}	X _E	X _R	Q _{IN}	Q _W	Q _R	HRT	HRT _{EFF}	SRT
L	L	L	mg/L	mg/L	mg/L	m ³ /d	m ³ /d	m ³ /d	h	h	d
1739	461	2200	232	99	4515	26.4	0.096	0	2.0	2.0	0.74
Heights			Mass Loads			Mass		Removal Efficiency			
H _{TOT}	H ₁	SBH	L _{IN}	L _E	L _W	m _{BLANKET}	Accumulation	E%TSS			
m	m	m	g/d	g/d	g/d	g	g	%			
2.29	1.49	0.80	6138	2380	433	2081	2470	61%			

The removal efficiency of TSS slightly differ to what reported in Table 9 due to the fact that in Table 34 the calculation is based on the outlet and inlet mass loads, rather than the solely concentrations. Regarding the SRT, it should be said that the X_R value (contained in the SRT equation) comes from the waste composite sample, and not from the 2.00 m immersion sample. In addition, the sludge age equals to 0.74 d is close to the desired value of 1 day.

The mass accumulation, given by Equation 4, is almost equal to the estimated mass of the sludge blanket. This underlines the fact that the SRT was indeed equal to 1 d.

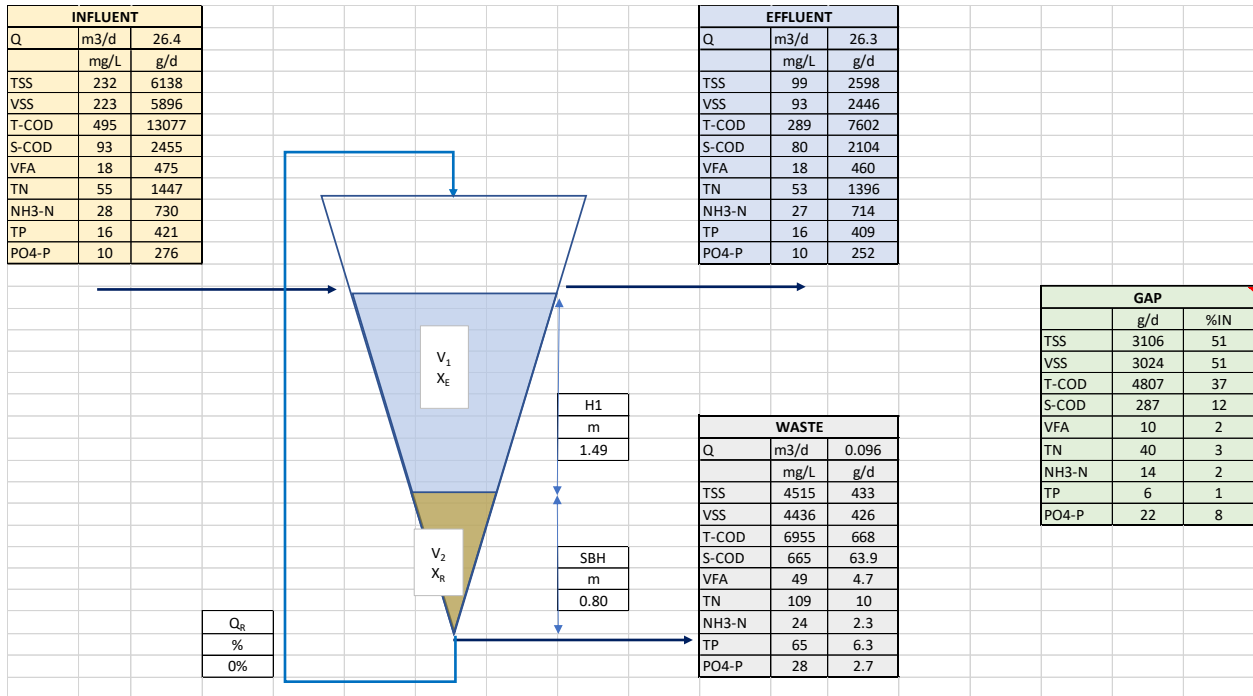


Figure 54: Mass balance for Stage #1.

A.2: One day SRT and no internal recirculation flow rate (Stage #2)

Probe values

The data collected by the online probes located at the primary effluent are compared with the lab measurement values on composite samples (straight line). In these graphs, the time period between the starting time (11:00 AM) to around 05:00 PM should be not considered. In fact, the probes' values were affected by fouling. Once sensor cleaning was completed, the values became again reasonable and in line with laboratory results.

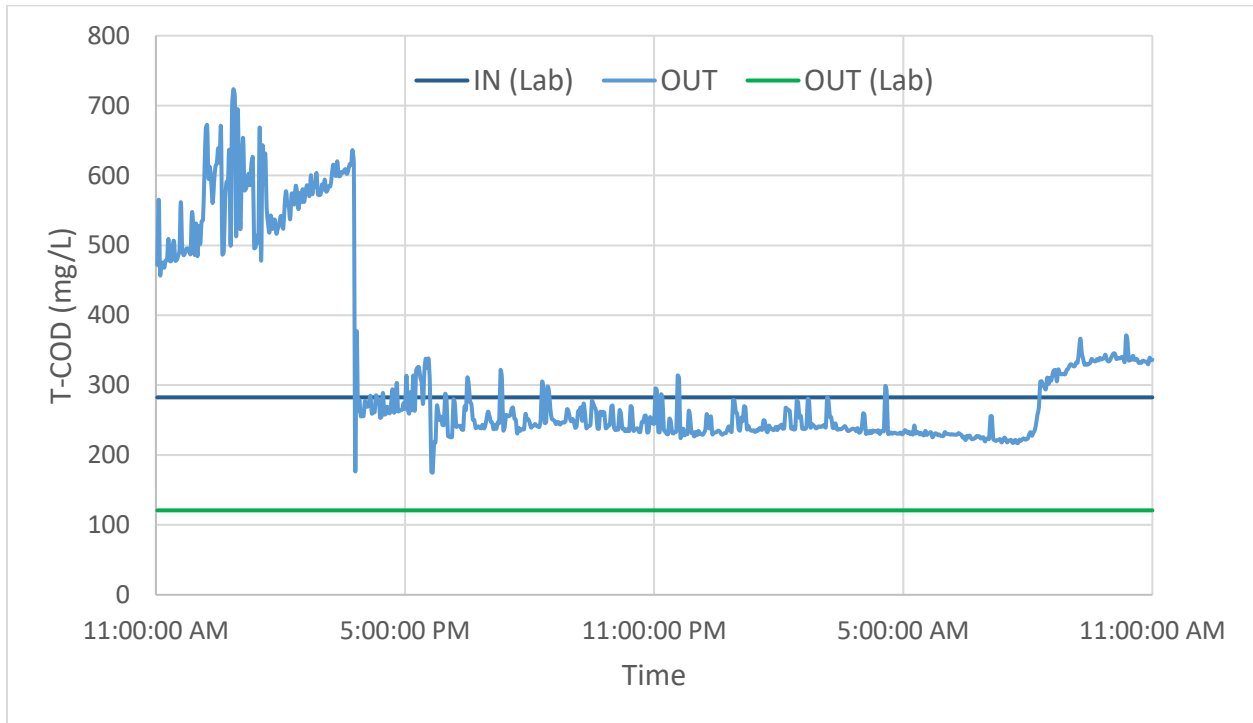


Figure 55: Total COD concentrations from lab measurements on composite samples (influent and outlet) and online probe located at the outlet (Stage #2).

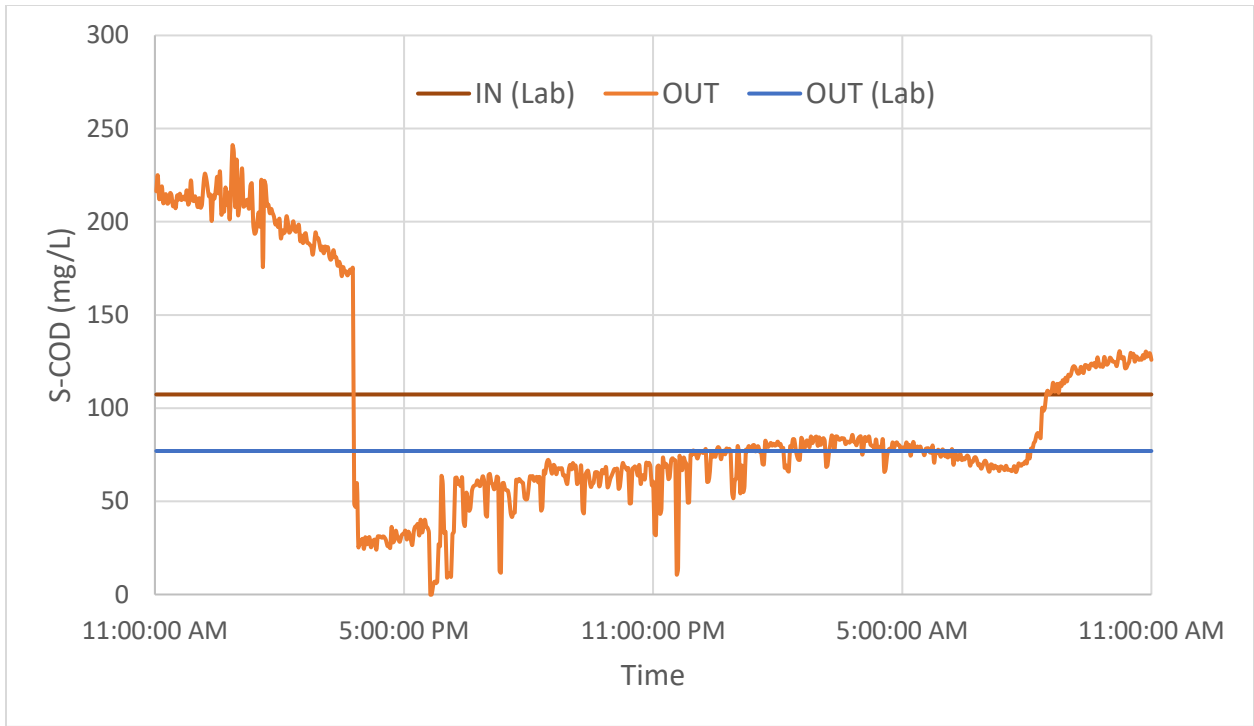


Figure 56: Soluble COD concentrations from lab measurements on composite samples (influent and outlet) and online probe located at the outlet(Stage #2).

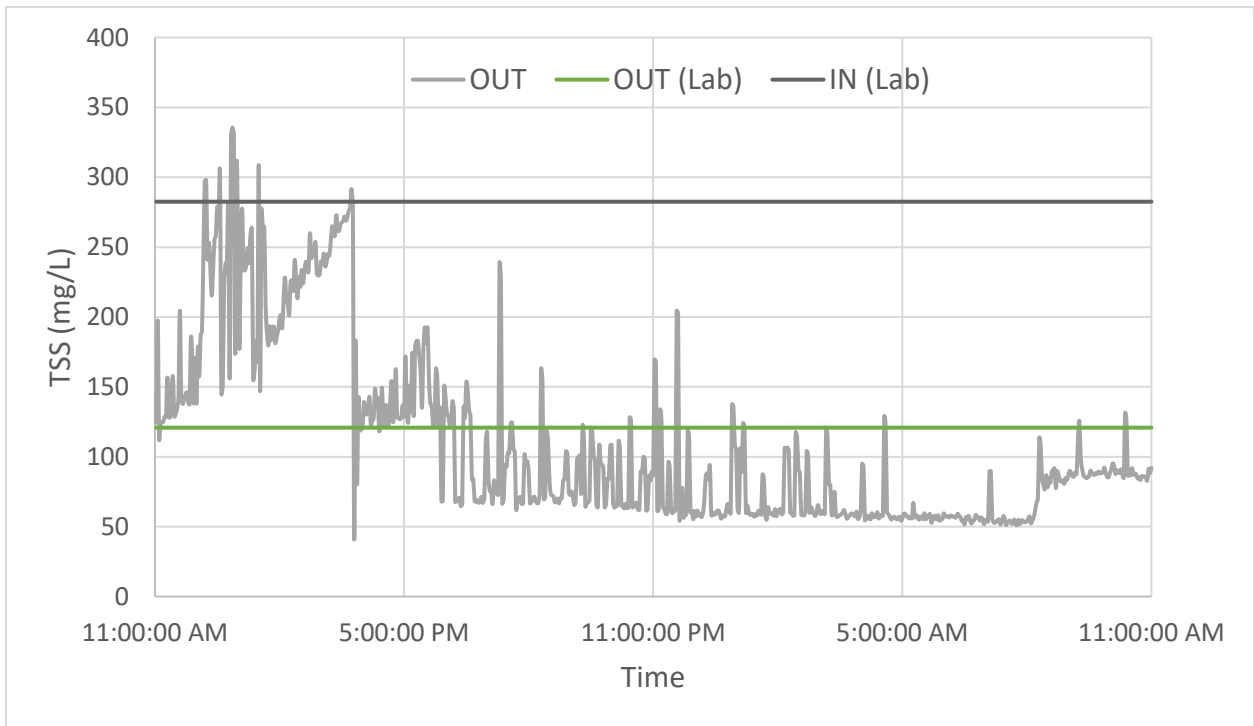


Figure 57: TSS concentrations from lab measurements on composite samples (influent and outlet) and online probe located at the outlet (Stage #2).

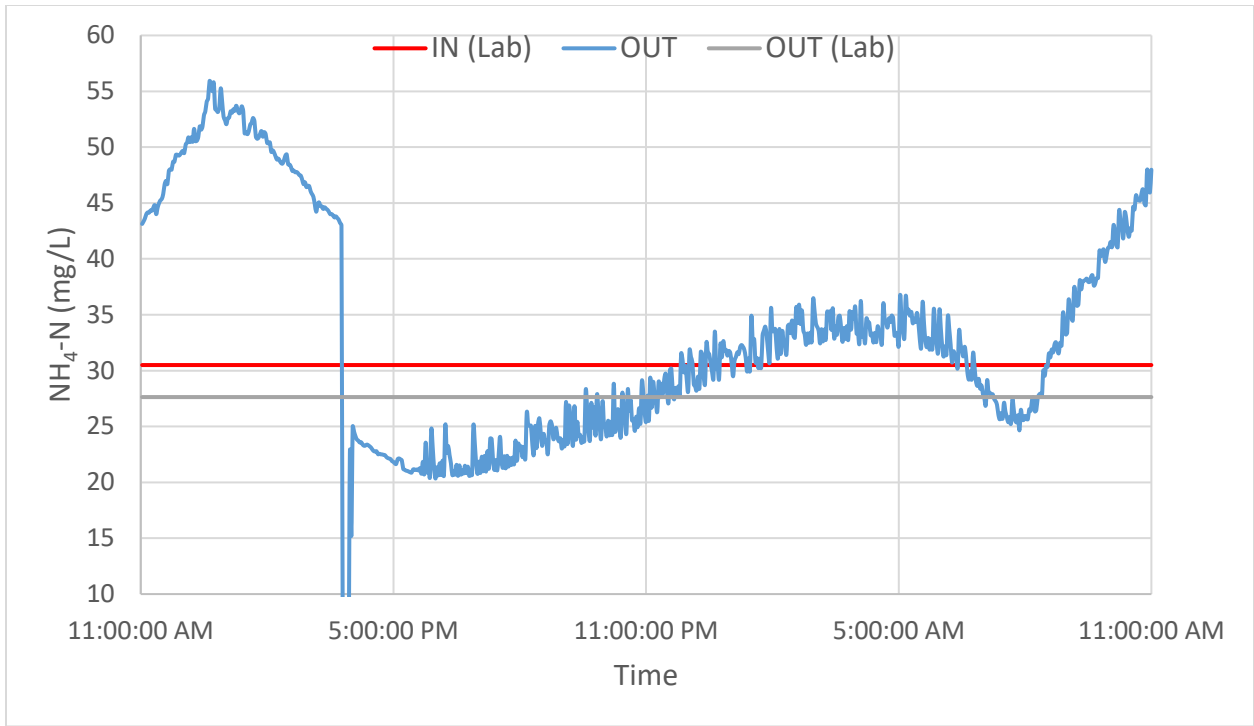


Figure 58: Ammonium concentrations from lab measurements on composite samples (influent and outlet) and online probe located at the outlet (Stage #2).

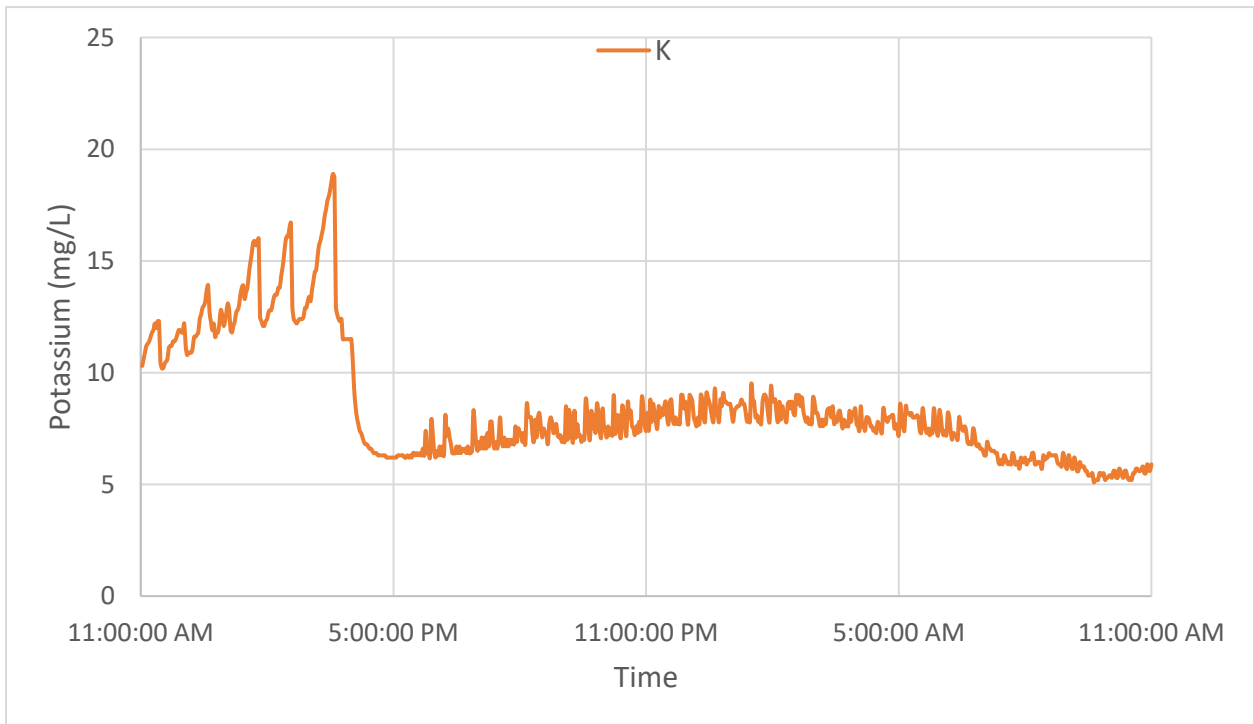


Figure 59: Potassium concentration trend at the outlet (Stage #2).

The big difference in potassium values between the previous stage (Figure 51) and this stage (Figure 59) is due to a calibration carried out just after the first stage. Therefore, the data from the second stage are more reliable than the first one.

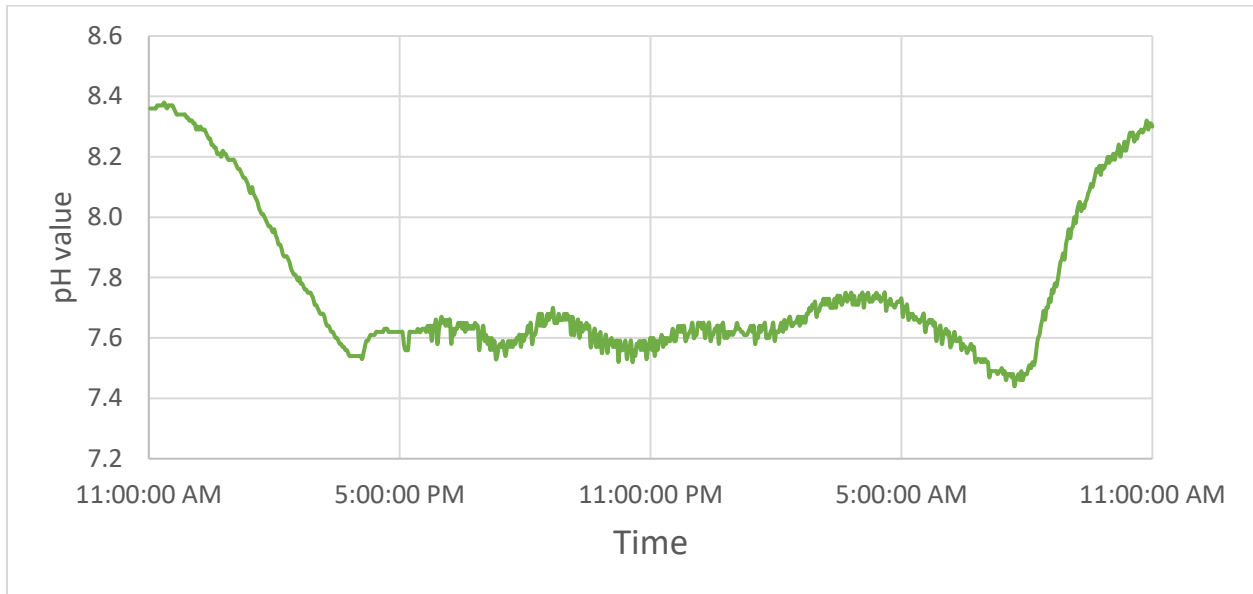


Figure 60: pH trend at the outlet (Stage #2).

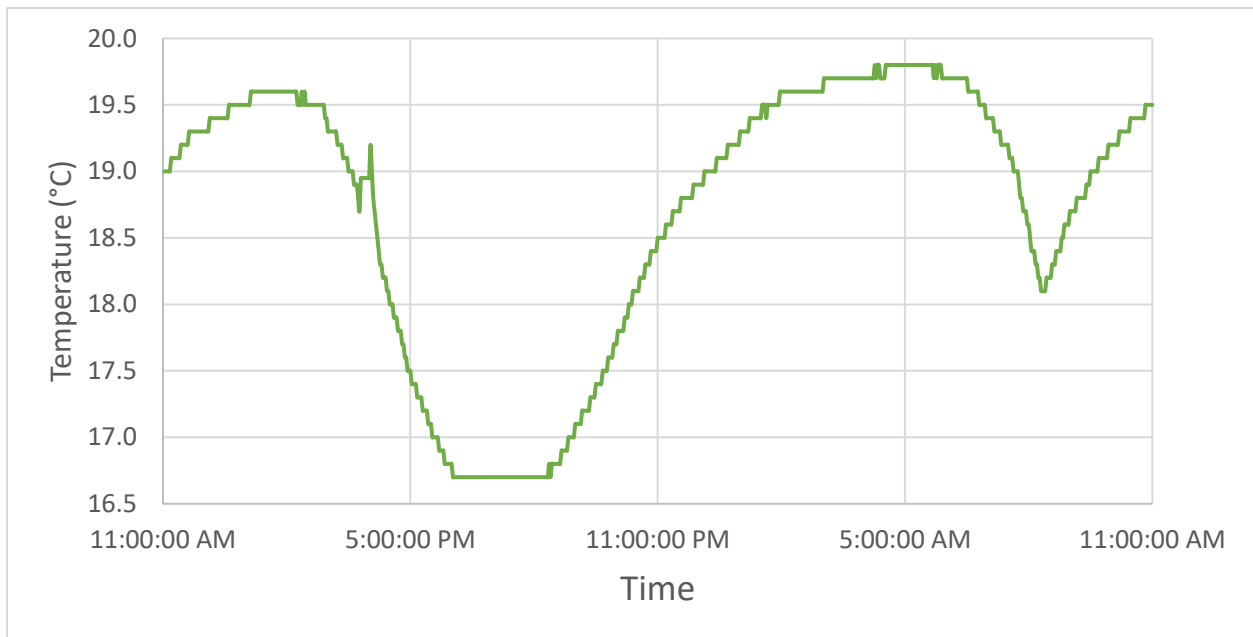


Figure 61: Temperature trend at the outlet (Stage #2).

The increase from 08:00AM onwards reported in all the graphs is due to the human activities in the morning.

Main parameters and mass balance

Table 35: Summary of the main parameters for Stage #2.

Set-Up condition summary - Main operating parameters											
Volumes			TSS concentrations			Flow rates			Retention Times		
V ₁	V ₂	V _{TOT}	X _{IN}	X _E	X _R	Q _{IN}	Q _W	Q _R	HRT	HRT _{EFF}	SRT
L	L	L	mg/L	mg/L	mg/L	m ³ /d	m ³ /d	m ³ /d	h	h	d
1510	690	2200	283	121	10826	38.4	0.04	0	1.4	1.4	1.51

Heights			Mass Loads			Mass		Removal Efficiency
H _{TOT}	H ₁	SBH	L _{IN}	L _E	L _W	m _{BLANKET}	Accumulation	
m	m	m	g/d	g/d	g/d	g	g	
2.29	1.29	1.00	10848	4524	433	7466	8890	58%

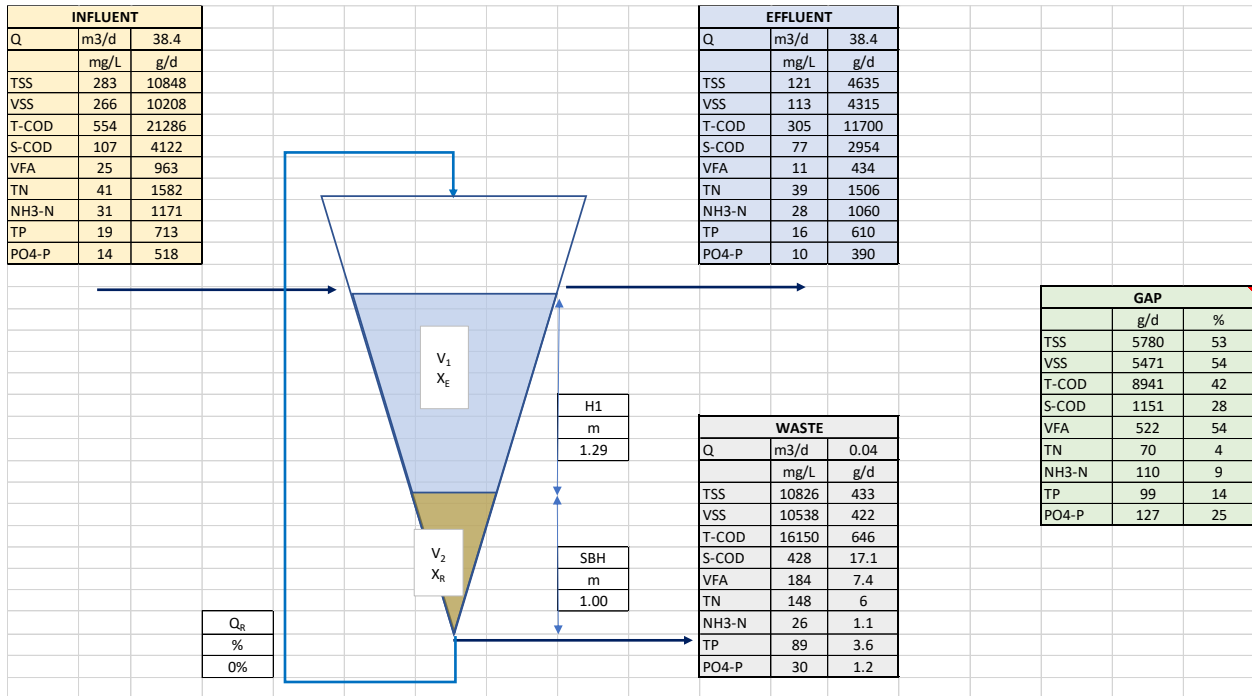


Figure 62: Mass balance for Stage #2.

A.3: One day SRT and high internal recirculation flow rate (Stage #3)

Probe values

For this period, online data are limited due to the on site unavailability of probes. Thus, only TSS concentration and temperature data are illustrated.

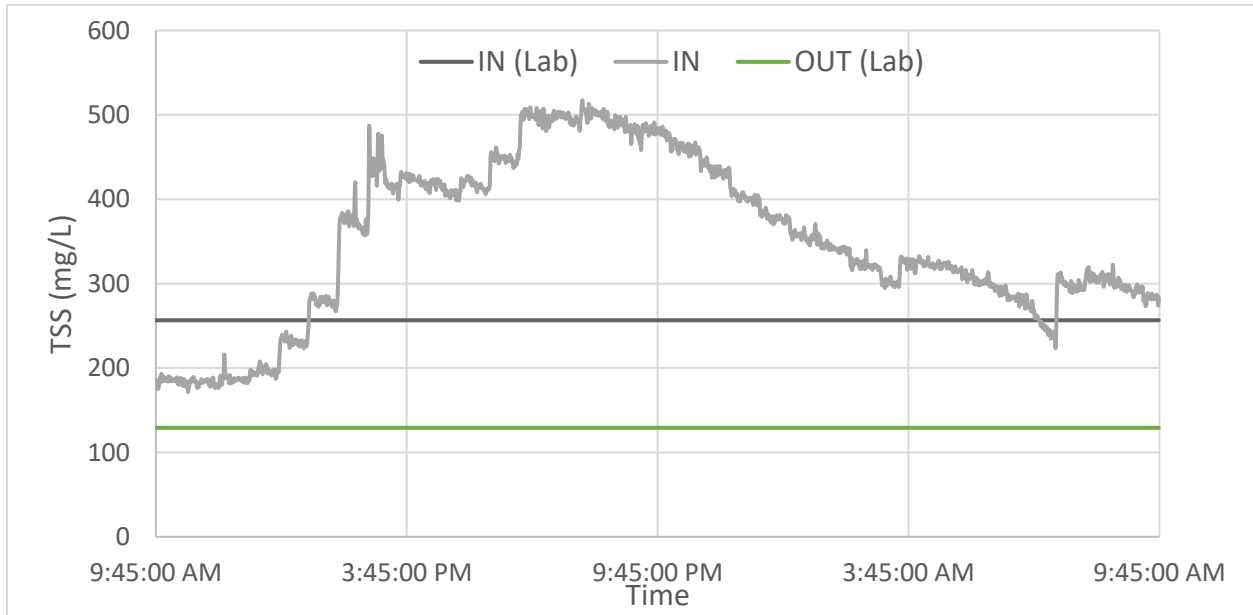


Figure 63: TSS concentrations from lab measurements on composite samples (influent and outlet) and online probe located at the outlet (Stage #3).

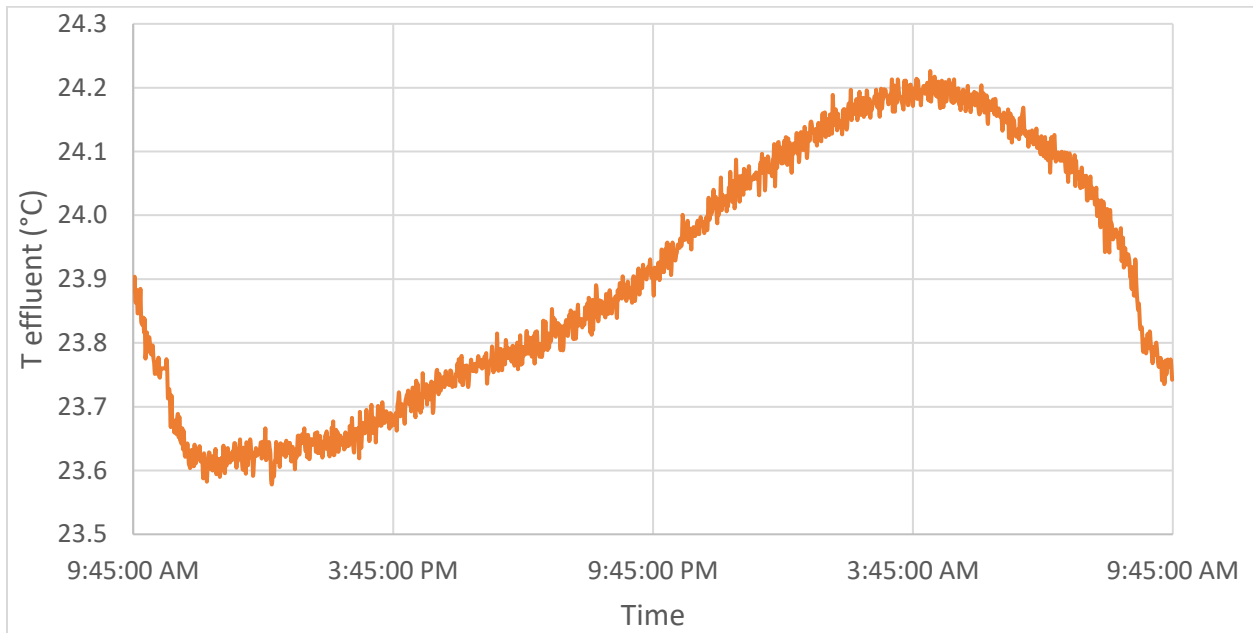


Figure 64: Temperature trend at the outlet (Stage #3).

Mass balance

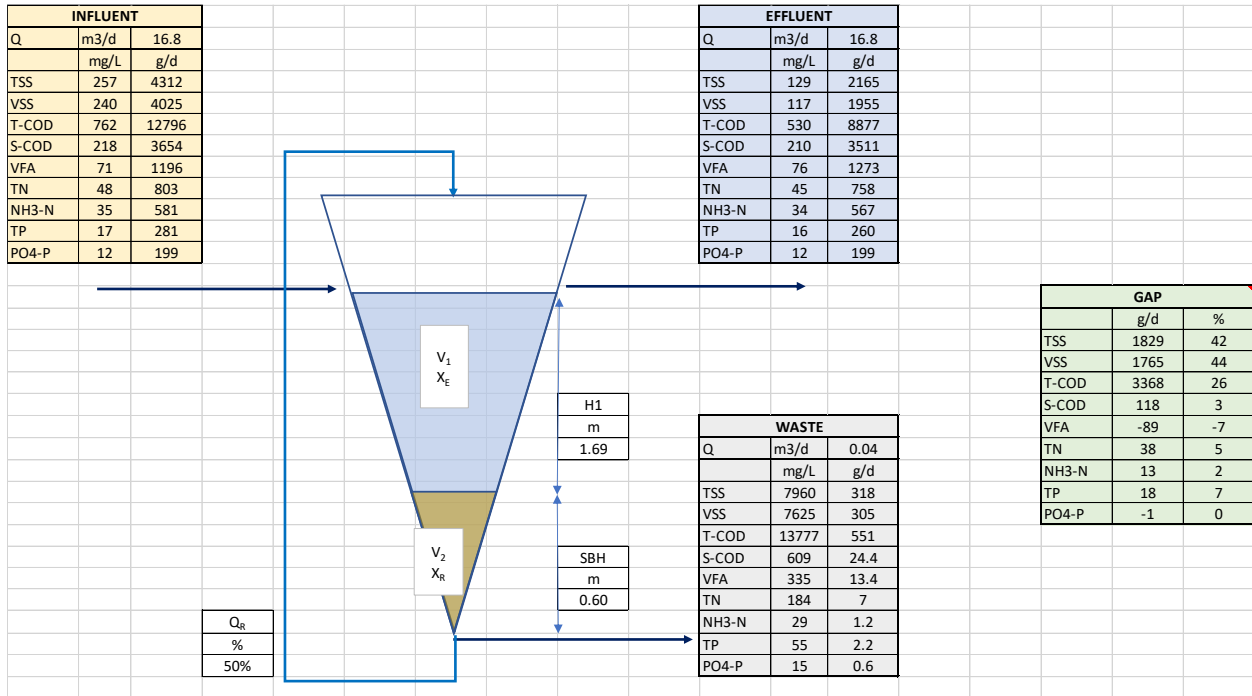


Figure 65: Mass balance Stage #3.

A.4: Three days SRT and high internal recirculation flow rate (Stage #4)

Probe values

As can be seen in Figure 66 and Figure 67 the TSS concentration and temperature follow the same trend, i.e. their values are increasing during the studied period and they tend to stabilize around 02:00 AM. An incorrect placement of the probes (i.e. not completely immersed in the wastewater) could be the cause of this kind of failure, especially for the TSS probe that measures a fixed value of 0 mg/L until 01:00 PM.

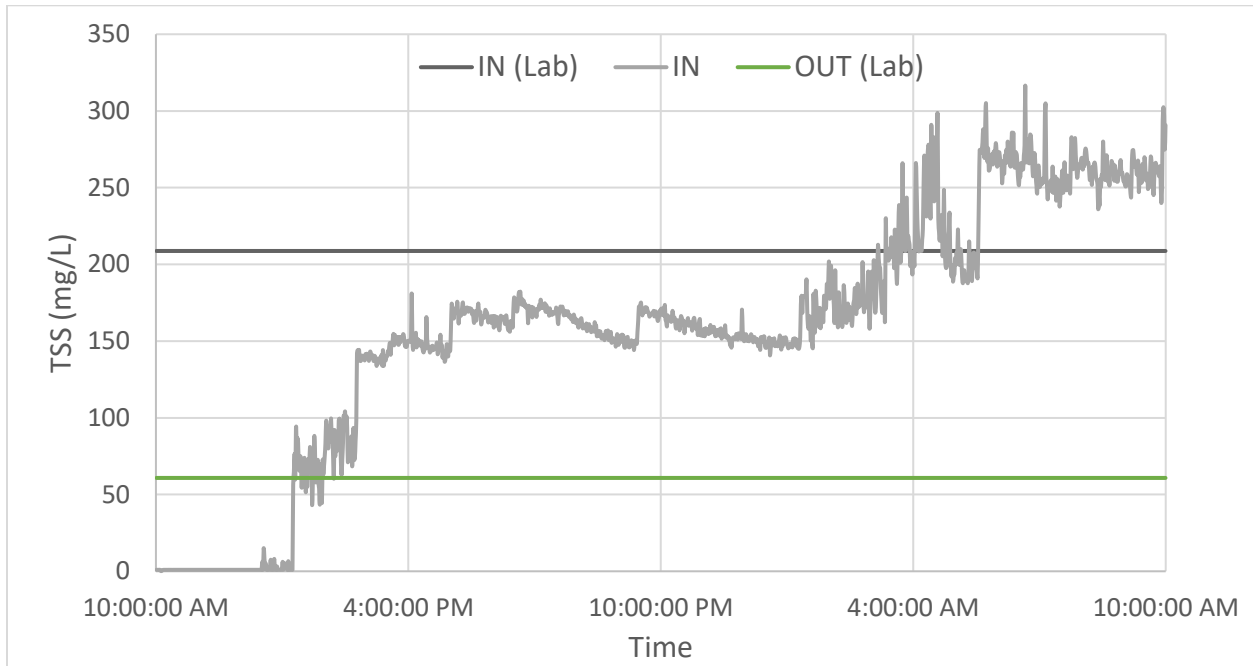


Figure 66: TSS concentrations from lab measurements on composite samples (influent and outlet) and online probe located at the outlet (Stage #4).

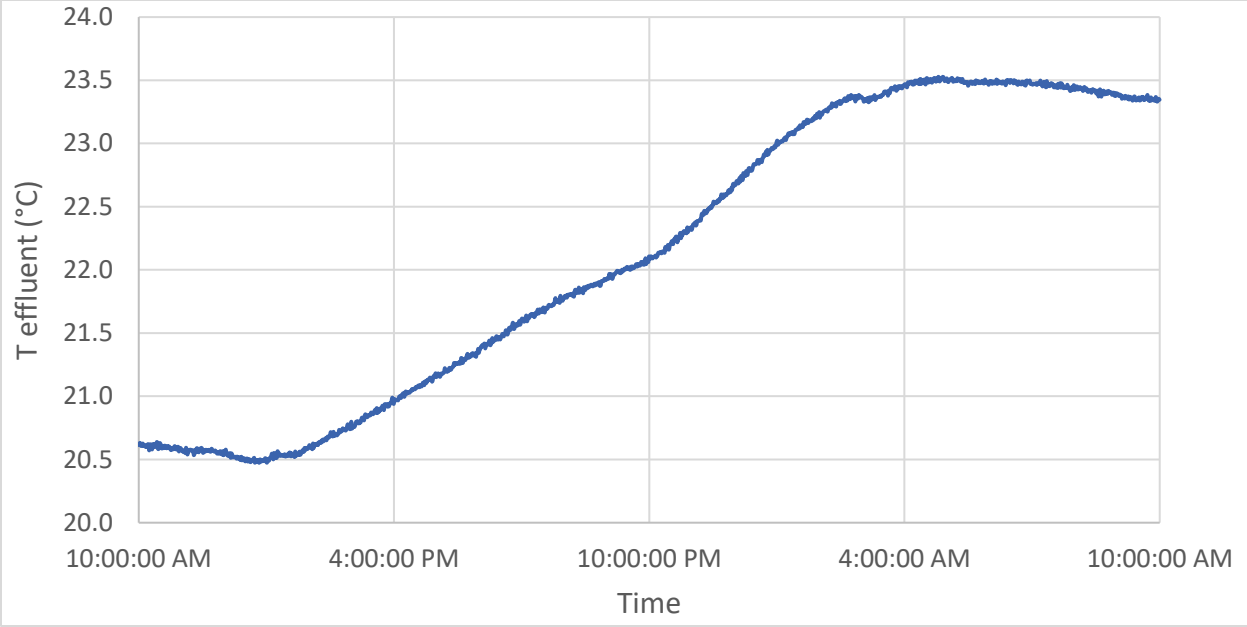


Figure 67: Temperature trend at the outlet (Stage #4).

A.5: Three days SRT and low internal recirculation flow rate (Stage #5)

Probe values

In Figure 68, values for the TSS concentrations measured with the probe significantly differ from the lab values, showing values of around 40 mg/L and 305 mg/L, respectively. An improper probe calibration could be a possible reason of this difference.

It should be noted that during this stage, the temperature reached an average value of 27.7°C, which is the highest ever recorded.

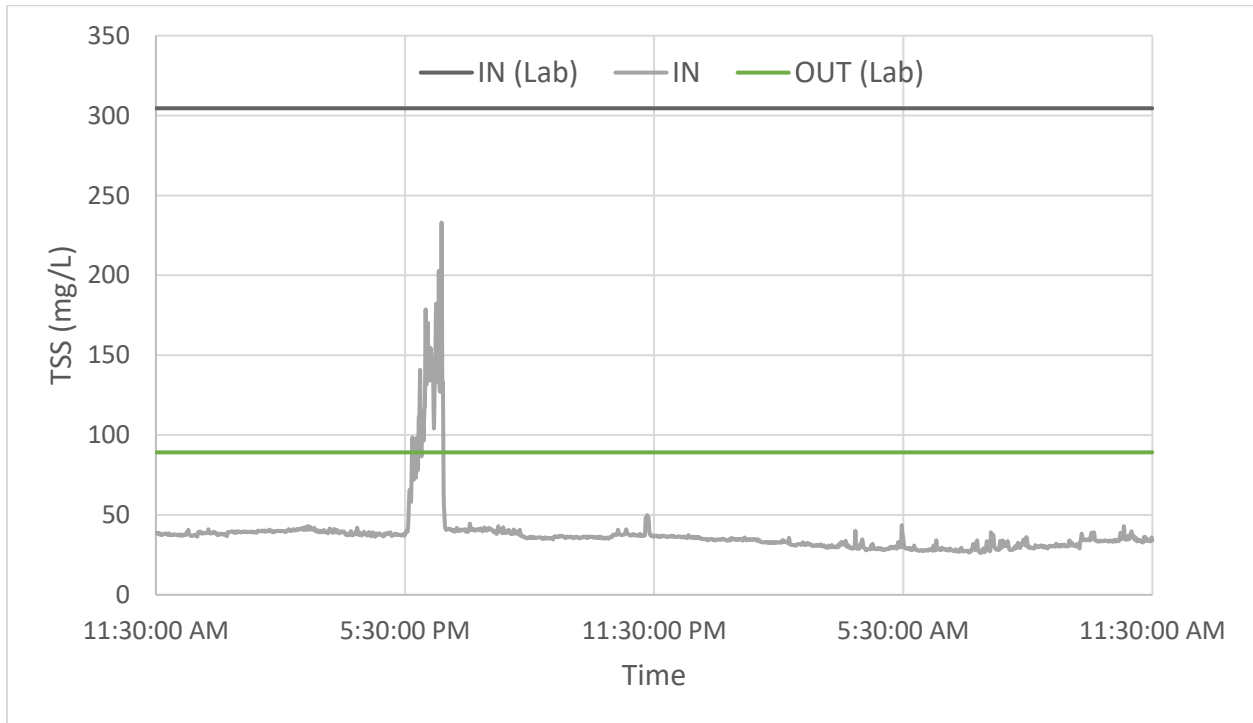


Figure 68: TSS concentrations from lab measurements on composite samples (influent and outlet) and online probe located at the outlet (Stage #5).

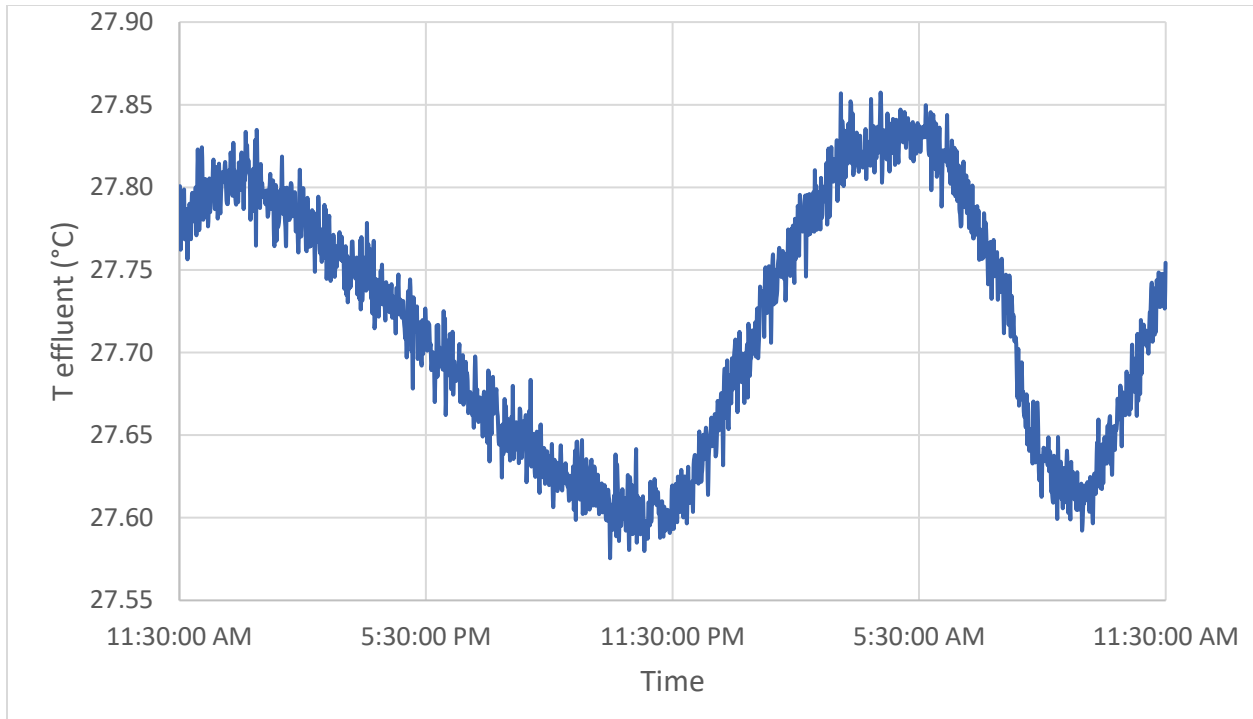


Figure 69: Temperature trend at the outlet (Stage #5).

Mass balance

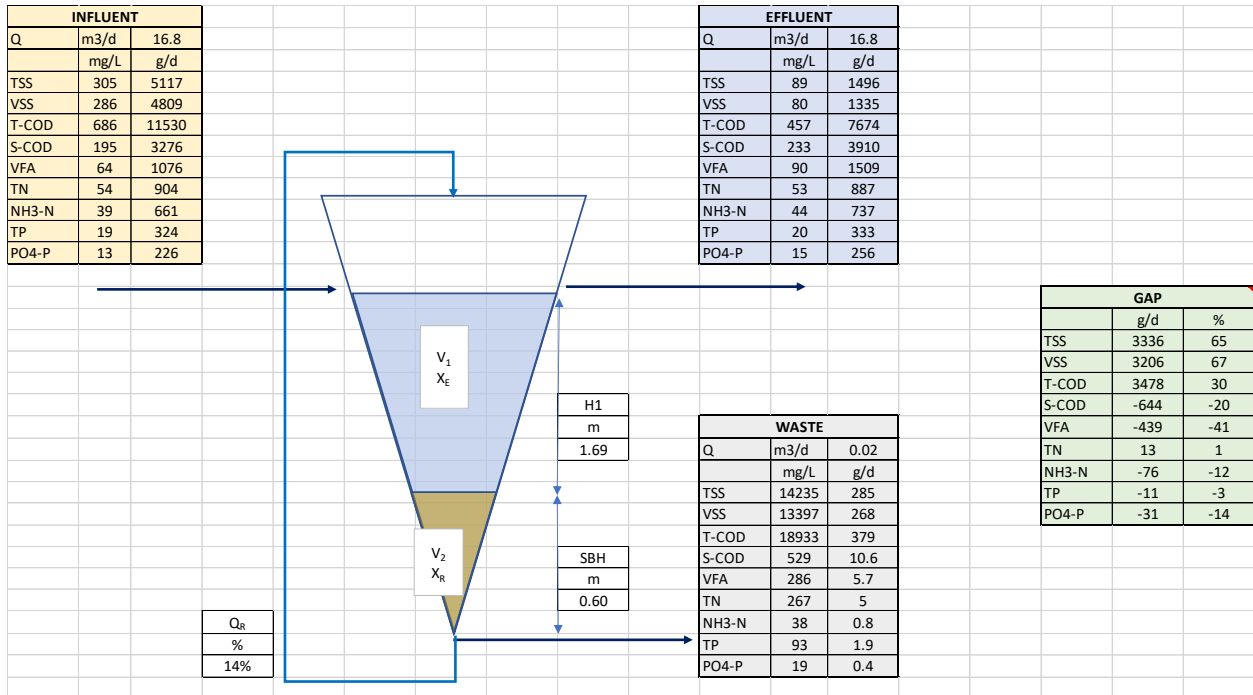


Figure 70: Mass balance Stage #5.

A.6: Three days SRT and low internal recirculation flow rate, and alkalinity dosing (Stage #6)

Alkalinity demand and NaHCO₃ solution dosage

The VFA and alkalinity dynamics during a 27 hours period can be seen on Figure 71 and Figure 72. In order to consider the HRT of the clarifier, the outlet values were delayed by three hours. Also, it should be said that the inlet values from 06:30 AM to 09:30 AM, as well as the inlet values from 09:30 PM to 05:30 AM, and the last 08:30 AM outlet values, were predicted based on the real measurements (filled markers in Figure 71).

The prediction of the unfilled markers in Figure 71 and Figure 72 for the i^{th} sample, was given by:

$$VFA_{IN,i} = VFA_{OUT,i}(1 - \mu_{diff})$$

or

$$Alk_{IN,i} = Alk_{OUT,i}(1 - \mu_{diff})$$

where μ_{diff} is the mean of the relative difference between the measured outlet VFA (Alk) concentration and the measured inlet VFA (Alk) concentration, per the outlet VFA (Alk) concentration.

$$\mu_{diff} = \frac{1}{n} \sum_n \mu_i$$

$$\mu_{VFA,i} = (VFA_{OUT,i} - VFA_{IN,i})/VFA_{OUT,i}$$

or

$$\mu_{Alk,i} = (Alk_{OUT,i} - Alk_{IN,i})/Alk_{OUT,i}$$

Whereas an overall VFA production can be observed throughout the sampling period, the alkalinity is consumed. Figure 72 shows how the bicarbonate alkalinity concentration drops to 100 mgHCO₃/L during the very early morning when there are is little human activity.

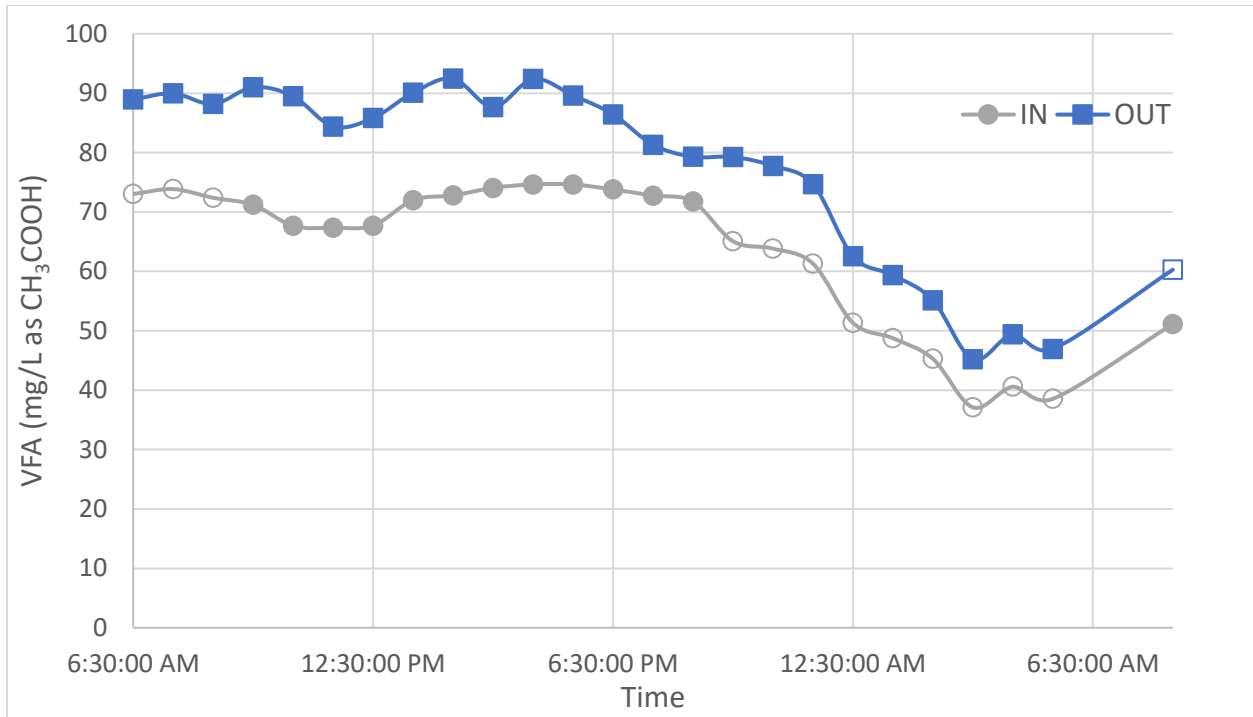


Figure 71: VFA concentration dynamics at the primary clarifier inlet and outlet on July 25th and 26th.

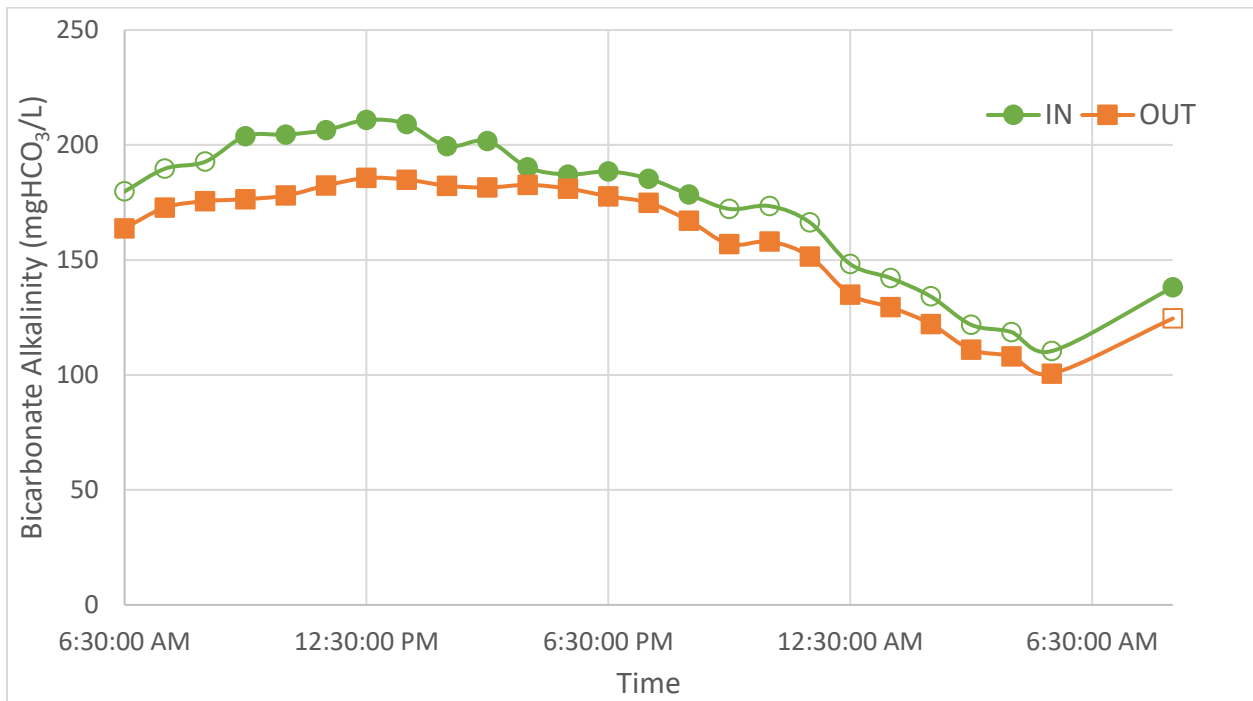


Figure 72: Alkalinity concentration dynamics at the primary clarifier inlet and outlet on July 25th and 26th.

In order to fulfill the $100\text{mgHCO}_3/\text{L}$ gap, a basin of 50L volume, equipped with a stirrer, and filled with tap water and sodium bicarbonate, was used. A peristaltic tube, connected with a peristaltic pump, was dosing the bicarbonate saturated solution to the upper part of the clarifier, as illustrated on Figure 73.

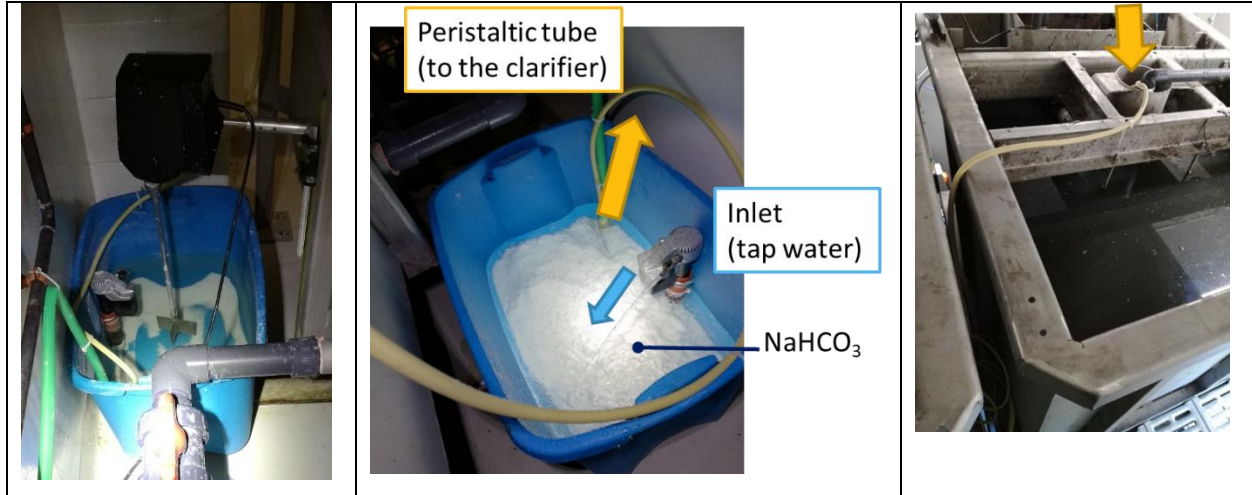


Figure 73: Set-up of the basin for saturated sodium bicarbonate solution dosage.

After one day of NaHCO_3 solution dosage, a thin film layer was noticed on the clarifier's surface (see Figure 74). In terms of alkalinity concentration there was no clear benefit due to the low alkalinity concentration (823 mg/L , see Table 36) of the saturated solution that was dosed at around $40\text{mL}/\text{min}$.



Figure 74: Film on the clarifier's surface after NaHCO_3 dosage.

Furthermore, between Day 4 and 5, an additional sampling campaign for VFA and alkalinity dynamics was carried out and the values showed almost no improvement on alkalinity

needs. The results are shown in Figure 76. In this case, only the first three inlet values and the last three outlet values were predicted, while the other points illustrated are based on real measurements. Also, no NaHCO_3 seemed to be consumed during that period since there was no need to refill the basin after five days of dosage.

However, once an overhead stirrer was implemented (i.e., on day 5), the alkalinity concentration increased to 52.4 g/L (see Table 36), which is almost 64 times the value of Day 1. It even increased to 71.1 g/L the day after.

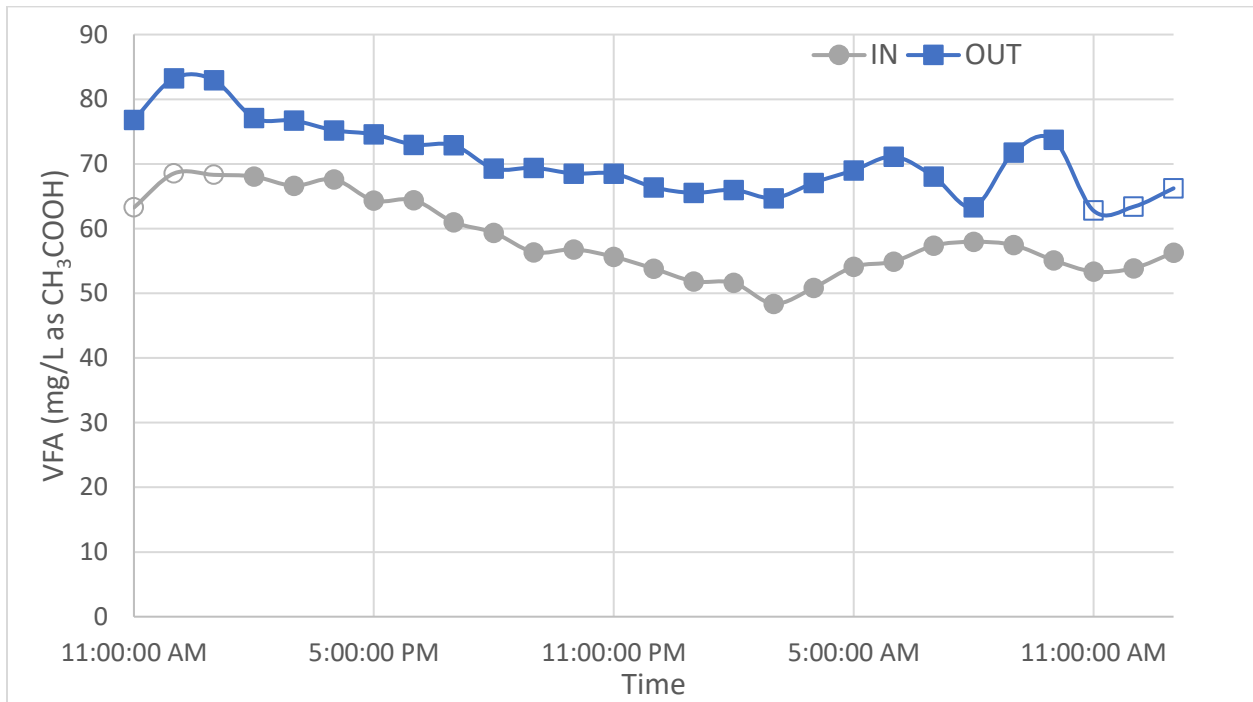


Figure 75: VFA concentration dynamics at the primary clarifier inlet and outlet on Day 4 and 5.

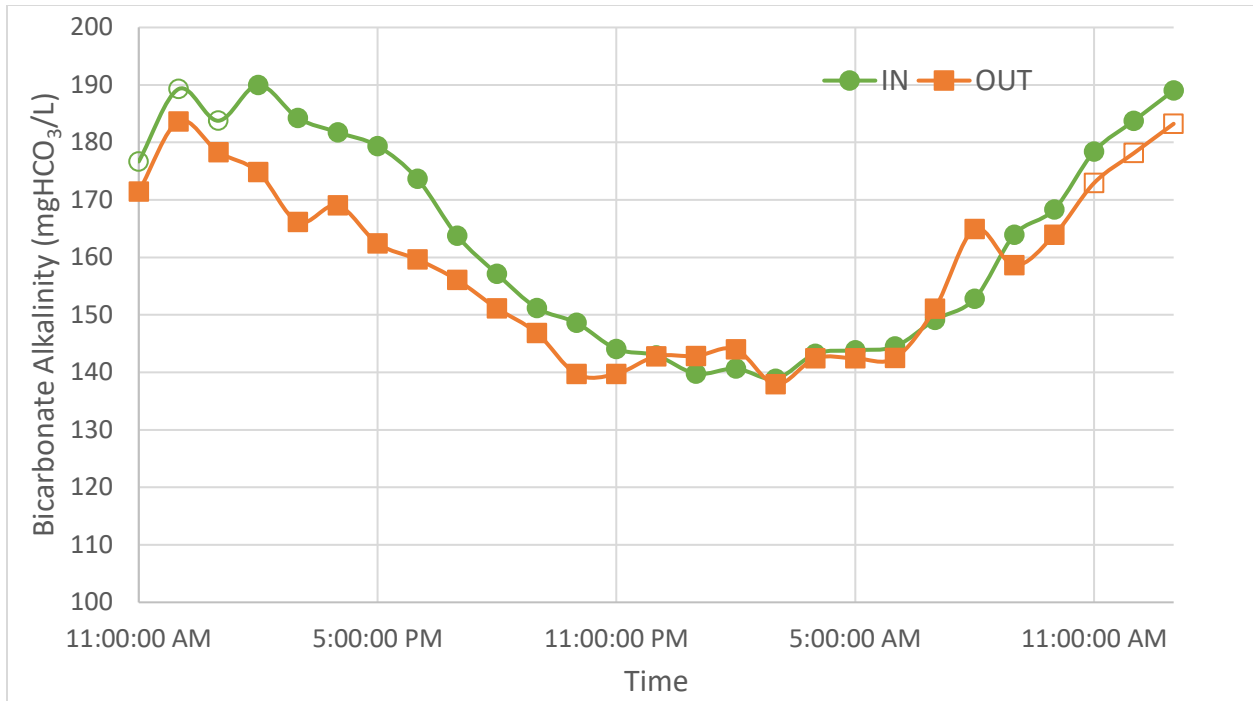


Figure 76: Alkalinity concentration dynamics at the primary clarifier inlet and outlet on Day 4 and 5.

Table 36: pH, VFA and alkalinity values during NaHCO₃ dosage (Stage #6).

Day	Primary inlet (storage tank)			Primary outlet			Added NaHCO ₃ solution		
	pH	VFA (mg/L as CH ₃ COOH)	Alkalinity (mg/L as HCO ₃)	pH	VFA (mg/L as CH ₃ COOH)	Alkalinity (mg/L as HCO ₃)	pH	VFA (mg/L as CH ₃ COOH)	Alkalinity (mg/L as HCO ₃)
Day1	7.31	77	252	7.34	82	234	7.86	0	823
Day6	6.96	64	174	7.16	79	342	8.67	0	52,403
Day7	6.97	60	154	7.21	91	346	8.76	0	71,127

Probe values

As indicated on Figure 77 the TSS inlet concentration measured at the lab perfectly agrees with the online trend measured by the probe.

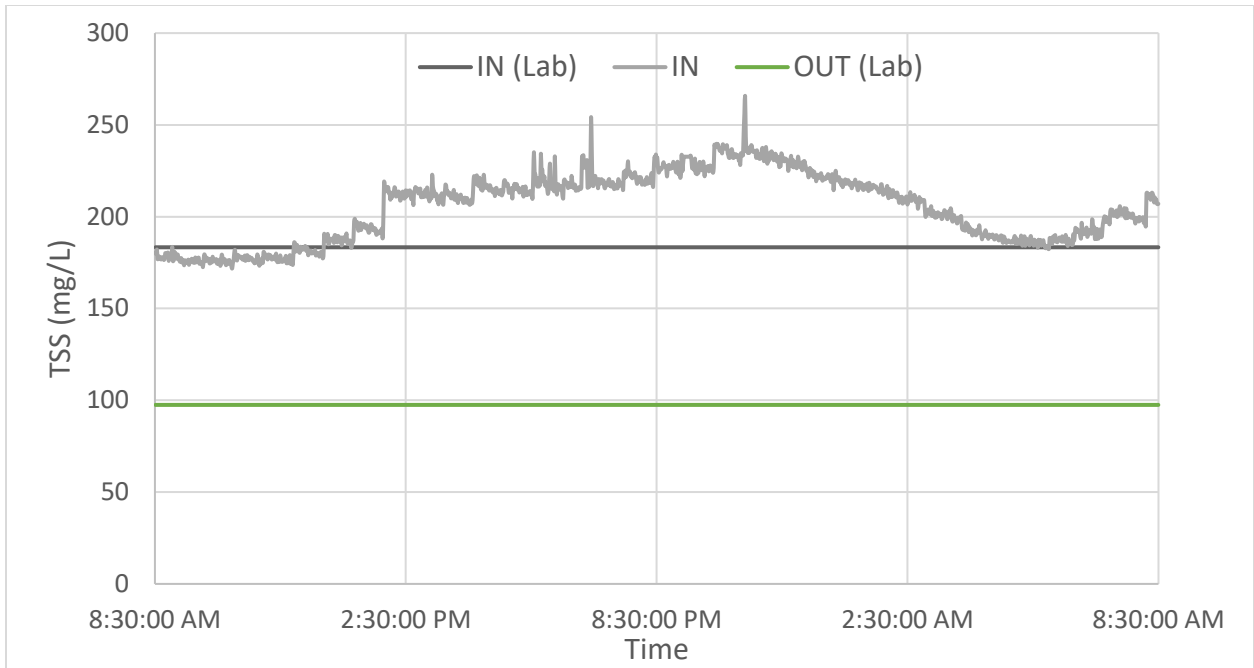


Figure 77: TSS concentrations from lab measurements on composite samples (influent and outlet) and online probe located at the outlet (Stage #6).

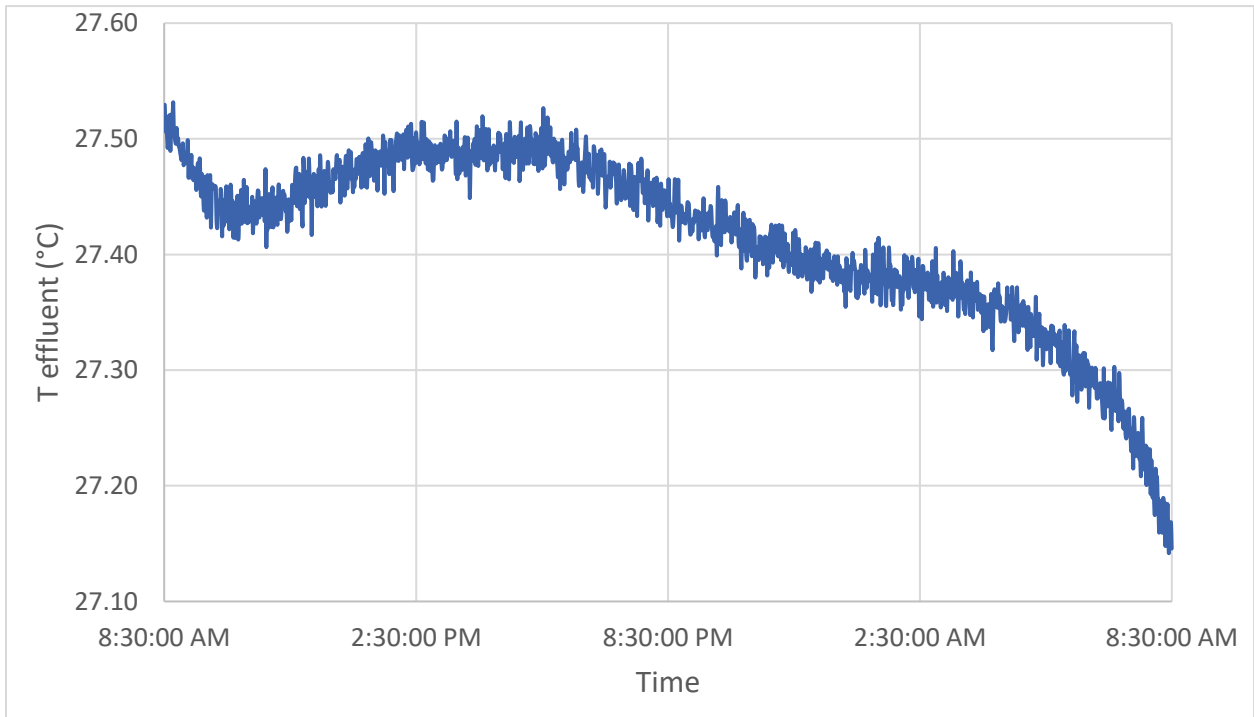


Figure 78: Temperature trend at the outlet (Stage #6).

Mass balance

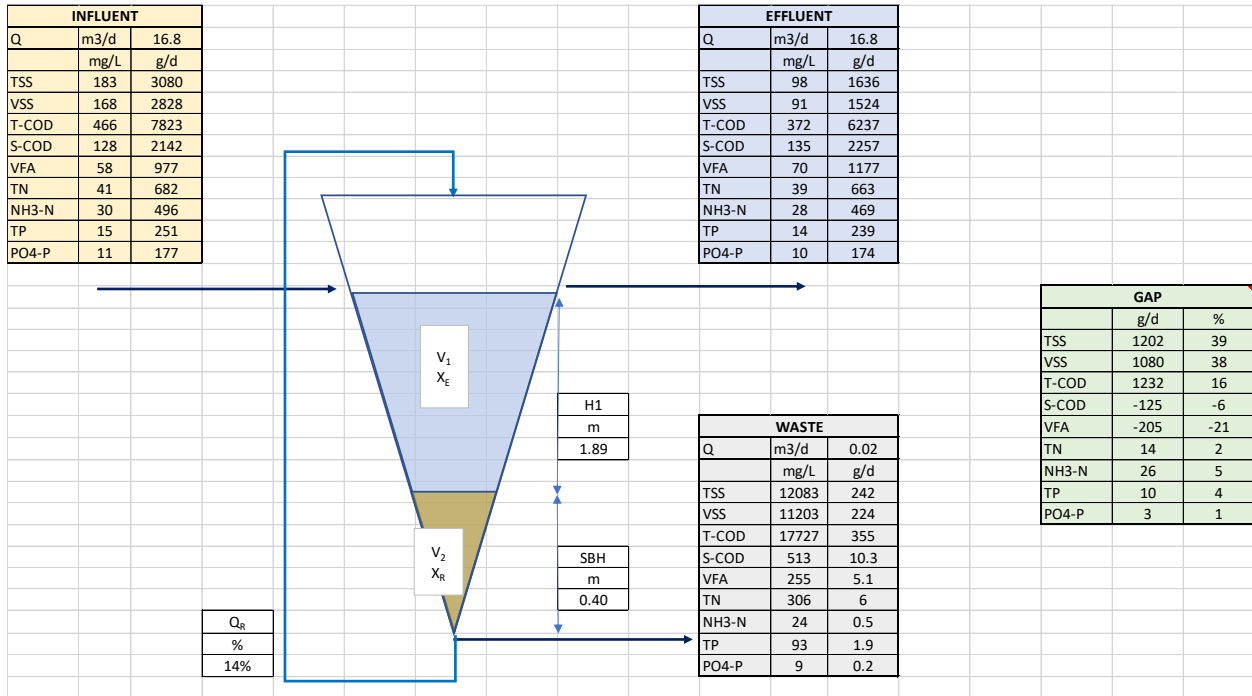


Figure 79: Mass balance Stage #6.

A.7: Three days SRT, low internal recirculation flow rate, and FeCl₃ dosing (Stage #7)

Jar-tests for optimum FeCl₃ dosage

In order to identify the optimal concentration for FeCl₃ addition in terms of solids removal efficiency (i.e, E% TSS), wastewater samples of dry weather and wet weather conditions (DWP and WWP) were tested. The investigated ferric chloride dosages were 0, 10, 20, 30, 45, and 60 mg/L. By means of the jar test equipment (see Figure 80) a rapid mixing of 1 min at 200rpm, followed by a slow stirring of 15 minutes at 30rpm were applied. After an hour of sedimentation (0 rpm), 0.6L of supernatant out of the 1L sample were siphoned off by using a peristaltic pump.

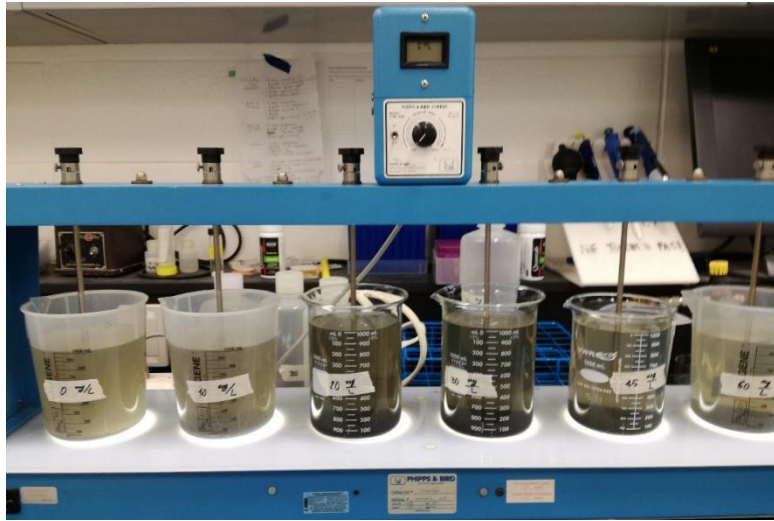


Figure 80: Jar test equipment.

Table 37: Raw wastewater quality characteristics for dry and wet weather period.

	TSS _{IN} (mg/L)	pH
WWP	161	7.35
DWP	247	7.27

Figure 81 indicates that during the DWP the coagulant is more effective, and that the optimum concentration for FeCl₃ in terms of TSS removal efficiency is 20 mg/L, for both dry and wet weather periods.

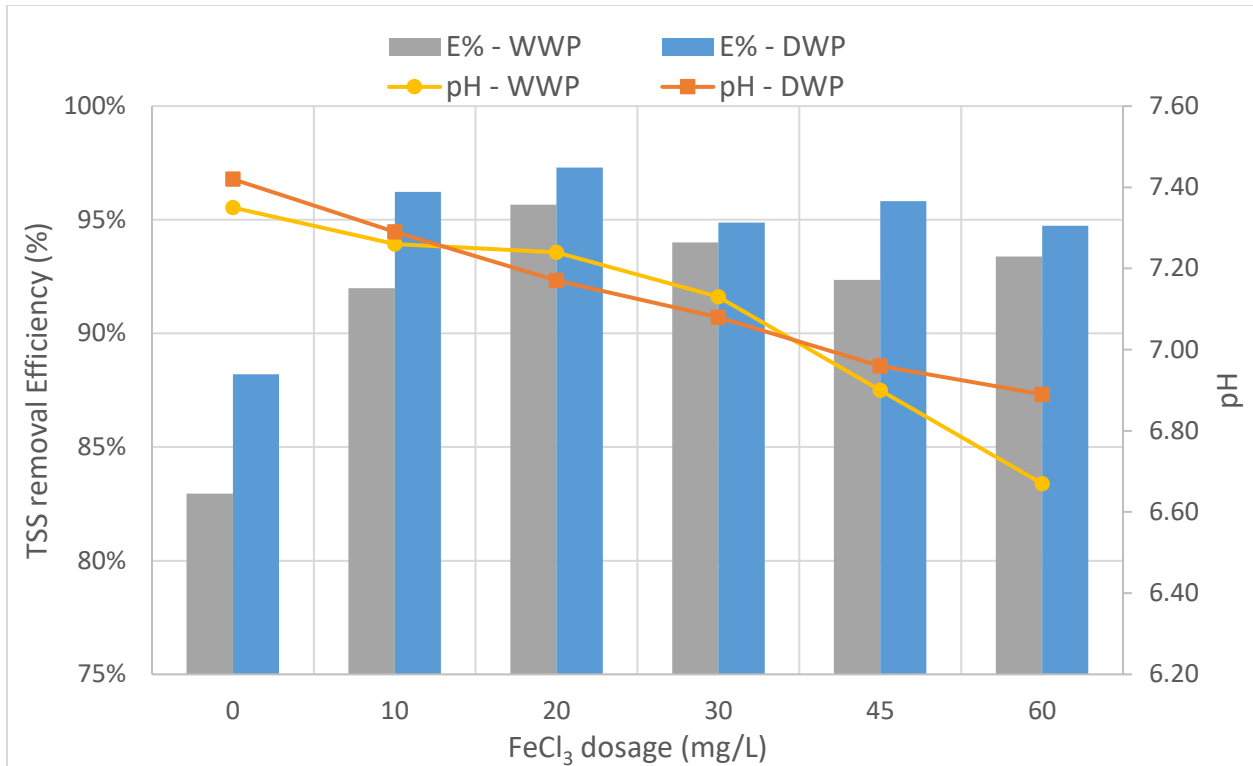


Figure 81: Jar test results for different FeCl₃ dosages with dry weather (DWP) and wet weather (WWP) samples.

Probe values

More probes were available during this experimental period and the different plots are reported below.

Except until 03:00 PM, the TSS outlet concentration measured on the composite sample by the laboratory analysis almost agrees with the online trend measured by the probe, as indicated on Figure 82. A probe cleanup was probably executed at that time, i.e. around 03:00 PM. On the other hand, the TSS inlet value, measured by the probe, is lower than the lab one for the whole 24 hours.

The total COD measured by the probe is overall higher compared to the value measured through laboratory analysis (see Figure 83). Probably, a probe calibration should be carried out to reduce this difference.

As illustrated in Figure 85 the temperature trends follow the same pattern for the two different probes, but their values slightly differ from each other.

As can be seen on Figure 84, the pH trend at the outlet is very different to what was measured on the composite sample, indicating a value of about 6.9 and 7.35, respectively. A probe calibration is certainly needed here.

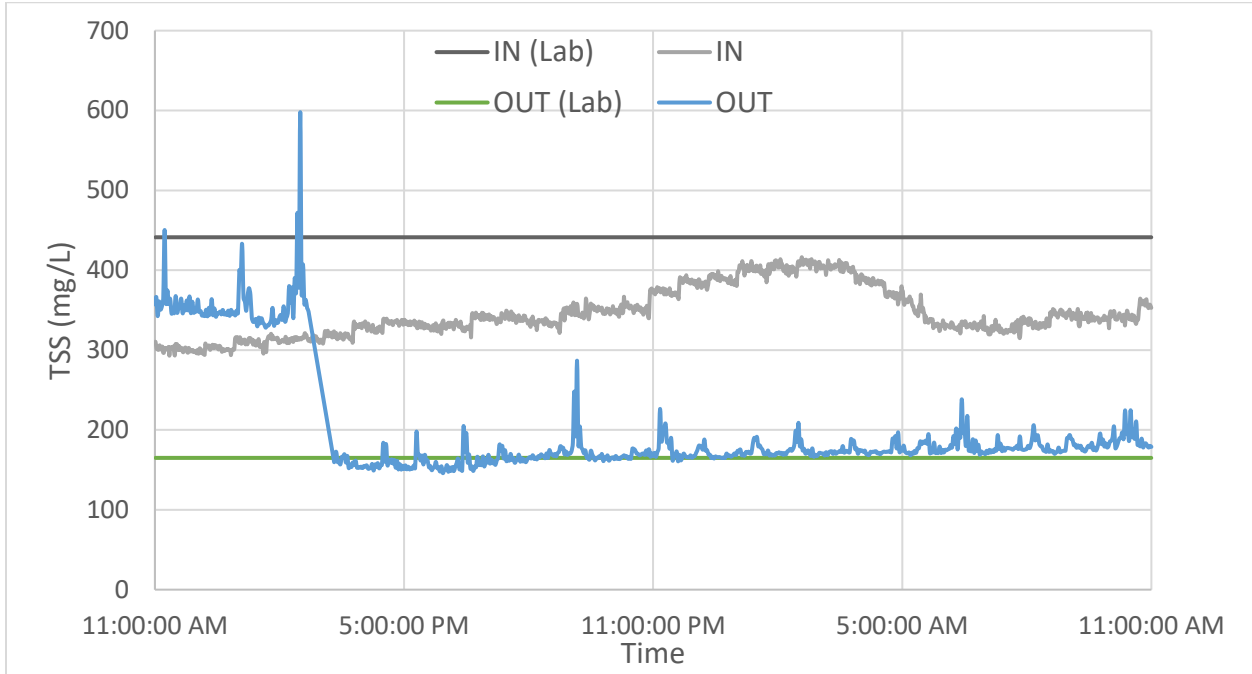


Figure 82: TSS concentrations from lab measurements on composite samples (influent and outlet) and online probes located at the inlet and outlet (Stage #7).

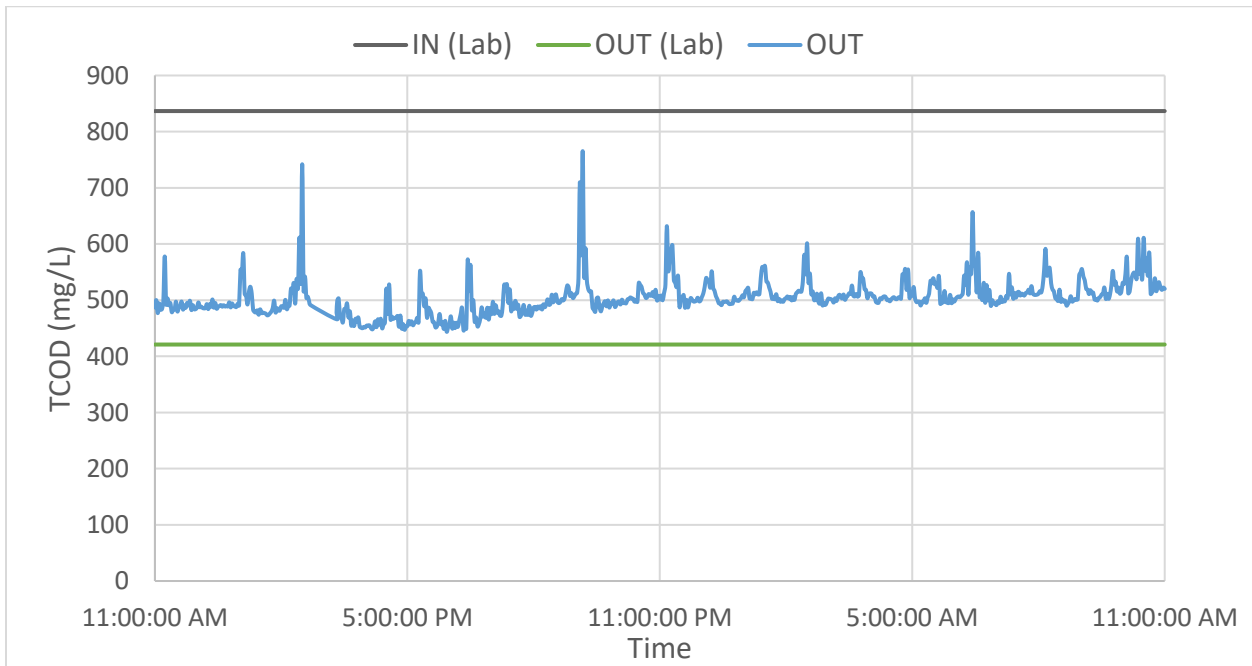


Figure 83: Total COD concentration from lab measurements on composite samples (influent and outlet) and online probe located at the outlet (Stage #7).

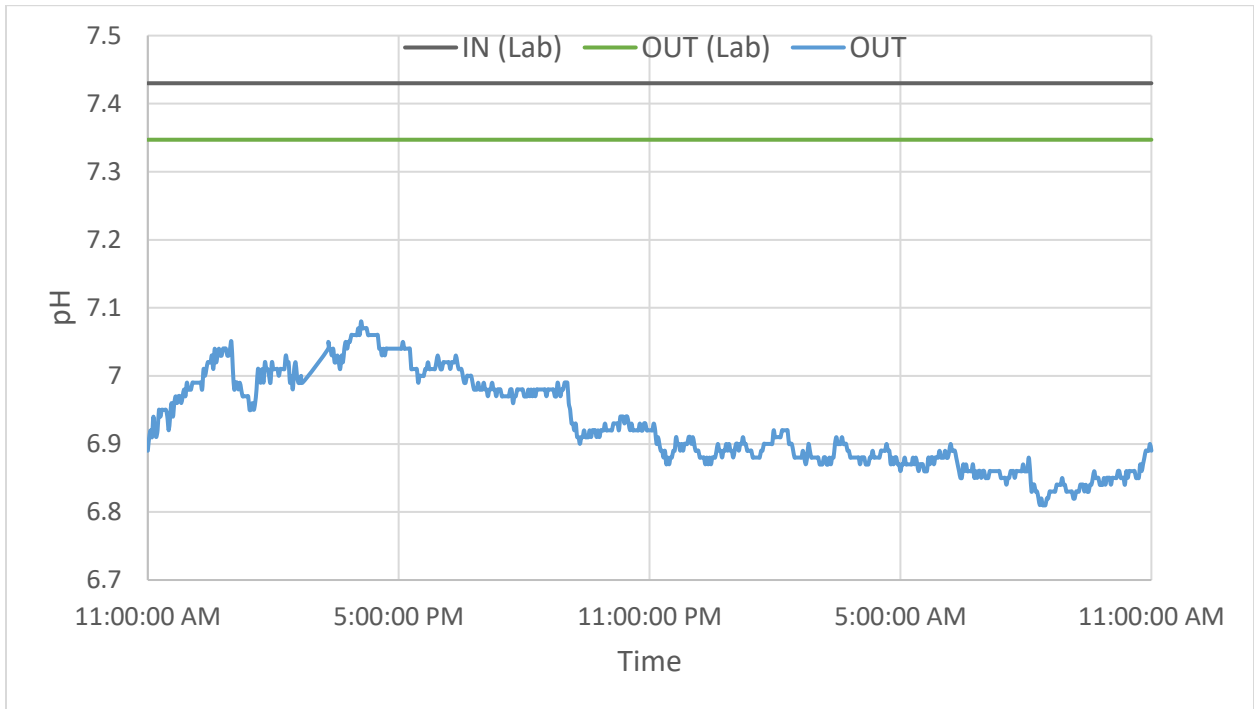


Figure 84: pH trend at the outlet and from lab measurements on composite samples (influent and outlet) (Stage #7).

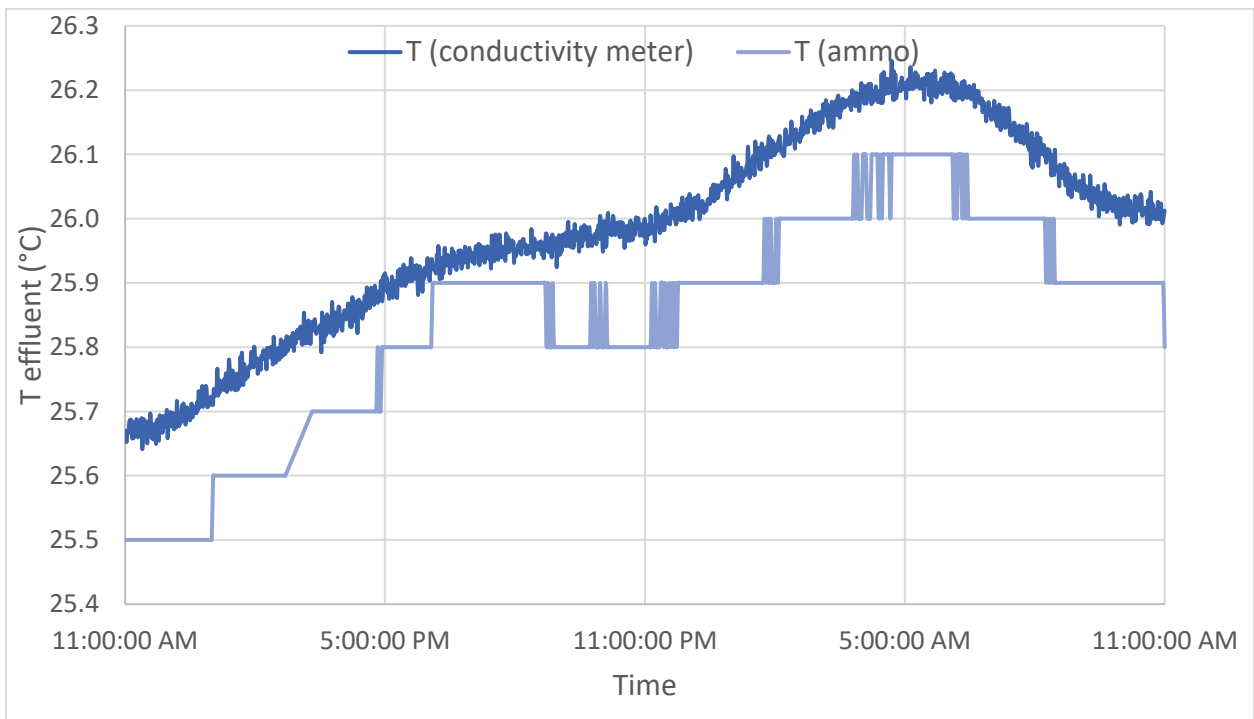


Figure 85: Temperature trend at the outlet for conductivity meter and ammo::lyser probe (Stage #7).

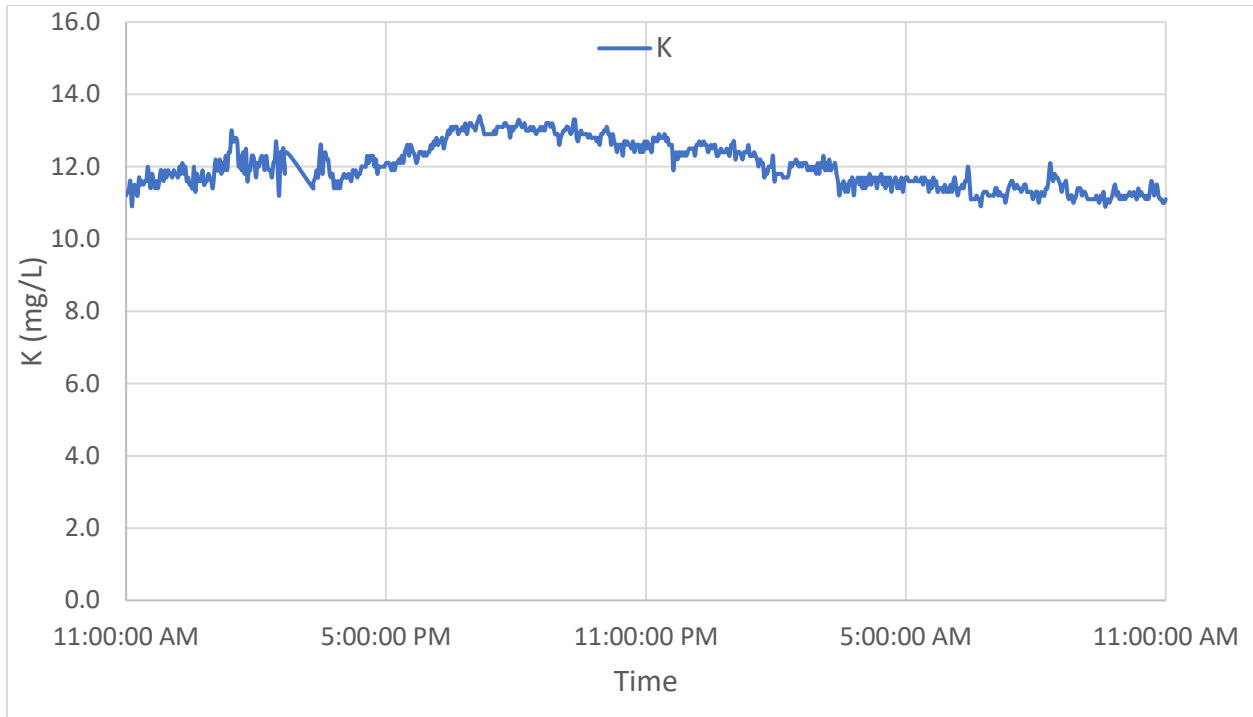


Figure 86: Potassium concentration trend at the outlet (Stage #7).

Main parameters and mass balance

Table 38: Summary of the main parameters for Stage #7.

Set-Up condition summary - Main operating parameters											
Volumes			TSS concentrations			Flow rates			Retention Times		
V ₁	V ₂	V _{TOT}	X _{I,N}	X _E	X _R	Q _{I,N}	Q _W	Q _R	HRT	HRT _{EFF}	SRT
L	L	L	mg/L	mg/L	mg/L	m ³ /d	m ³ /d	m ³ /d	h	h	d
1968	232	2200	441	165	15034	16.8	0.02	2.4	3.1	2.8	1.16
Heights			Mass Loads			Mass		Removal Efficiency			
H _{TOT}	H ₁	SBH	L _{I,N}	L _E	L _W	m _{BLANKET}	Accumulation	E%TSS			
m	m	m	g/d	g/d	g/d	g	g	%			
2.29	1.69	0.60	7413	2693	422	3490	4975	64%			

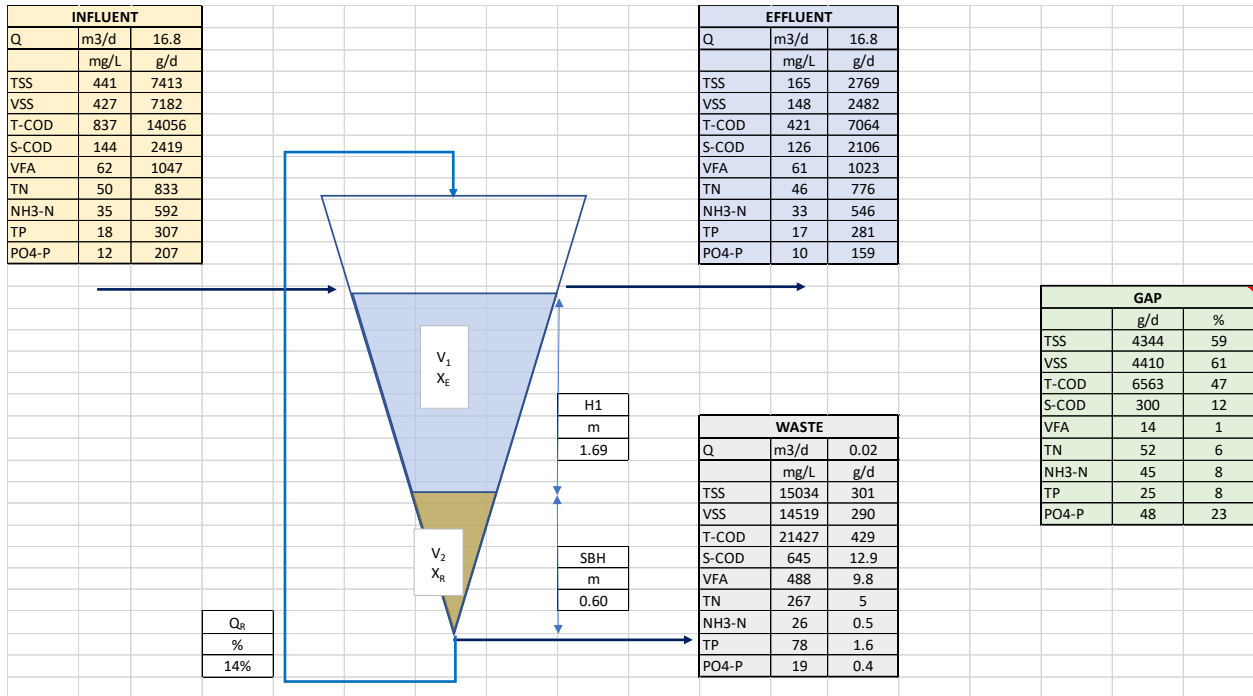


Figure 87: Mass balance Stage #7.

A.8: Three days SRT, low internal recirculation flow rate, and alkalinity and FeCl₃ dosing (Stage #8)

Probe values

As can be noticed from Figure 88, the online TSS data agreed well with the lab measurements for both the outlet and the inlet values.

Instead, for the T-COD (Figure 89), and pH (Figure 90), a discrepancy between the lab and the probe values is observed.

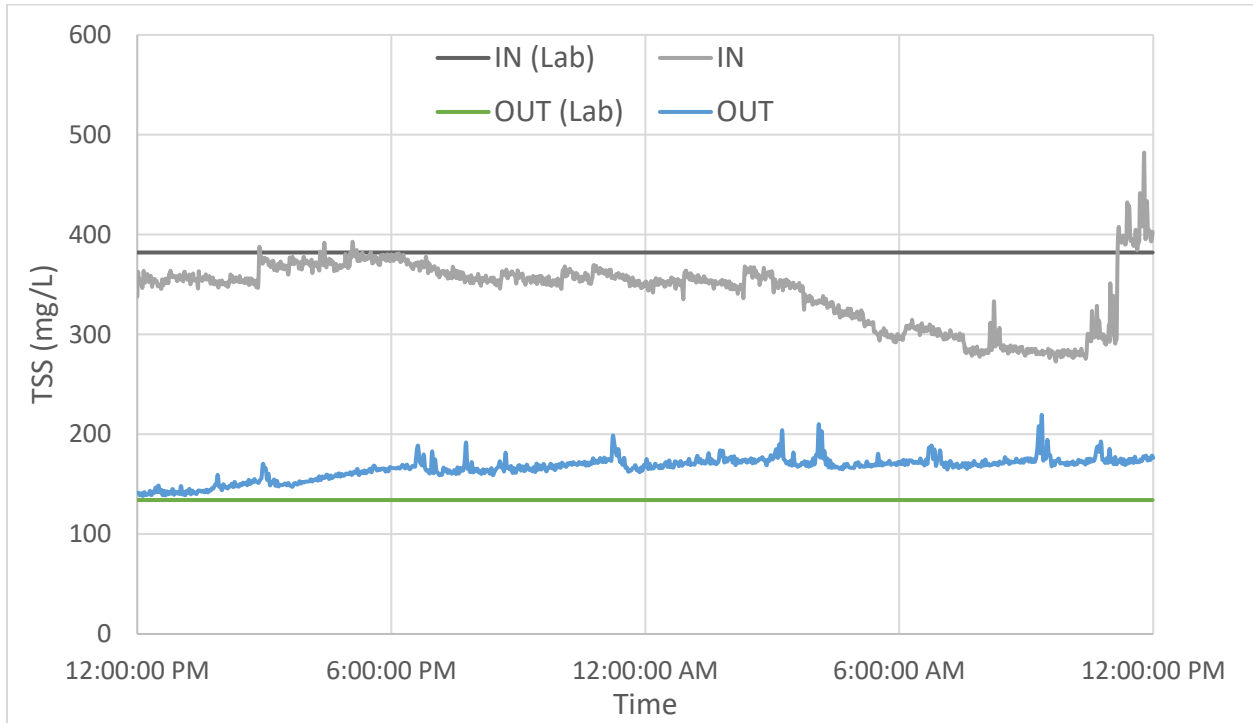


Figure 88: TSS concentrations from lab measurements on composite samples (influent and outlet) and online probes located at the inlet and outlet (Stage #8).

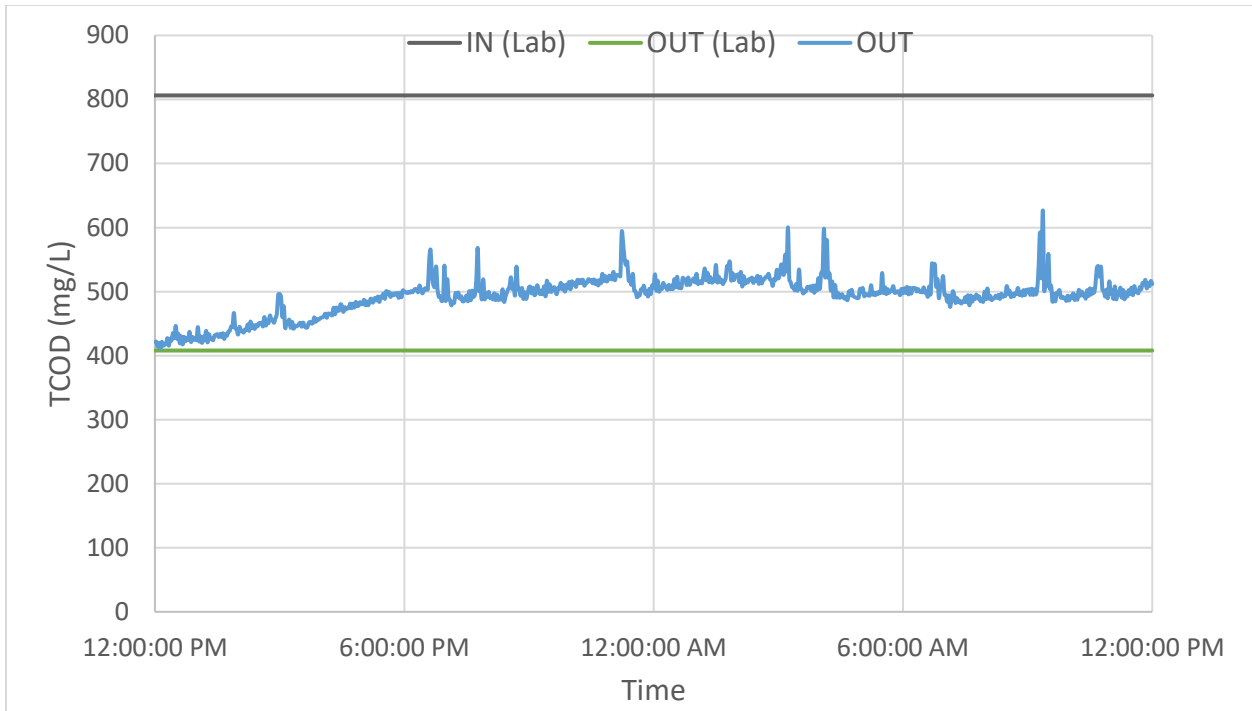


Figure 89: Total COD concentration from lab measurements on composite samples (influent and outlet) and online probe located at the outlet (Stage #8).

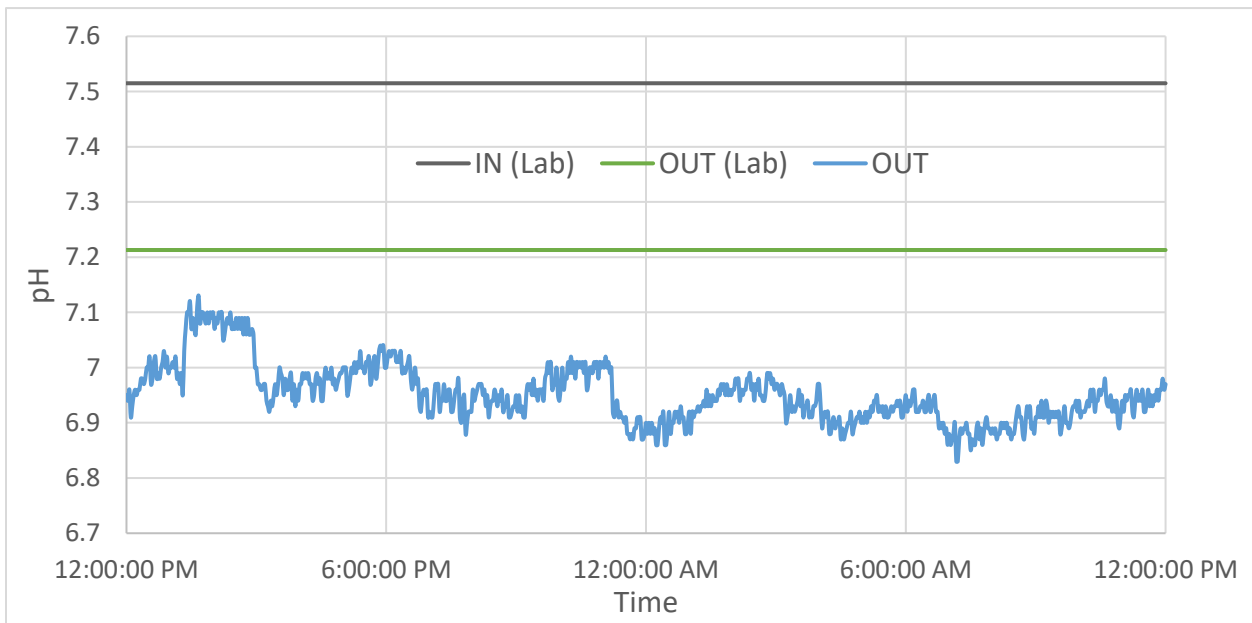


Figure 90: pH trend at the outlet and from lab measurements on composite samples (influent and outlet) (Stage #8).

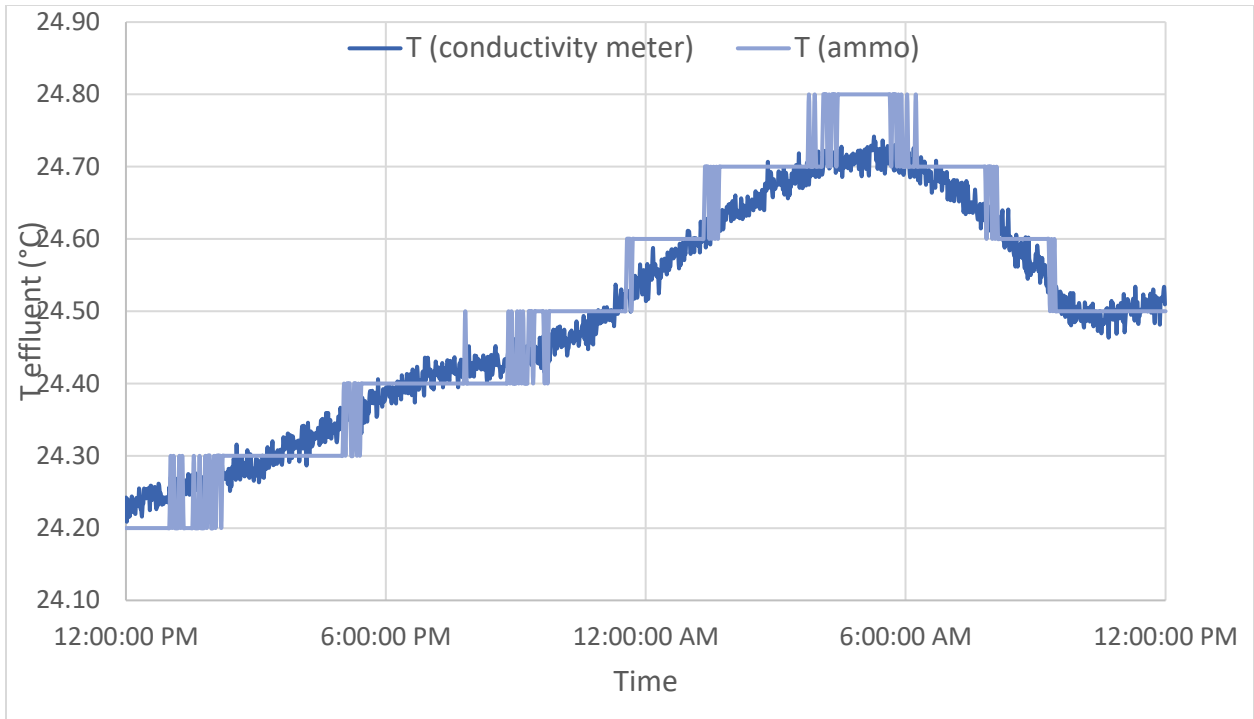


Figure 91: Temperature trend at the outlet for conductivity meter and ammo:lyser probe (Stage #8).

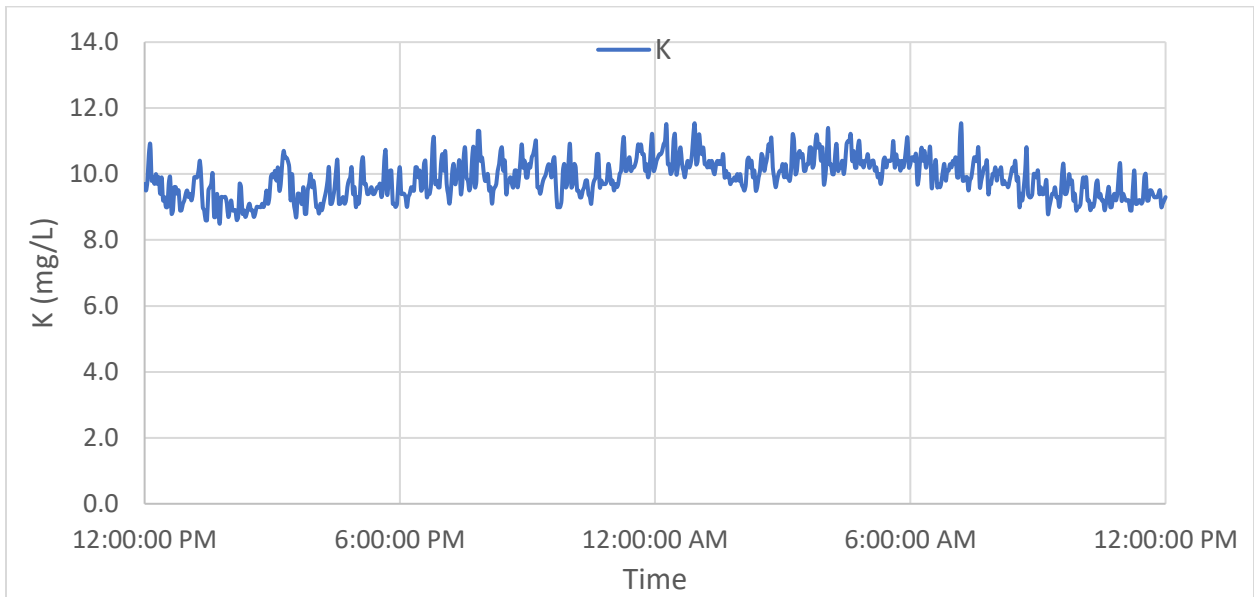


Figure 92: Potassium concentration trend at the outlet (Stage #8).

Main parameters and mass balance

Table 39: Summary of the main parameters for Stage #8.

Set-Up condition summary - Main operating parameters											
Volumes			TSS concentrations			Flow rates			Retention Times		
V ₁	V ₂	V _{TOT}	X _{IN}	X _E	X _R	Q _{IN}	Q _W	Q _R	HRT	HRT _{EFF}	SRT
L	L	L	mg/L	mg/L	mg/L	m ³ /d	m ³ /d	m ³ /d	h	h	d
1968	232	2200	382	134	16201	16.8	0.02	2.4	3.1	2.8	1.00

Heights			Mass Loads			Mass		Removal Efficiency
H _{TOT}	H ₁	SBH	L _{IN}	L _E	L _W	m _{BLANKET}	Accumulation	E%TSS
m	m	m	g/d	g/d	g/d	g	g	%
2.29	1.69	0.60	6419	2190	383	3761	3847	66%

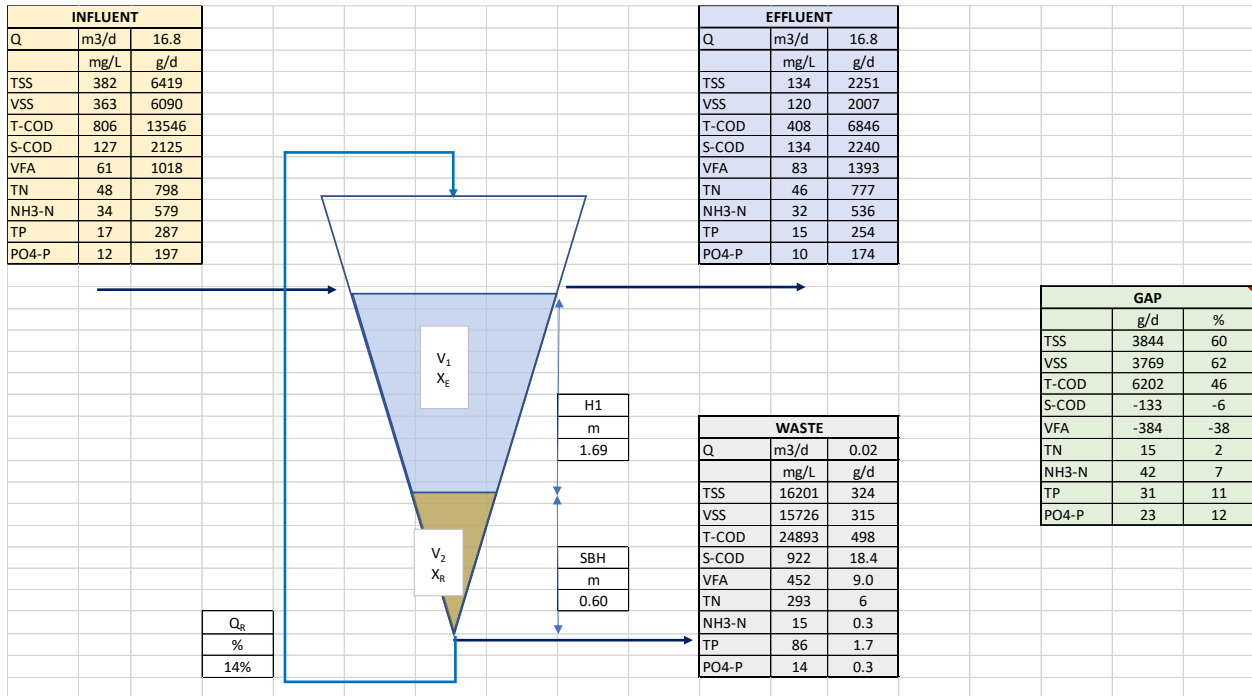


Figure 93: Mass balance Stage #8.

A.9: Data Analysis – Plots

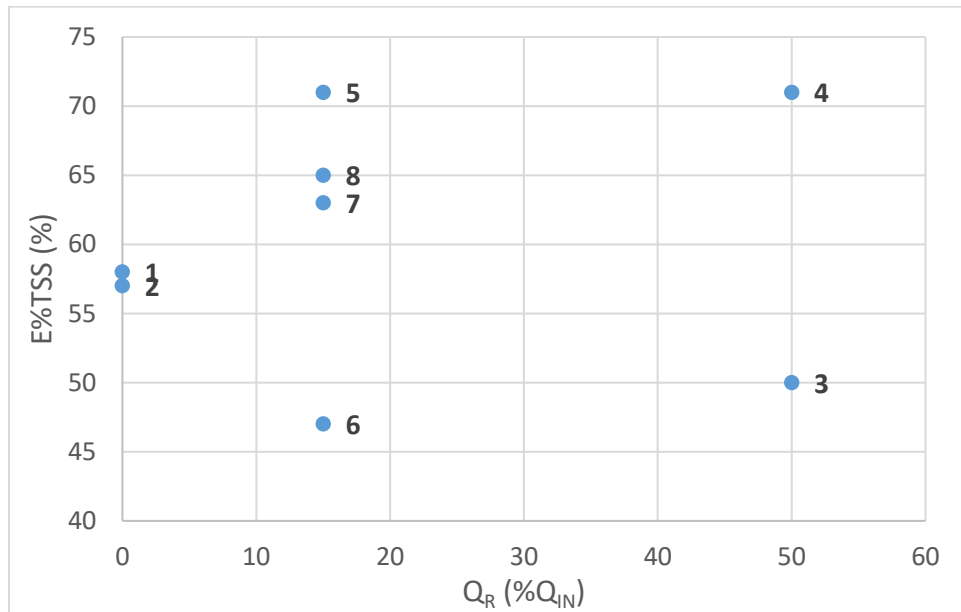


Figure 94: Effect of internal recirculation ratio on the TSS removal efficiency for stage #1 to #8.

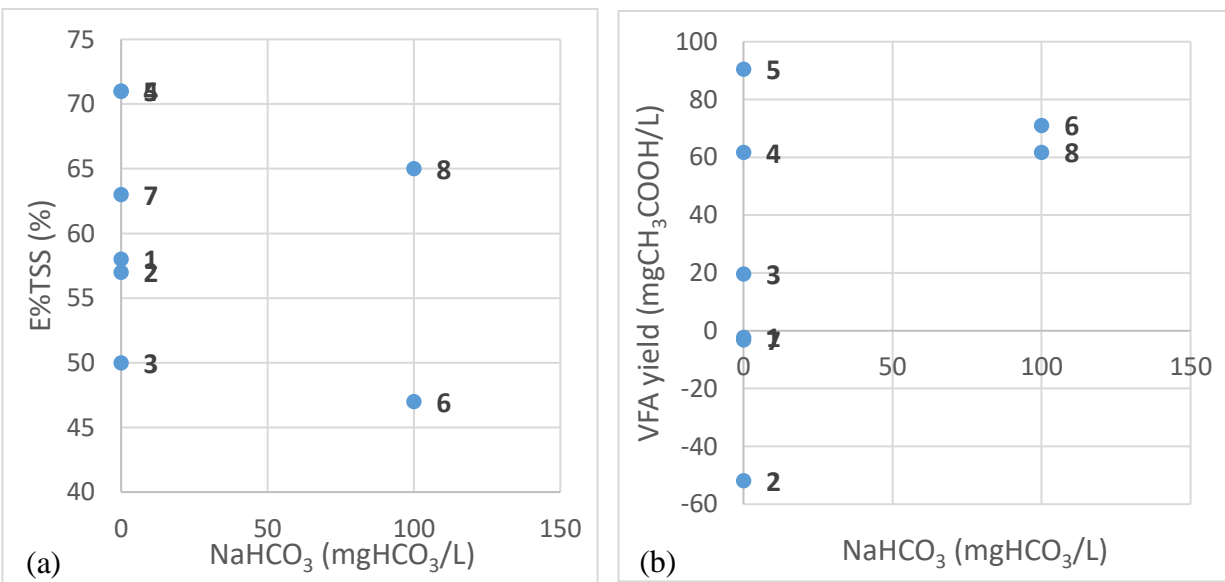


Figure 95: Effect of sodium bicarbonate dosage on (a) TSS removal efficiency and (b) VFA yield for stage #1 to #8.

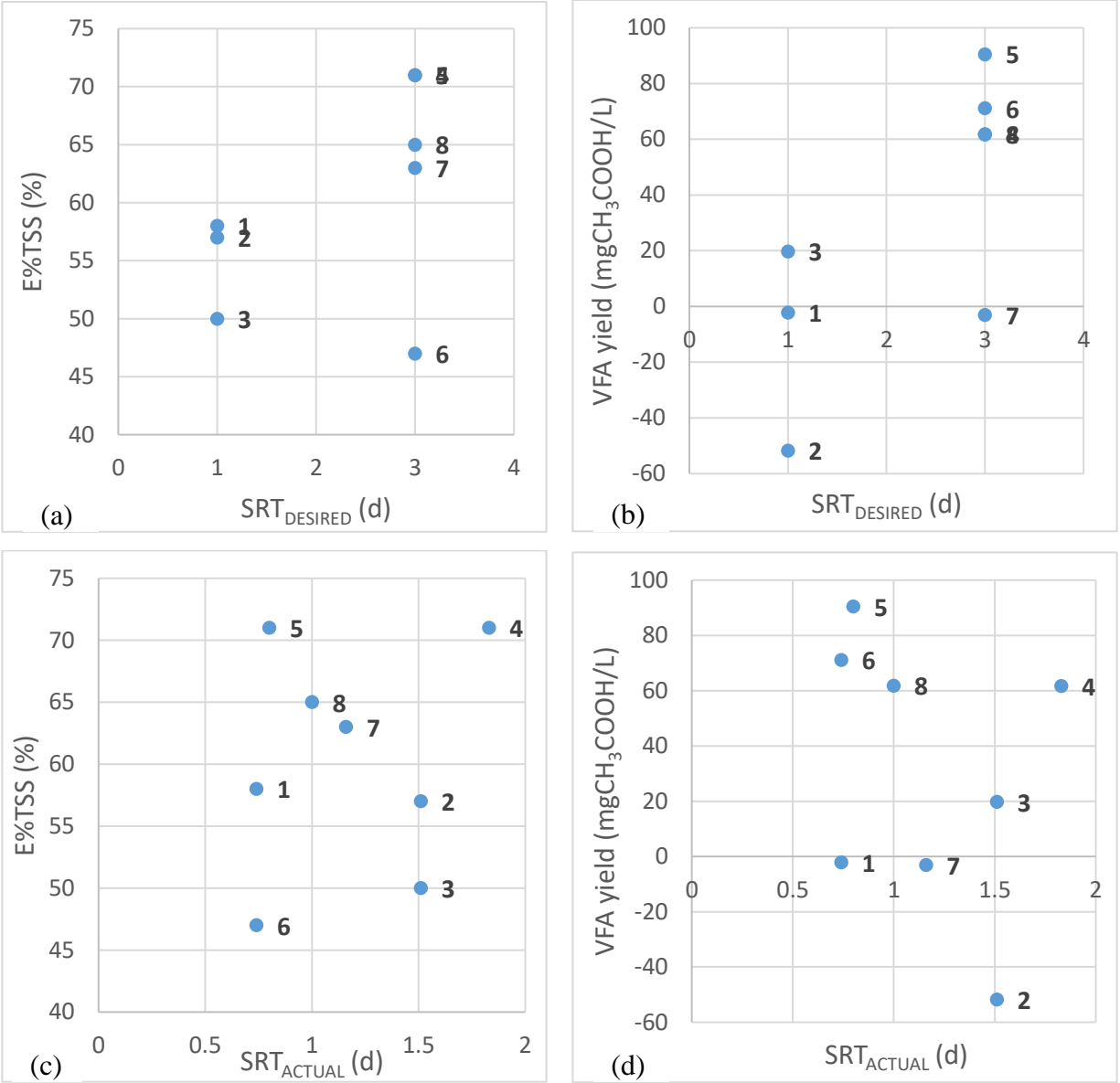


Figure 96: Effect of the desired and actual SRT on (a, c) TSS removal efficiency and (b, d) VFA yield, respectively, for stage #1 to #8.

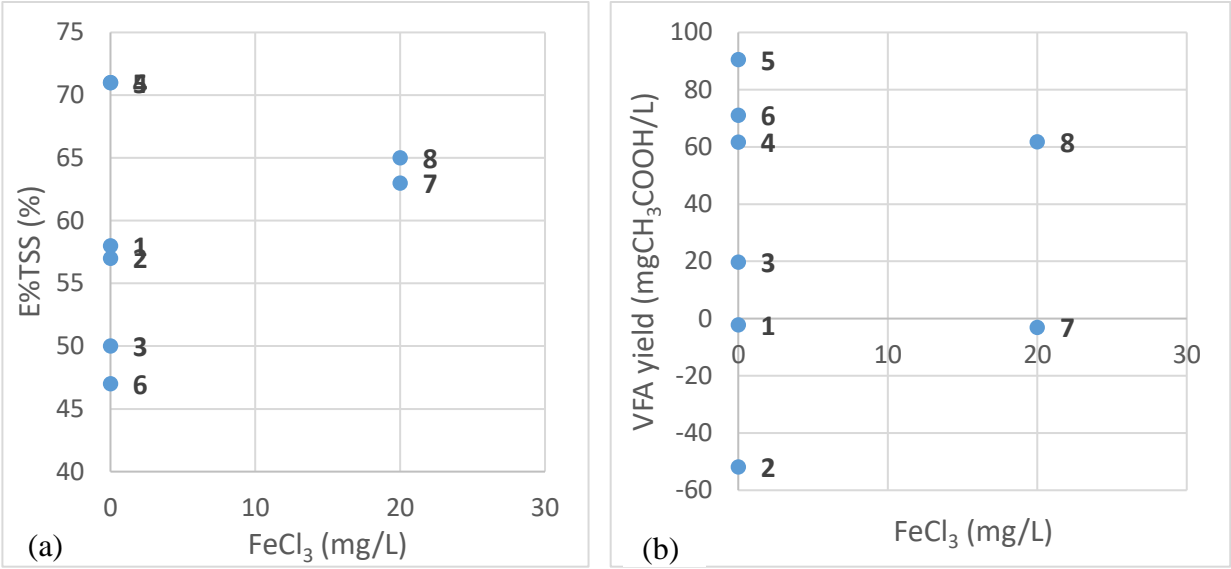


Figure 97: Effect of ferric chloride addition on (a) TSS removal efficiency and (b) VFA yield for stage #1 to #8.

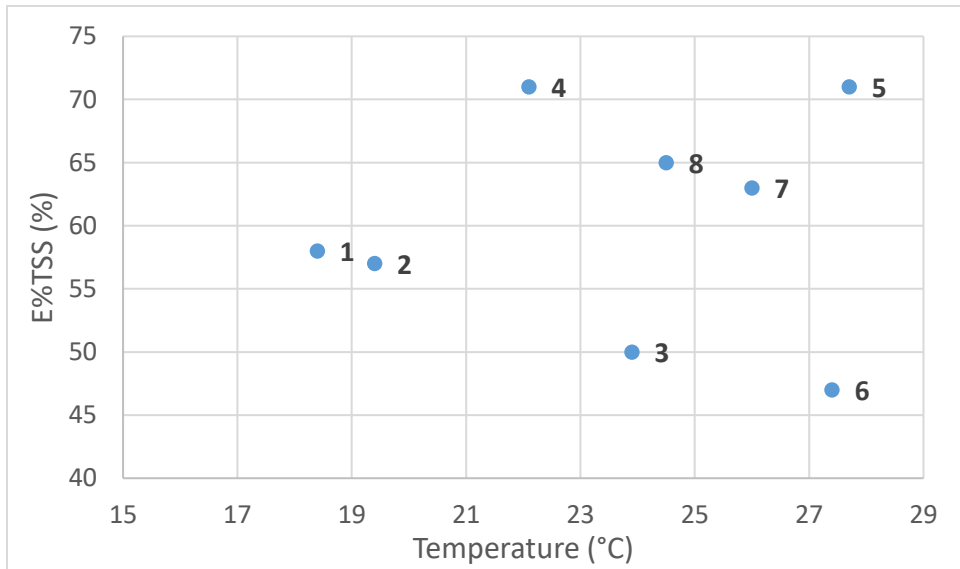


Figure 98: Temperature effect on TSS removal efficiency for stage #1 to #8.

Steady state

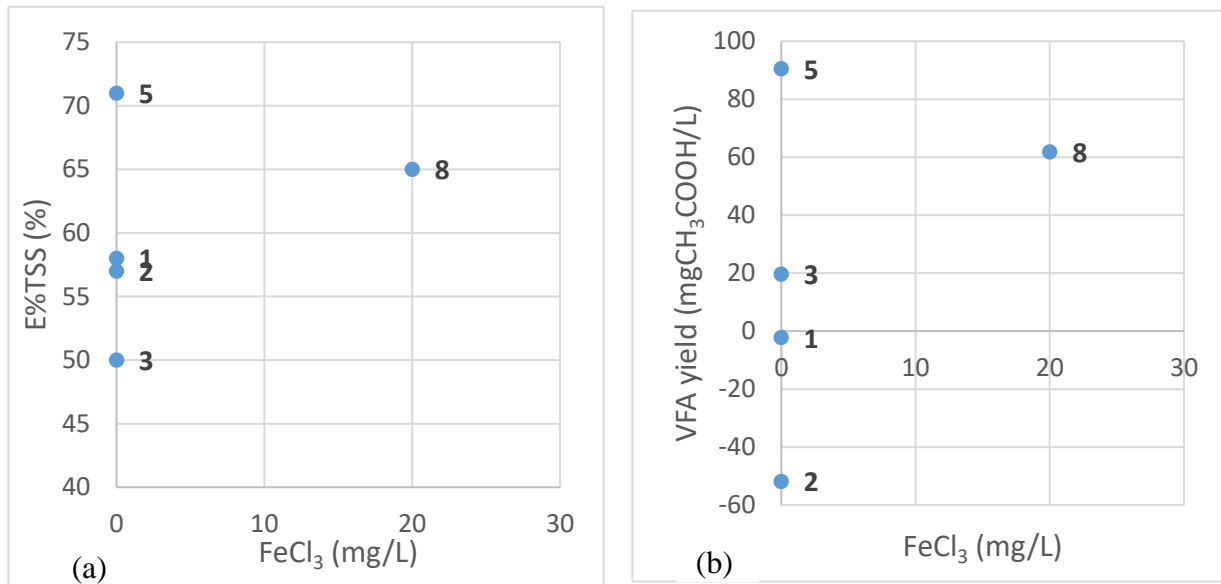


Figure 99: Effect of ferric chloride addition on (a) TSS removal efficiency and (b) VFA yield for stages in steady state conditions.

A.10: R code and data

```
data<-read.csv("OnlySSdata.csv")
model1=lm(VFA~SRTdes*Recirculation*NaHCO3*FeCl3, data=OnlySSdata)
model1
summary.aov(model1)
model2=lm(TSS~SRTdes*Recirculation*NaHCO3*FeCl3, data=OnlySSdata)
model2
summary.aov(model2)
```

Table 40: Coefficient estimates for VFA yield response.

Coefficient	Intercept	SRTdes	Q _R (14%)	Q _R (14%)	NaHCO ₃	FeCl ₃	NaHCO ₃ :FeCl ₃
Estimate	-48.000	21.000	75.500	46.700	-0.194	-4.68	0.04215

A.11: Conditions, Parameters, and Performance Values

Stage	Conditions											
	Flow rates				HRT		SRT		Chemical Dosages		Min time needed for steady-state	Start-up Period
	Q _{IN}	Q _R		Q _W	HRT	HRT _{EFF}	SRT _{DESIRED}	SRT _{ACTUAL}	NaHCO ₃	FeCl ₃		
	m ³ /d	m ³ /d	%Q _{IN}	m ³ /d	h	h	d	d	mgHCO ₃ /L	mg/L	d	d
1d	26.4	0	0%	0.096	2.0	2.0	1	0.74	-	-	3	6
1d	38.4	0	0%	0.04	1.4	1.4	1	1.51	-	-	3	3
1d, high Qr	16.8	8.4	50%	0.04	3.1	2.1	1	1.51	-	-	3	4
3d, high Qr	16.8	8.4	50%	0.02	3.1	2.1	3	1.83	-	-	9	7
3d, low Qr	16.8	2.4	14%	0.02	3.1	2.8	3	0.80	-	-	9	18
3d, low Qr, NaHCO ₃	16.8	2.4	14%	0.02	3.1	2.8	3	0.74	100	-	9	8
3d, low Qr, FeCl ₃	16.8	2.4	14%	0.02	3.1	2.8	3	1.16	-	20	9	7
3d, low Qr, NaHCO ₃ +FeCl ₃	16.8	2.4	14%	0.02	3.1	2.8	3	1.00	100	20	9	14

Stage	Main parameters									
	SBH	pH				Temperature		VFAs		
		IN	OUT	WASTE	Delta	OUT (ammo.)	OUT (cond.)	IN	OUT	WASTE
	m					°C	°C	mgCH ₃ COO/L	mgCH ₃ COO/L	mgCH ₃ COO/L
1d	0.80	-	7.45	-	-	17.6	18.4	18.0	17.5	49.0
1d	1.00	7.32	7.46	6.24	0.14	18.7	19.4	25.1	11.3	183.8
1d, high Qr	0.60	7.54	7.64	5.57	0.10	-	23.9	71.2	75.9	334.5
3d, high Qr	0.60	7.39	7.22	5.61	-0.17	-	22.1	28.8	40.8	222.2
3d, low Qr	0.60	7.47	7.28	6.08	-0.19	-	27.7	64.0	89.9	286.2
3d, low Qr, NaHCO ₃	0.40	7.39	7.63	7.27	0.24	-	27.4	58.2	70.1	254.9
3d, low Qr, FeCl ₃	0.60	7.43	7.35	5.47	-0.08	25.9	26.0	62.3	61.0	488.4
3d, low Qr, NaHCO ₃ +FeCl ₃	0.60	7.52	7.21	5.16	-0.30	24.5	24.5	60.6	83.0	451.5

Stage	Main parameters											
	Alkalinity				TSS				VSS			
	IN	OUT	WASTE	Delta	IN	OUT	WASTE	E%	IN	OUT	WASTE	E%
	mgHCO ₃ /L	mgHCO ₃ /L	mgHCO ₃ /L	mgHCO ₃ /L	mg/L	mg/L	mg/L	%	mg/L	mg/L	mg/L	%
1d	-	-	-	-	232	99	4515	58%	223	93	4436	58%
1d	152	146	137	-6	283	121	10826	57%	266	113	10538	58%
1d, high Qr	176	160	74	-16	257	129	7960	50%	240	117	7625	51%
3d, high Qr	148	135	828	-12	209	61	9481	71%	194	56	9056	71%
3d, low Qr	199	203	77	4	305	89	14235	71%	286	80	13397	72%
3d, low Qr, NaHCO ₃	161	368	105	208	183	98	12083	47%	168	91	11203	46%
3d, low Qr, FeCl ₃	206	191	205	-15	441	165	15034	63%	427	148	14519	65%
3d, low Qr, NaHCO ₃ +FeCl ₃	189	210	1191	21	382	134	16201	65%	363	120	15726	67%

Stage	Solids and COD										
	VSS/TSS			Total COD				Soluble COD			
	IN	OUT	WASTE	IN	OUT	WASTE	E%	IN	OUT	WASTE	E%
	%	%	%	mg/L	mg/L	mg/L	%	mg/L	mg/L	mg/L	%
1d	96%	94%	98%	495	289	6955	42%	93	80	665	14%
1d	94%	93%	97%	554	305	16150	45%	107	77	428	28%
1d, high Qr	93%	90%	96%	762	530	13777	30%	218	210	609	4%
3d, high Qr	93%	92%	96%	417	252	13033	40%	89	98	431	-10%
3d, low Qr	94%	89%	94%	686	457	18933	33%	195	233	529	-19%
3d, low Qr, NaHCO ₃	92%	93%	93%	466	372	17727	20%	128	135	513	-5%
3d, low Qr, FeCl ₃	97%	90%	97%	837	421	21427	50%	144	126	645	13%
3d, low Qr, NaHCO ₃ +FeCl ₃	95%	89%	97%	806	408	24893	49%	127	134	922	-6%

Stage	Nitrogen											
	Total TN				Soluble TN				NH ₃ -N			
	IN	OUT	WASTE	E%	IN	OUT	WASTE	E%	IN	OUT	WASTE	E%
	mg/L	mg/L	mg/L	%	mg/L	mg/L	mg/L	%	mg/L	mg/L	mg/L	%
1d	54.8	53.1	108.5	3%	44.1	43.6	39.1	1%	27.7	27.1	24.3	2%
1d	2.5	1.6	4.2	35%	1.2	0.6	2.9	49%	0.4	0.6	0.1	-58%
1d, high Qr	47.8	45.2	183.7	5%	43.2	39.3	32.4	9%	34.6	33.9	29.4	2%
3d, high Qr	33.8	31.6	209.3	6%	29.7	27.1	22.3	8%	22.6	21.9	16.0	3%
3d, low Qr	53.8	52.8	267.0	2%	44.6	46.2	42.8	-4%	39.4	43.9	37.9	-12%
3d, low Qr, NaHCO ₃	40.6	39.5	306.0	3%	33.6	35.4	29.5	-5%	29.5	28.0	23.6	5%
3d, low Qr, FeCl ₃	49.6	46.3	266.7	7%	41.6	36.3	35.2	13%	35.3	32.6	26.2	8%
3d, low Qr, NaHCO ₃ +FeCl ₃	47.5	46.3	292.7	2%	40.2	39.1	22.8	3%	34.5	32.0	14.8	7%

Stage	Phosphorus											
	Total P				PO ₄ -P				PO ₄ -P / TP			
	IN	OUT	WASTE	E%	IN	OUT	WASTE	E%	IN	OUT	WASTE	E%
	mg/L	mg/L	mg/L	%	mg/L	mg/L	mg/L	%	%	%	%	%
1d	16.0	15.5	65.3	3%	10.5	9.6	28.3	9%	66%	62%	43%	
1d	0.9	0.2	9.9	81%	0.3	0.2	0.7	21%	29%	120%	7%	
1d, high Qr	16.7	15.5	54.7	7%	11.8	11.9	15.2	0%	71%	76%	28%	
3d, high Qr	10.7	9.8	65.7	8%	7.0	7.2	9.4	-3%	65%	73%	14%	
3d, low Qr	19.3	19.8	93.5	-3%	13.4	15.3	18.8	-14%	70%	77%	20%	
3d, low Qr, NaHCO ₃	15.0	14.2	93.3	5%	10.5	10.4	9.4	1%	70%	73%	10%	
3d, low Qr, FeCl ₃	18.3	16.7	78.4	8%	12.4	9.5	19.2	23%	68%	57%	24%	
3d, low Qr, NaHCO ₃ +FeCl ₃	17.1	15.2	86.3	11%	11.8	10.4	14.5	12%	69%	68%	17%	

Stage	Performance										
	TSS removal	VFAs yield		VFAs yield tot		Hydrolysis yield	(VFA _{OUT} -VFA _{IN})/TCOD	SCOD/TCOD			
		mgCH ₃ COO/ g VSS	mgCOD/ g VSS	mgCH ₃ COO/ g VSS	mgCOD/ g VSS			IN	OUT	WASTE	Delta
	E%					%	%	%	%	%	
1d	58%	-2.5	-2.7	-1.7	-1.8	-2.6%	-0.1%	19%	28%	10%	9%
1d	57%	-51.9	-55.5	-51.1	-54.7	-5.5%	-2.5%	19%	25%	3%	6%
1d, high Qr	50%	18.9	20.2	22.2	23.8	-1.1%	0.6%	29%	40%	4%	11%
3d, high Qr	71%	61.4	65.7	62.8	67.2	2.0%	2.9%	21%	39%	3%	17%
3d, low Qr	71%	90.1	96.4	91.3	97.7	5.5%	3.8%	28%	51%	3%	23%
3d, low Qr, NaHCO ₃	47%	70.6	75.5	72.4	77.4	1.5%	2.6%	27%	36%	3%	9%
3d, low Qr, FeCl ₃	63%	-3.3	-3.5	-1.9	-2.1	-2.2%	-0.2%	17%	30%	3%	13%
3d, low Qr, NaHCO ₃ +FeCl ₃	65%	61.6	65.9	63.1	67.5	0.9%	2.8%	16%	33%	4%	17%

Stage	Performance				
	VFA/SCOD				COD solubilisation
	IN	OUT	WASTE	Delta	
	%	%	%	%	mg/L
1d	19%	22%	7%	3%	-13.0
1d	23%	15%	43%	-9%	-30.3
1d, high Qr	33%	36%	55%	3%	-8.0
3d, high Qr	32%	42%	52%	9%	8.5
3d, low Qr	33%	39%	54%	6%	38.0
3d, low Qr, NaHCO ₃	46%	52%	50%	7%	7.0
3d, low Qr, FeCl ₃	43%	49%	76%	5%	-18.5
3d, low Qr, NaHCO ₃ +FeCl ₃	48%	62%	49%	14%	7.0

References

- [1] P. M. Glibert, “Eutrophication , harmful algae and biodiversity — Challenging paradigms in a world of complex nutrient changes,” *Mar. Pollut. Bull.*, vol. 124, pp. 591–606, 2017.
- [2] M. Geissdoerfer, P. Savaget, N. M. P. Bocken, and E. Jan, “The Circular Economy - A new sustainability paradigm?,” *J. Clean. Prod.*, vol. 143, pp. 757–768, 2017.
- [3] Metcalf & Eddy, “Wastewater Engineering: Treatment and Reuse.” McGrawHill, Fourth Edition, 2003.
- [4] M. Atasoy, I. Owusu-agyeman, E. Plaza, and Z. Cetecioglu, “Bio-based volatile fatty acid production and recovery from waste streams: Current status and future challenges,” *Bioresour. Technol.*, vol. 268, pp. 773–786, 2018.
- [5] W. S. Lee, A. Seak, M. Chua, H. K. Yeoh, and G. C. Ngoh, “A review of the production and applications of waste-derived volatile fatty acids,” *Chem. Eng. J.*, vol. 235, pp. 83–99, 2014.
- [6] L. Appels, J. Baeyens, J. Degève, and R. Dewil, “Principles and potential of the anaerobic digestion of waste-activated sludge,” *Prog. Energy Combust. Sci.*, vol. 34, pp. 755–781, 2008.
- [7] G. Yanga and J. Wang, “Fermentative hydrogen production from sewage sludge,” *Crit. Rev. Environ. Sci. Technol.*, vol. 47, pp. 1219–1281, 2017.
- [8] W. S. Lee, A. S. M. Chua, H. K. Yeoh, and G. C. Ngoh, “A review of the production and applications of waste-derived volatile fatty acids,” *Chem. Eng. J.*, vol. 235, pp. 83–99, 2014.
- [9] “Elutriation,” 2019. [Online]. Available: <https://en.wikipedia.org/wiki/Elutriation>. [Accessed: 11-Apr-2019].
- [10] J. Chanona, J. Ribes, A. Seco, and J. Ferrer, “Optimum design and operation of primary sludge fermentation schemes for volatile fatty acids production,” *Water Res.*, vol. 40, pp. 53–60, 2006.
- [11] A. Bouzas, J. Ribes, J. Ferrer, and A. Seco, “Fermentation and elutriation of primary sludge: Effect of SRT on process performance,” *Water Res.*, vol. 41, pp. 747–756, 2007.
- [12] P. Jin, X. Wang, Q. Zhang, X. Wang, H. H. Ngo, and L. Yang, “A new activated primary tank developed for recovering carbon source and its application,” *Bioresour. Technol.*, vol. 200, pp. 722–730, 2016.
- [13] M. A. Khan *et al.*, “Optimization of process parameters for production of volatile fatty acid,

- biohydrogen and methane from anaerobic digestion,” vol. 219, pp. 738–748, 2016.
- [14] Y. H. Ahn and R. E. Speece, “Elutriated acid fermentation of municipal primary sludge,” *Water Res.*, vol. 40, pp. 2210–2220, 2006.
- [15] H. Wu, J. Gao, D. Yang, Q. Zhou, and W. Liu, “Alkaline fermentation of primary sludge for short-chain fatty acids accumulation and mechanism,” *Chem. Eng. J.*, vol. 160, pp. 1–7, 2010.
- [16] Y. Chen, X. Jiang, K. Xiao, N. Shen, R. J. Zeng, and Y. Zhou, “Enhanced volatile fatty acids (VFAs) production in a thermophilic fermenter with stepwise pH increase e Investigation on dissolved organic matter transformation and microbial community shift,” *Water Res.*, vol. 112, pp. 261–268, 2017.
- [17] E. U. Cokgor, S. Oktay, D. O. Tas, G. E. Zengin, and D. Orhon, “Influence of pH and temperature on soluble substrate generation with primary sludge fermentation,” *Bioresour. Technol.*, vol. 100, pp. 380–386, 2009.
- [18] H. Ma, X. Chen, H. Liu, H. Liu, and B. Fu, “Improved volatile fatty acids anaerobic production from waste activated sludge by pH regulation: Alkaline or neutral pH?,” *Waste Manag.*, vol. 48, pp. 397–403, 2016.
- [19] L. Lin, R. Li, Z. Yang, and X. Li, “Effect of coagulant on acidogenic fermentation of sludge from enhanced primary sedimentation for resource recovery: Comparison between FeCl₃ and PACl,” *Chem. Eng. J.*, vol. 325, pp. 681–689, 2017.
- [20] L. Lin, R. Li, Y. Li, J. Xu, and X. Li, “Recovery of organic carbon and phosphorus from wastewater by Fe-enhanced primary sedimentation and sludge fermentation,” *Process Biochem.*, vol. 54, pp. 135–139, 2017.
- [21] L. Lin and X. yan Li, “Acidogenic fermentation of iron-enhanced primary sedimentation sludge under different pH conditions for production of volatile fatty acids,” *Chemosphere*, vol. 194, pp. 692–700, 2018.
- [22] H. Liu, P. Han, H. Liu, G. Zhou, B. Fu, and Z. Zheng, “Full-scale production of VFAs from sewage sludge by anaerobic alkaline fermentation to improve biological nutrients removal in domestic wastewater,” *Bioresour. Technol.*, vol. 260, pp. 105–114, 2018.
- [23] D. C. Montgomery, “Design and Analysis of Experiments.” Wiley, 7th Ed., 2009.
- [24] H. Wu, D. Yang, Q. Zhou, and Z. Song, “The effect of pH on anaerobic fermentation of primary sludge at room temperature,” *Hazard. Mater.*, vol. 172, pp. 196–201, 2009.

